

Poster Session

DISCIPLINE-INTEGRATED MODELLING APPROACH FOR DESCRIBING THE OLKILUOTO CRYSTALLINE SITE IN FINLAND

J. Andersson¹, J. Mattila², J.A Hudson³, L. Koskinen², P. Pitkänen⁴, M. Yllä-Mella², P. Hellä⁵

¹JA, Streamflow AB, Sweden; ²Posiva Oy, Finland; ³REC, UK; ⁴VTT, Finland;

⁵Pöyry Environment Oy, Finland

Abstract

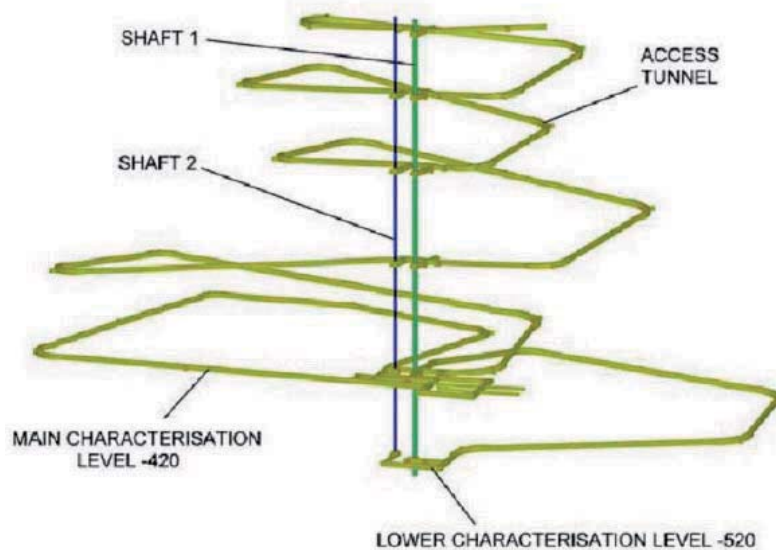
Posiva, the nuclear waste management organization in Finland, is currently constructing an underground research facility at the Olkiluoto site. The Olkiluoto Modelling Task Force (OMTF) has been established for planning and integrating the results and the modelling work in the different supporting disciplines. The main duty of the OMTF is to develop site descriptive models of the Olkiluoto site, as well as predicting and evaluating the disturbance created by construction of the ONKALO ramp and characterization tunnels. Various approaches are utilised including cross-discipline workshops to ensure a common basis for modelling; prediction/outcome studies; and carrying out an overall confidence assessment are key synthesizing and integrating tools. The resulting geosynthesis is reported in a series of Site Reports. Future updates of the Site Report will be part of the Safety Case portfolio supporting a licence application for constructing a final repository for Finland's spent nuclear fuel at the site.

Introduction

Posiva, the nuclear waste management organization in Finland, is currently constructing an underground research facility, ONKALO, at the Olkiluoto site. The ONKALO, as well as other characterisation activities at Olkiluoto, produces a substantial amount of data, Figure 1. These data need to be incorporated into models of the site to be used as input, both for the further construction of the ONKALO and for use in subsequent safety analyses and licence applications.

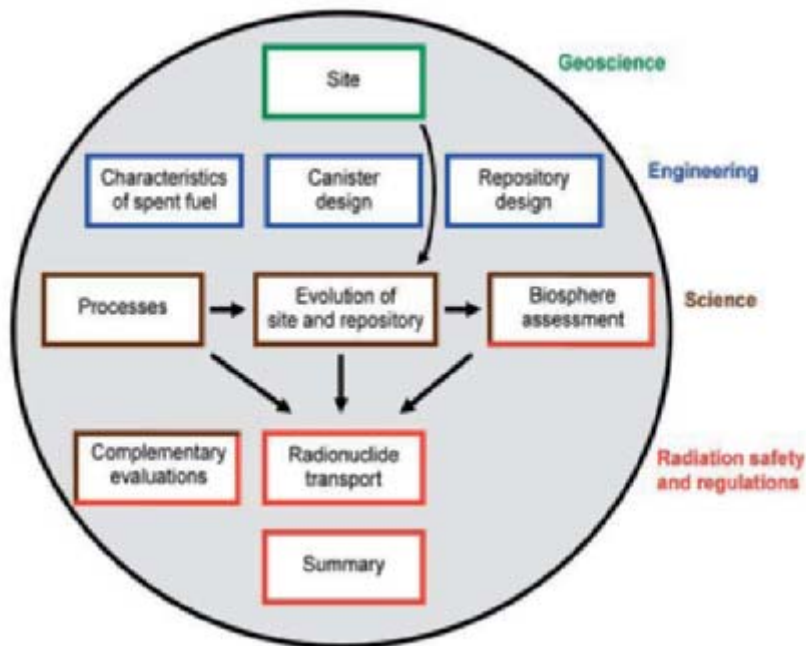
The Olkiluoto Modelling Task Force (OMTF) has been established for planning and integrating the results and the modelling work in the different supporting disciplines. The OMTF consists of modelling teams covering the subjects of Geology, Rock Mechanics, Hydrogeology and Hydrogeochemistry. A Task Force Core Group, consisting of representatives from the modelling teams, plus the Task Force Leader, has been established. The main duty of the OMTF is to develop site descriptive models of the Olkiluoto site, as well as predicting and evaluating the disturbance created by construction of the ONKALO ramp and characterisation tunnels.

Figure 1. The general layout of ONKALO according to the current design



The resulting geosynthesis is reported in a series of Site Reports. A first version, Site Report 2004 (Posiva, 2005) as well as an updated version, Site Report 2006 (Andersson *et al.*, 2007) have already been published. Future updates of the Site Report will be part of the Safety Case portfolio, Figure 1 supporting a licence application for constructing a final repository for Finland's spent nuclear fuel at the site

Figure 2. The Site report will be part of the Posiva Safety Case portfolio



Site descriptive model

The main product of the modelling is a descriptive model of the site, i.e. a model describing the geometry, properties of the bedrock and the water, and the interacting processes and mechanisms that are relevant for understanding the evolution of the site to the present day and the potential for future radionuclide migration. This Site Descriptive Model (SDM) is, therefore, distinct from the measured data themselves. Modelling involves interpreting data, extrapolating or interpolating between measurement points and calibrating the numerical models used to simulate the system against data, based on the various assumptions inherent in the conceptual model(s) being employed.

Geological model

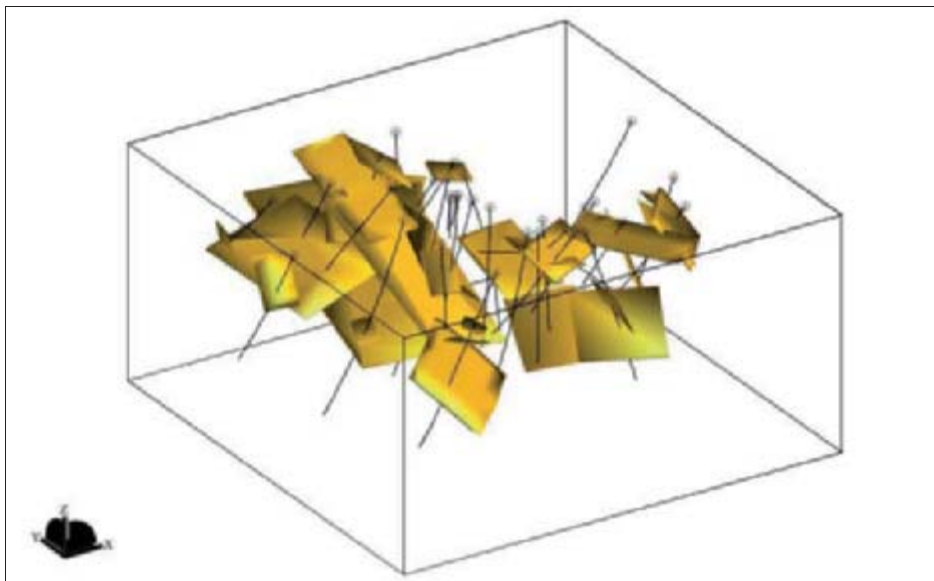
For convenience of description and handling, the geological model has been subdivided into a series of subsidiary descriptions covering lithology, alteration, ductile deformation, brittle deformation and fracturing. This sub-division is for the convenience of handling different types of data and should not be regarded as of fundamental significance. For example, the deformation zone model and fracture system model (DFN-model) both represent the effects of brittle deformation at the site, describing deterministic large-scale features and stochastic small-scale features, respectively. However, this is clearly an artificial sub-division, geologically, since these features are closely related with regard to their mode of formation. Similarly, the lithological model may have considerable significance for the distribution of fracturing in space.

The rocks at Olkiluoto can be divided into high-grade metamorphic rocks and igneous rocks on the basis of texture, migmatite structure and major mineral composition. The metamorphic rocks include various migmatitic gneisses and homogeneous, banded or only weakly migmatized gneisses, such as mica gneisses, quartz gneisses, mafic gneisses and tonalitic-granodioritic-granitic gneisses.

The bedrock at Olkiluoto belongs to the Svecofennian domain of Southern Finland, which was deformed in a ductile manner during the Svecofennian Orogeny ca. 1.91 – 1.80 Ga ago. The bedrock, except for the diabases and certain pegmatitic granite dykes, has been affected by five stages of ductile deformation, as determined on the basis of refolding and cross-cutting relationships. The ductile deformation models essentially concerns the 3-D model of the orientation of the composite foliation S2/3/4 dipping gently to the S and SE.

After the Svecofennian Orogeny ca. 1 910 – 1 800 Ma ago, the Fennoscandian shield was dominated by several tectonic events, resulting in brittle deformation, and a brittle deformation zone model is developed for describing this deformation. The starting point for the brittle deformation modelling was the observed intersections of deformation zones (brittle fault intersections and brittle joint intersections) in the drillholes, their kinematic data and geophysical indications. Since the brittle fault zones were supposed to be the spatially most continuous brittle features, the modelling work was strongly focussed on them. Tentatively, five groups of brittle faults (Groups A to E) can be defined from the total number of brittle faults. Fault-slip directions are sub-horizontal, N-S trending for group A, see Figure 3, gently NE or SW plunging for group B, gently SSE plunging for group C, gently ENE plunging for group D and gently SE plunging for group E. In all of the groups, most of the fault planes dip gently to the SE. In fault groups A and B there are also fault planes dipping steeply to the E and SE, respectively.

Figure 3. Fault zones of fault group A. View from the SW



The main advance since Site Report 2004 is the development of the brittle deformation model where the starting point for the brittle deformation modelling was the observed intersections of deformation zones in the drillholes, their kinematic data and geophysical indications, whereas hydrogeological data have deliberately not been used to allow for an independent assessment of the these data.

Rock mechanics model

The rock mechanics model consists of the geometrical, mechanical and thermal descriptions of the rock mass. The geometrical description is based on the bedrock geological model, as described above. The mechanical description includes the in situ stress state and the deformation and strength properties of the intact rock, the fractures, the rock mass between deformation zones and the deformation zones themselves. The thermal description is based on the thermal properties of the intact rock. The rock mechanics model also includes a description of the effects of excavation and considers the interaction of the rock mechanics model with the hydrogeological model.

Uniaxial compressive strengths are assessed from the field tests from drillhole cores. The strength values of the samples show noticeable variation, which is significant, even when different rock types are considered separately. The high standard deviation (approximately 30 MPa) may be assumed to reflect the heterogeneous nature of the different rock types at Olkiluoto. It may also be due to the difficulty in defining the rock types for the samples, as their locations in the boreholes were not known accurately and there are frequent variations in rock types; with rock type boundaries often coinciding with the locations defined for the samples.

The stress field is assessed from overcoring measurements, hydraulic fracturing stress data, and results from the Kaiser Effect measurements. However, the scatter in the data makes it difficult to determine a single, representative stress profile for each stress component, rather, estimated lower and upper limits were defined. When determining these, it was assumed (as is often inferred from actual

near-surface measurements in Fennoscandia) that the stress state comprises a significant non-zero horizontal component near the surface, whereas the vertical stress is governed primarily by the overburden pressure (zero at the surface). These linear profiles were subjectively defined to encompass the majority (but not all) of the data, thus providing reasonable input data for future work. The orientations of the maximum horizontal stress show a larger scatter, but are generally in the interval of 050–130°.

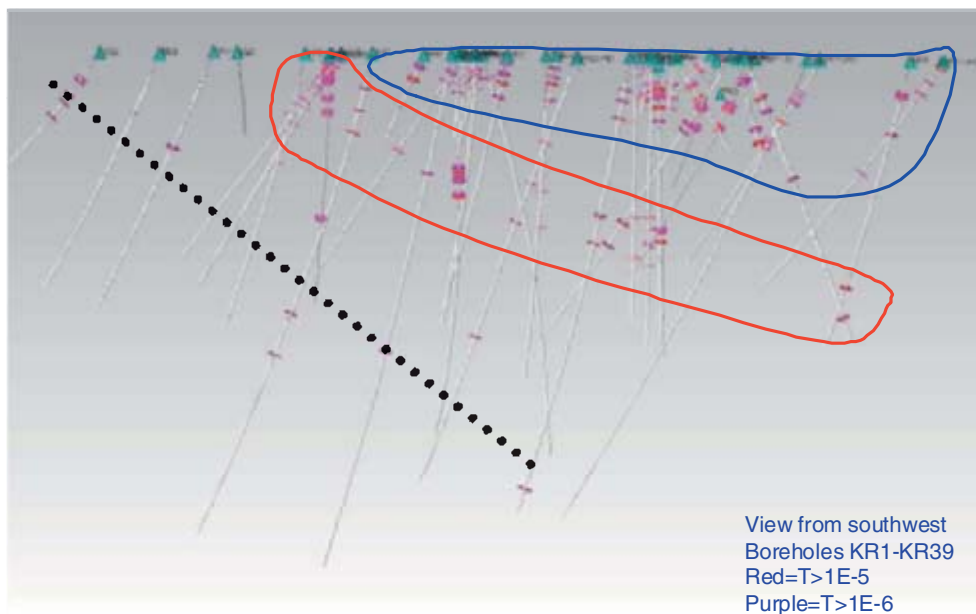
Site scale hydrogeological model

The site scale hydrogeological model consists of the hydrostructure model and the flow model. The hydrostructure model describes the location and extent, i.e. geometry of each water bearing (transmissive) zone of the bedrock. Although it is closely related to the geometrical structure of the geological bedrock model, the geometrical structures, including the deformation zones of the geological model, are not necessarily identical to the geometrical structure of the hydrogeological model. One of the modelling tasks is to describe its relationship with the geological model. From the viewpoint of the practical groundwater flow modelling on the site scale there is a need to introduce “hydrogeological zones” or to combine geological features into less complex hydraulic ones. The groundwater simulation model with its boundary conditions for the groundwater pressure and salinity, and specification of their initial states, and assigned hydraulic and transport properties is called the flow model.

Measured transmissivities, as displayed in Figure 4, form, in addition to the geological structures, the basis of defining the hydrogeological zones as well as determining the effective properties of both these zones and the properties of the sparsely fractured rock mass between these zones. Figure 4 shows that the spatial distribution of transmissivities greater than 10⁻⁹ m²/s exhibits a strong concentration close to the surface and to three major hydraulic zones. The customary assumption attributes such a distinct vertical trend in the transmissivity to the lithostatic stress, which increases linearly at shallow depths, thus reducing the apertures of fractures – in particular those having sub-horizontal orientations. This is not, however, the only explanation, as the density (frequency) of fractures clearly decreases at a depth of several tens of metres. In Figure 4 the high transmissivities at shallow depths are enclosed within a blue loop. Below this group the frequency of high transmissivities abruptly decreases, but at greater depth another spatial grouping of high transmissivities is met. This group of elevated transmissivities below sounder rock is associated with an important hydrogeological zone HZ20 (the domain of high transmissivities above it encloses the HZ19 hydrogeological zone system). A more careful examination uncovers the fact that at yet greater depth, another group of enhanced transmissivities is encountered (indicated with a dotted line in the figure), but is clearly of less significance.

The main geological input to the hydrogeological bedrock model describes a number of brittle deformation zones (BFZ) whose hydrogeological properties have been determined with drillhole measurements of transmissivity. The extensive dataset gathered clearly indicates that not all the BFZs are hydrogeologically significant. Furthermore, in some cases clearly elevated transmissivities cannot be associated with modelled structures in the brittle deformation model. This is important feedback for the next version of the BFZ-model, since extensive hydraulic zones are expected to be connected to deformation zones, even if the rock mass between the zones can contain connected and transmissive individual fractures.

Figure 4. Measured transmissivities higher than $T = 10^{-6} \text{ m}^2/\text{s}$. Three distinct areas of spatial grouping of high transmissivities are indicated



Hydrogeochemical model

The hydrogeochemical model consists of a description of the groundwater composition and an assessment of the processes controlling the evolution of the groundwater composition in time and space. Hydrogeochemical conditions are of importance for the durability of engineered barriers (canister, bentonite buffer and other sealing materials) and for determining the solubility and migration of radionuclides. The most critical chemical parameters in groundwater for safety are salinity, pH, oxygen, the concentration of divalent cations and dissolved sulphide.

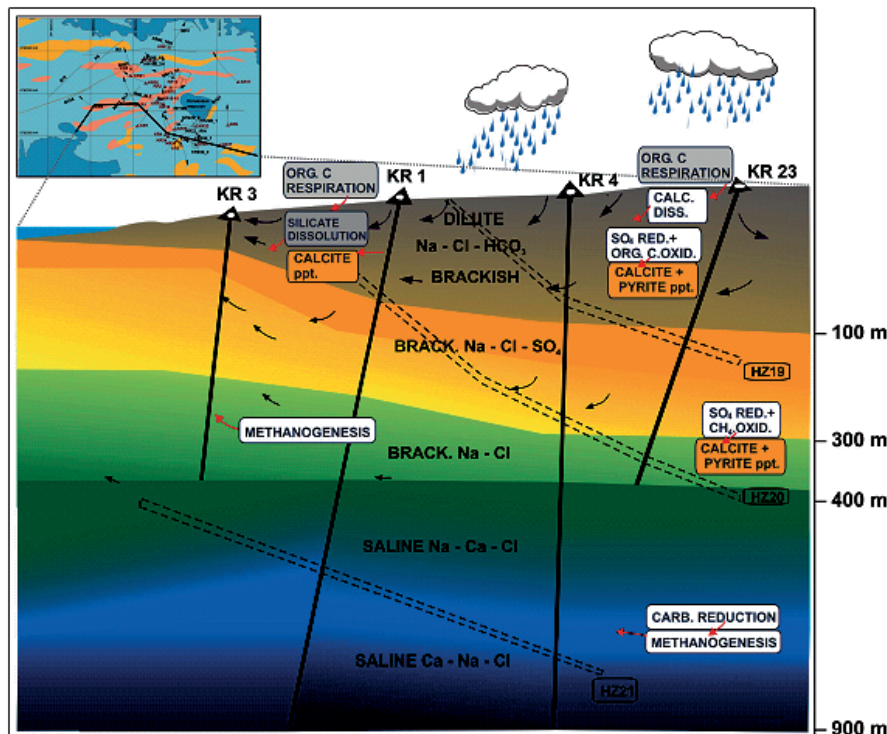
Generally chemical groundwater conditions are stable at depth at Olkiluoto and reactions and transport processes proceed very slowly. However, chemical interactions may be enhanced, and thus may also consume the buffering capacity of the system, if groundwaters with different chemical states are mixed, or other materials (in contact with water) are in significant disequilibrium with groundwater. Therefore, it is necessary to have a good understanding of the hydrogeochemical evolution of the site, regarding former interactions induced by the mixing of groundwaters. The ultimate goal is to create a site-specific model that reliably describes changes in groundwater composition and explains their causes.

The groundwater chemistry over the depth range 0-1 000 m at Olkiluoto is characterised by a significant range in salinity. Fresh groundwater with low total dissolved solids ($\text{TDS} \leq 1 \text{ g/l}$) is found only at shallow depths, in the uppermost tens of metres. Brackish groundwater, with TDS up to 10 g/l dominates at depths varying from 30 m to 450 m. Saline groundwater ($\text{TDS} > 10 \text{ g/l}$) dominates below 400 m depth. Sodium and calcium dominate as main cations in all groundwaters and Mg is notably enriched in SO_4 -rich groundwaters, supporting their marine origin.

The hydrogeochemical conditions and their distribution in the bedrock are the result of progressive mixing and reactions between various initial water types, which represent some of the major events at the site during its geological history. The initial waters have reference compositions in current groundwater data, which are most evident in combinations of conservative parameters, such as values of stable isotopes of water, Cl and Br contents. A comparison of $\delta^{18}\text{O}$ and Cl data indicates four extreme reference groundwaters, which can govern the other groundwater compositions by mixing. The waters are according to age: brine reference, glacial reference, Littorina reference and meteoric water which, with the addition of Baltic seawater (basically diluted Littorina), enables the mixing traces of the other samples to be determined.

The interpretation of hydrogeochemical data indicates that mixing has controlled the wide salinity variations in groundwaters at Olkiluoto at low temperature conditions. However, water-rock interactions, such as carbon and sulphur cycling and silicate reactions, buffer the pH and redox conditions and stabilise the groundwater chemistry. The baseline hydrogeochemical system at Olkiluoto, outlined in Figure 5, seems to include two natural metastable interfaces at which the majority of chemical processes are concentrated. The upper is an infiltration zone, mainly in the overburden, and the lower lies between two brackish groundwater types at 200-300 m depth, where SO_4 -rich groundwater changes to be SO_4 -poor, but becomes methane-rich. The disequilibrium at both interfaces is caused by differences in redox states. At the upper interface oxic waters from the surface (meteoric or seawater) infiltrate the anoxic organic rich layer. Respiration of organic matter releases CO_2 in groundwater (carbonic acid) that activates weathering processes, e.g. calcite and silicate dissolution, that buffer groundwater pH to neutral levels. At the lower interface between the sulphidic and methanic redox environments, SO_4 -rich, marine-derived groundwater mixes with methane to produce, in places, exceptionally high dissolved sulphide contents and carbonate as microbially-mediated reaction products, which may precipitate as pyrite and calcite.

Figure 5. Illustrated hydrogeochemical site model of baseline groundwater conditions with main water-rock interactions at Olkiluoto



Prediction outcome studies

The adequacy of the site model is tested by making different kinds of predictions, A, B and C as the tunnel work progresses:

- Type A predictions only use the latest version of the overall Site Model.
- Type B predictions also use data that were not available at the time of producing the Site Model, such as results from recently completed tunnel mapping and pilot holes.
- Type C predictions occur after excavation and involve establishing whether the modelling methods applied could indeed have predicted the known outcome by judicious adjustment of input parameters.

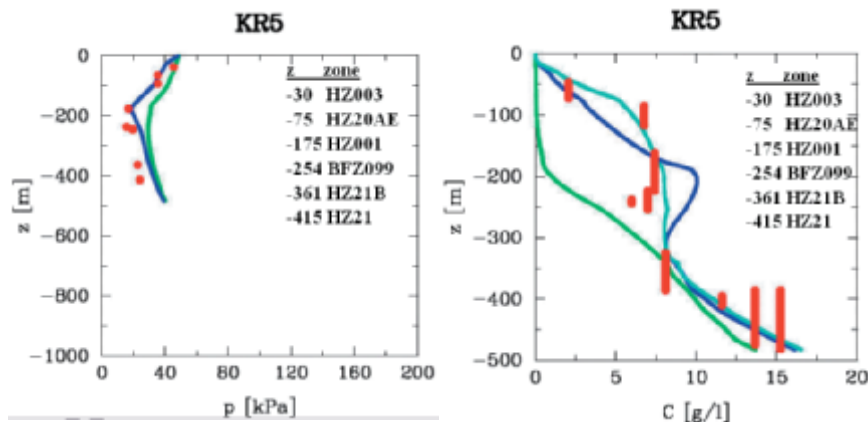
Predictions concern both what will be encountered during construction of the ONKALO, such as the lithology of the rock mass and the rock mechanics properties, and the disturbance caused by the construction, such as drawdown and upconing, and any rock spalling that may occur. Clearly, strong deviations between the A, B and C predictions are reasons to update the overall Site Model, however, it may not be feasible to formulate strict criteria for determining the level of “success” or “failure” for all parameters. Instead a set of principles for the prediction/outcome studies have been established. It is important to understand that the objective of the studies is not to strive for exact matches or for fully-calibrated models, but to develop a prediction methodology that is sufficient with regard to the needs of the Design work and the Safety Case.

Groundwater flow and evolution of groundwater composition

An essential part of the groundwater flow analyses is calibration, which strives to ensure that the flow model corresponds to the hydraulic characteristics of the real system as much as possible. The calibration is carried out using a manual trial-and-error technique evaluating the flow model against the measured pressure and salinity in the drillholes.

Simulations computed with the initial geometric mean transmissivities obtained from hydraulic tests, show a fairly good agreement between the simulated and measured pressures, apart from some drill holes intersecting a hydraulic zone in the upper 300 m. Thus, it was considered justified to increase the transmissivity of this zone in the upper layer. This results in quite good fits, Figure 6, although some discrepancies remain with measured values (red).

Figure 6. Pressure and salinity in drillhole KR5 simulated using the initial model (green), with the calibrated model for two different initial salinities (blue and light blue) compared



Uncertainty and confidence assessment

The Site Descriptive Modelling involves uncertainties and it is necessary to assess the confidence in such modelling. This has been assessed through special protocols in a technical auditing exercise. These protocols investigate: whether all data have been considered and understood; where the uncertainties lie and what the potential is for alternative interpretations; whether there is sufficient consistency between disciplines and consistency with the past evolution of the site; as well as comparisons with previous model versions.

Conclusions

Overall, the uncertainty and confidence assessment demonstrates an evolving confidence in the Site Description. The main remaining challenge of the site characterisation work is to properly assess the confidence in the Site Description outside the well-characterised ONKALO volume, and to enhance the resolution of the description of the spatial variability in potential repository volumes including discrete fracture network modelling, and resulting transport properties as well as stress and rock mechanics and thermal properties.

References

Andersson J., H. Ahokas, J.A. Hudson, L. Koskinen, A. Luukkonen, J. Löfman, V. Keto, P. Pitkänen, J. Mattila, AT.K. Ikonen, M. Ylä-Mella, 2007, Olkiluoto Site Description, (2006), Report POSIVA 2007-03, Posiva Oy.

Posiva, (2005), Olkiluoto Site Description 2004, Report POSIVA 2005-03, Posiva Oy.

STUDY ON CHARACTERISATION OF QUATERNARY TECTONIC MOVEMENT BY UPLIFT ESTIMATION USING FLUVIAL TERRACES

R. Hataya¹, M. Yanagida², M. Sato³

¹Central Research Institute of Electric Power Industry, ²Hanshin Consultants Co. Ltd.,

³Hanshin Consultants Co. Ltd.; Japan

Abstract

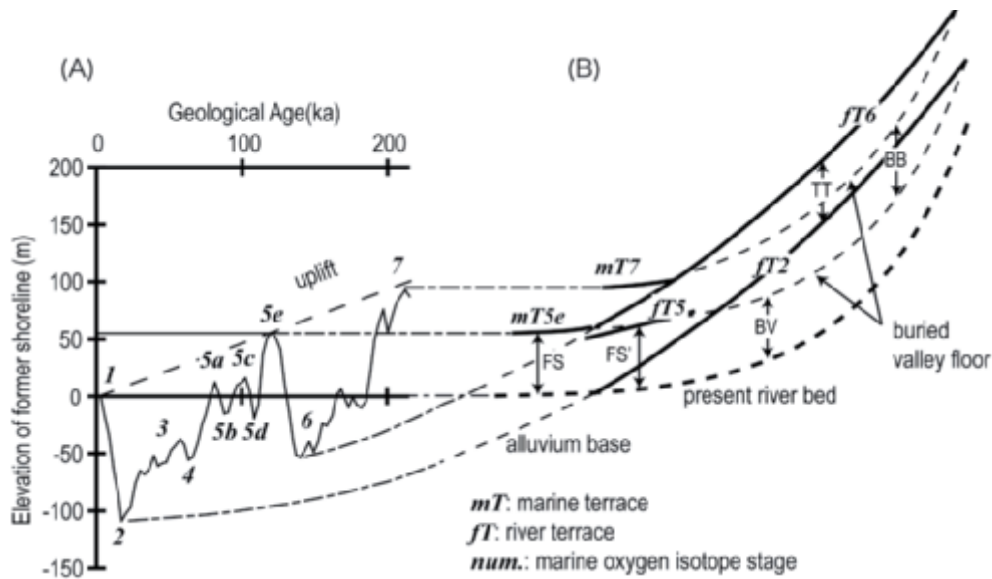
For quantitative estimation of late Quaternary uplift in an inland area, the method using fluvial terraces was proposed in previous studies. We verified this method by comparison with displacement of active faults. Furthermore, we showed that the method is available for estimating the uplift for late Quaternary in an inland area quantitatively. Hence, it enables characterisation of Quaternary tectonic movement in an inland, for example, tectonic movement of uplift/subsidence in late Quaternary. Methodology and concept proposed in this study give practical survey for the long-term safety of geological disposal of radioactive waste.

Introduction

Uplift estimation in an inland area that leave from the coast is very important for site screening and long-term safety of the geological disposal of high-level radioactive waste project. However it is delayed remarkably in comparison with those in a seaside area. For quantitative estimation of late Quaternary uplift in an inland area, the method using fluvial terraces in previous studies. It is based on the assumption that terraces are formed controlled by the cyclic glacio-eustasy, and relative height between terraces formed under the similar climate such as glacial age or inter-glacial age. In general, river profiles are steep in the glacial age and are gentle in the inter-glacial age, because they often depend on sea-level change. Yoshiyama and Yanagida (1995) defined FS, FS', TT, BV and BB values as indicators of uplift during late Quaternary (Figure 1), and concluded that TT, BB values are slightly larger and more reliable than FS' BV ones. However, reliability of TT, BB values wasn't yet proved concretely.

In this study, we verify that the fluvial terrace method is available for estimating the uplift for late Quaternary in an inland area quantitatively, using active faults. Furthermore, we discuss characterisation of Quaternary tectonic movement in an inland area by uplift estimation.

Figure 1. Uplift estimation using elevation of terraces. FS, FS', TT, BV and BB values show the quantities of uplift during late Quaternary, about 10^5 years (Yoshiyama and Yanagida, 1995). (A) Change of elevation of the former shoreline related both sea level change (Chappell, 1994) and uplift. (B) Terrace formation model (Dury, 1959; Kaizuka, 1977).



Verification of uplift estimation using fluvial terraces during late Quaternary

Method

If uplift estimation using fluvial terraces is practical, difference of uplift between hanging wall and footwall is equal to fault throw (vertical displacement) of terrace (Figure 2). So we have done geographical and geological investigation of terraces in two areas (Figure 3), which are Natori and Hirose Rivers area in Miyagi prefecture, and Naka and Hoki Rivers area in Tochigi and Ibaraki prefectures, to measure TT and BB values in both sides of active faults. TT and BB values were measured on the basis of terrace distribution maps and river profiles by our previous studies. Thickness of a covering layer on a terrace deposit was ignored. Elevations of fluvial terraces were read by 5m from 1/25 000 topographic maps of Geographical Survey of Japan.

Figure 2. Verification of uplift estimation method using fluvial terraces

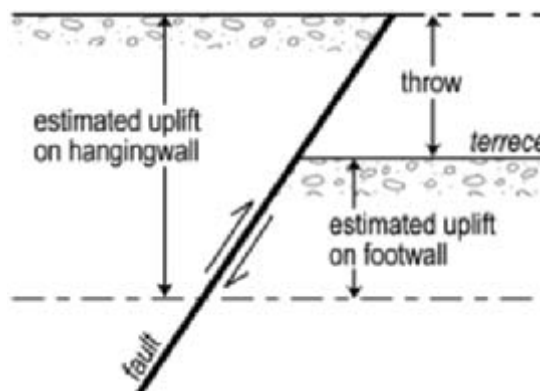
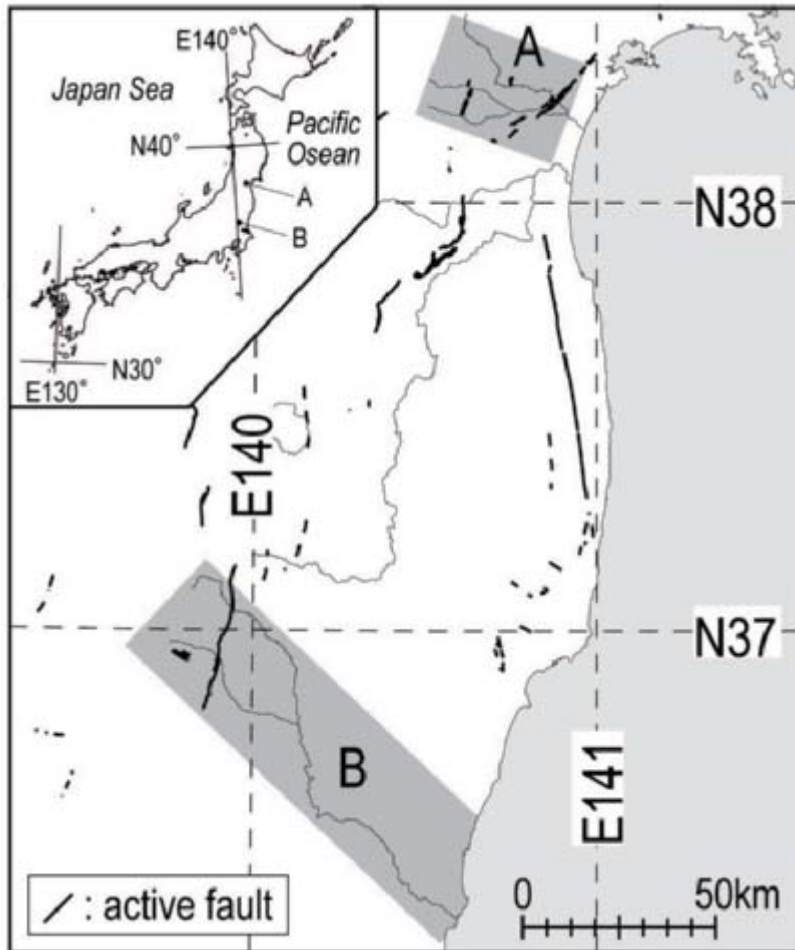


Figure 3. Study areas. A: Natori and Hirose Rivers area (Figure 5),
B: Naka and Hoki Rivers area (Figure 6)



Stratigraphic description of study areas

In Natori and Hirose Rivers area, the Ayashi fault, which is 2 km in length (The Research Group for Active Faults of Japan, 1991), is distributed. Hataya *et al.* (2005) described stratigraphic correlation and chronology of terraces along Natori River and its branches (Figure 4). We mapped out fluvial terraces along Hirose River, and carried out correlation of terraces between along Natori River and Hirose River, by air-photograph interpretation and field survey (Figure 5). As results, we could detect fluvial terraces of MIS6 and MIS3-MIS2.

Figure 4. Stratigraphic correlation and chronology of terraces in study areas. Numerical ages of Marine Oxygen Isotope Stage depend on Koike and Machida eds. (2001). Abbreviations, stratigraphic positions and fall ages of marker tephra layers, except Ac-Md (Adachi-Medeshima Pumice), MoP (Moka Pumice), are based on Machida and Arai (2003). Strayigraphic position of Ac-Md is shown by Hataya *et al.* (2005). That of MoP depends on Koike and Machida eds. (2001)

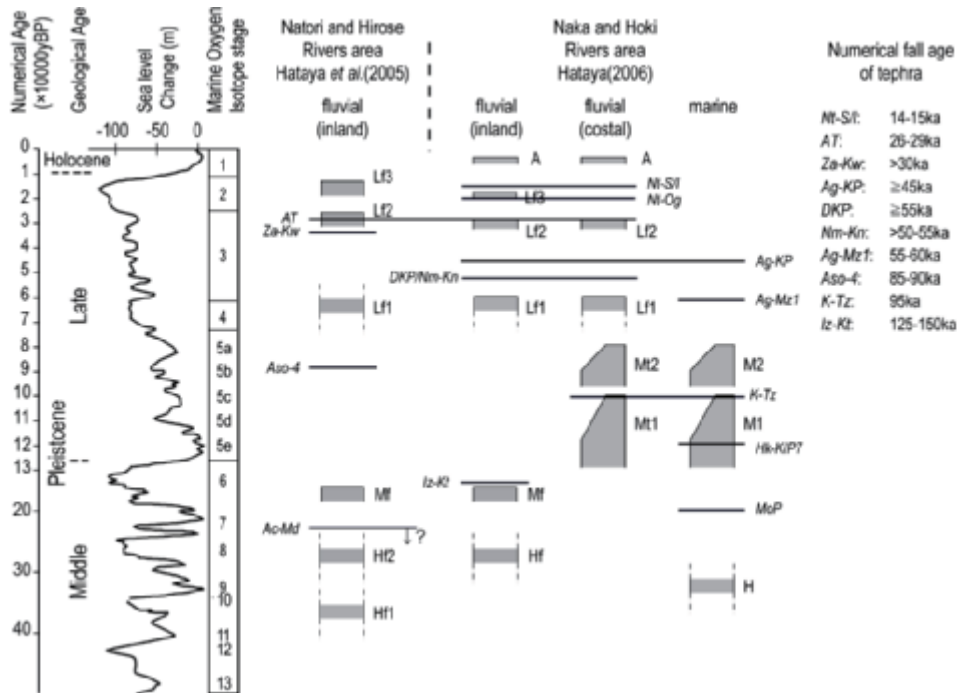
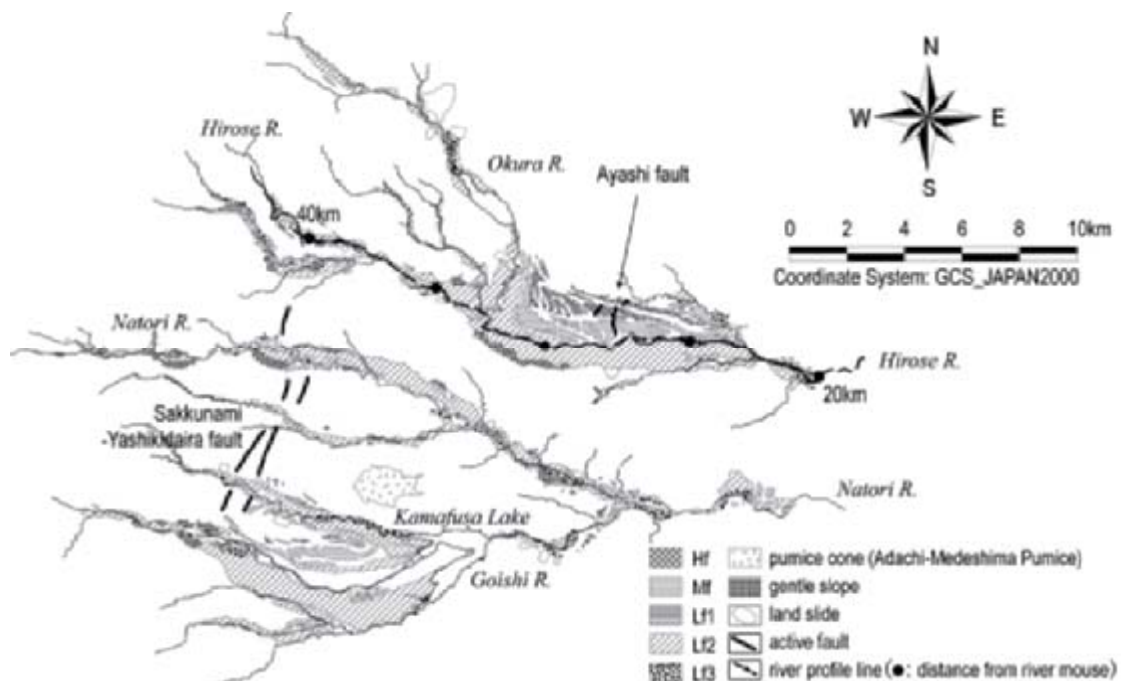
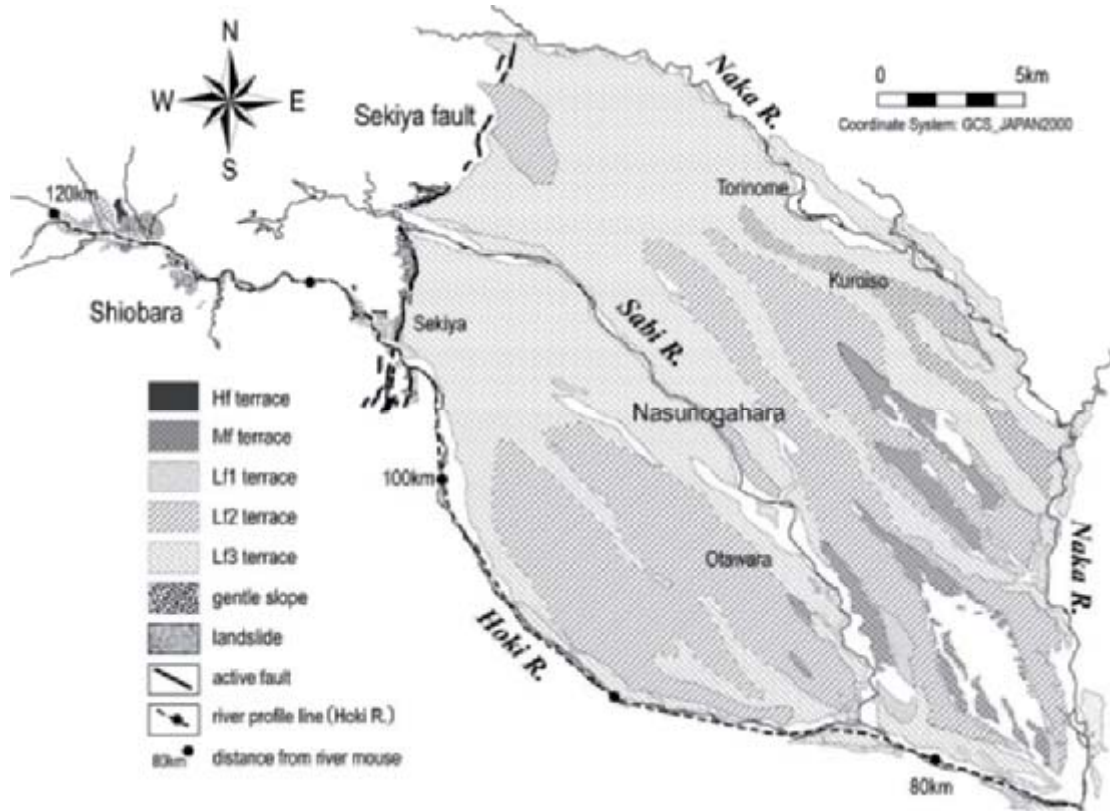


Figure 5. Distribution of terrace in the Natori and Hirose Rivers area



In Naka and Hoki Rivers area, the Sekiya fault, which is 40km in length, runs on the boundary between Nasunogahara and Shiobara districts (The Research Group for Active Faults of Japan, 1991). Hataya (2006) described stratigraphic correlation and chronology of terraces of this area and distribution of fluvial terraces of MIS6 and MIS3-MIS2 in the north part of this area (Figure 4, 6).

Figure 6. **Distribution of terrace in the North part of Naka and Hoki Rivers area (Hataya, 2006) Terrace distribution of Lf2 and Lf3 around Nasunogahara is followed Koike and Suzuki (2000)**



Results of verification of uplift estimation method using fluvial terraces

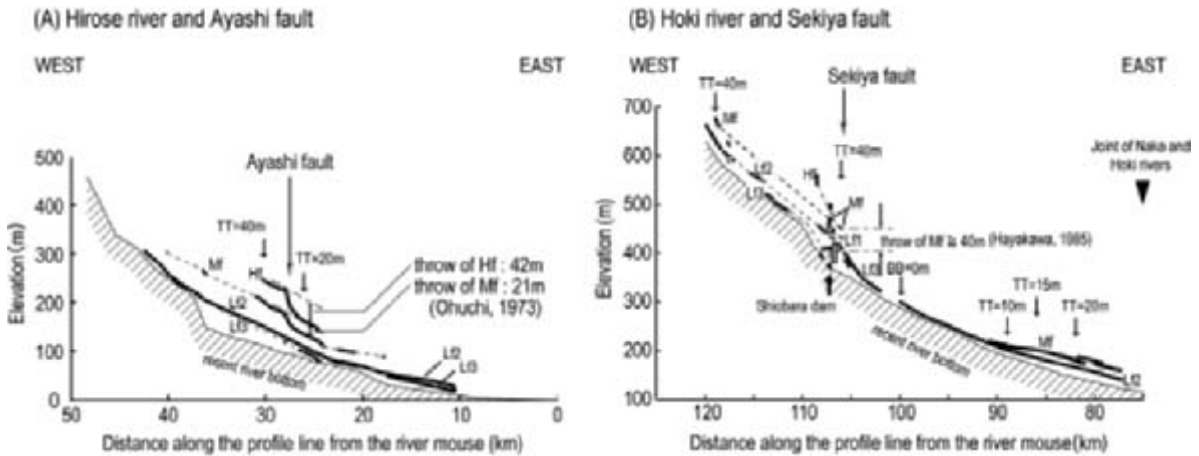
Differences of TT and/or BB values that are estimated in both sides of the Ayashi fault in Miyagi prefecture and the Sekiya fault in Tochigi Prefecture are almost equal to throws of these faults during late Quaternary (Figure 7).

Difference of TT values between hanging wall and footwall of the Ayashi fault along the Hirose River is 20 m, and the vertical slip rate was estimated with $0.2\text{m}/10^3\text{y}$. On the other hand, the throw of Ayashi fault after formation of the Mf terrace is 21m (Ouchi, 1973), and the vertical slip rate was calculated with $0.2\text{m}/10^3\text{y}$.

Near the Sekiya fault, difference of the TT values on the hanging wall is 40m, and the BB value on footwall are about 0m, and the vertical slip rate was estimated with about $0.4\text{m}/10^3\text{y}$. The vertical displacement of the Mf terrace is 40+m (Hayakawa, 1985), and the vertical slip rate was calculated with $0.3\text{m}/10^3\text{y}$.

Hence, it is concluded that relative heights of fluvial terraces surface and valley bottoms, TT and BB values, are good indicators of uplift estimation in late Quaternary in an inland area.

Figure 7. River profiles and comparison between difference of uplift and active fault throw. River profiles are along profile lines of both river shown in Figure 4 and 5.



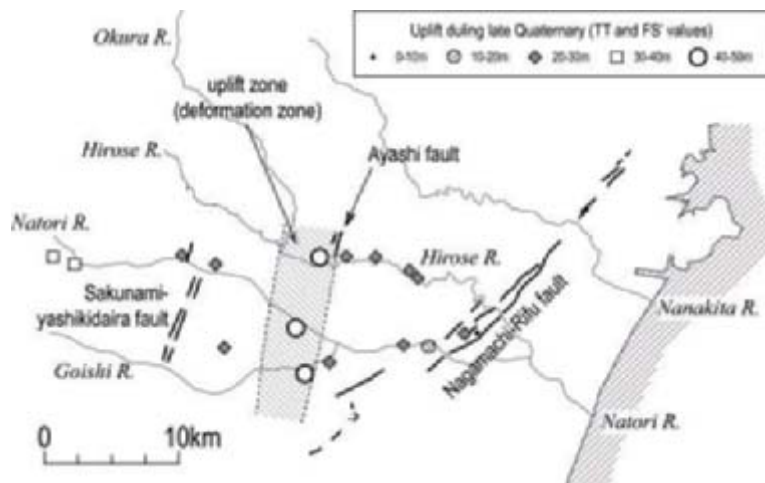
Tectonic movement in an inland area

Uplift estimation method using fluvial terraces is “long-term geodesy”. It is possible to find the geotectonic feature that were overlooked so far such as unknown active faults, de-formed zones along active fault, tectonic style of uplift and subsidence in an inland area, by obtaining the 3-dimensional distribution of uplift during late Quaternary.

Uplift zone around the Ayashi fault, Natori and Hirose Rivers area

The TT value is slightly larger in the hanging wall side of Ayashi fault. Furthermore, Hataya *et al.* (2005) shows that there are larger TT points along Natori River and Goishi River. The larger TT value zone suggests that there is an uplift zone of N-S direction (Figure 8). However, in previous studies, no tectonic relief/active fault was detected except the Ayashi fault of only 2km in length. It suggests that the uplift estimation method using fluvial terrace during late Quaternary enables to detect an unknown active structure that wasn't detected by “lineament survey” in an inland area.

Figure 8. Uplift zone detected from distribution of uplift estimated using fluvial terraces in the Natori and Hirose Rivers area



Tectonic style of uplift and subsidence

Terrace distribution in Naka and Hoki Rivers area (Figure 3) is showed by Hataya (2006). On the basis of its data, we obtained TT, BB, FS', FS values in Naka and Hoki River area (Figure 9).

Figure 9. Distribution of TT, BB, FS', FS values in Naka and Hoki Rivers area

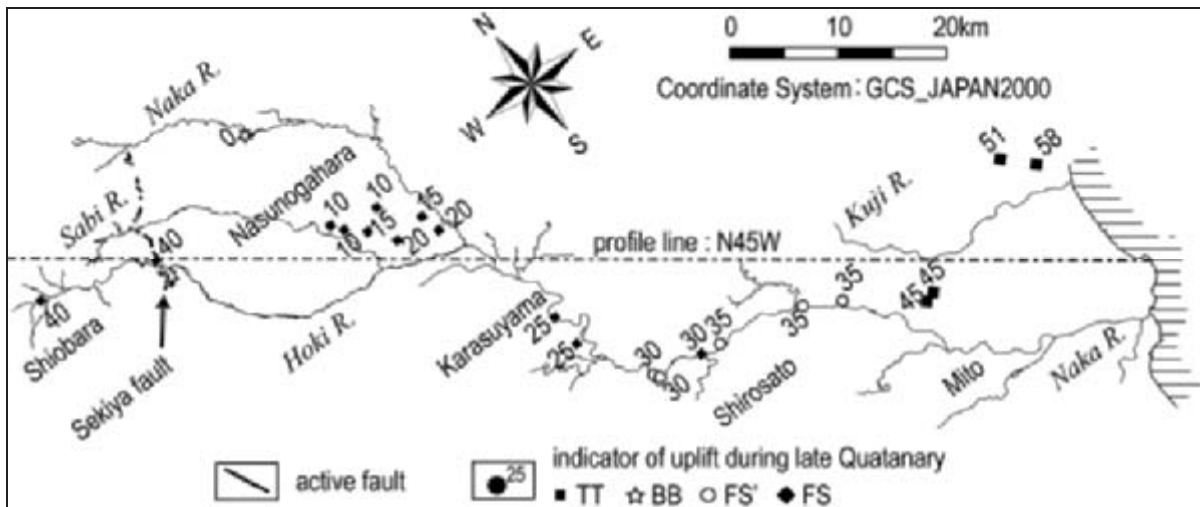
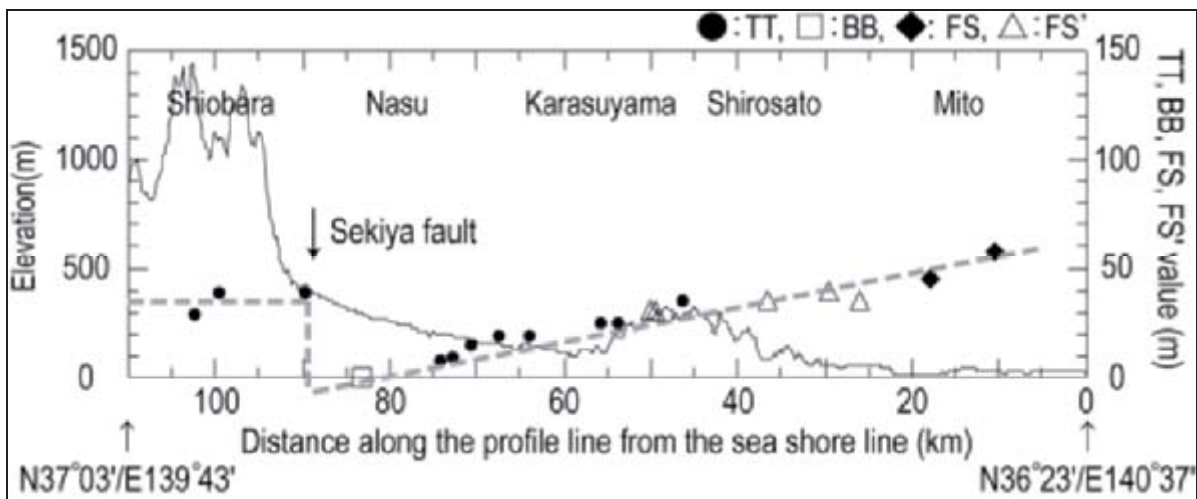


Figure 10. Tilting movement detected from distribution of uplift estimated using fluvial terraces in the Naka and Hoki Rivers area



Uplift during late Quaternary along Naka River decreases monotonously from the river mouse toward to Sekiya fault (Figure 10). It indicates that block tilting movement toward to the west and that there is a narrow subsidence area near the footwall of the Sekiya fault. Koike (1968) has shown tilting movement toward to the west during Quaternary by discussing distribution and stratigraphy of uplift peneplains. Our result is conformable to his conclusion. Furthermore, it shows that block tilting movement continues from early Quaternary to the recent, and gives new information, a quantitative tilting rate during late Quaternary.

Summary

Uplift/subsidence is a key process affecting the geosphere stability of host rock. In this study, we can verify the estimation method of uplift during late Quaternary using fluvial terraces. Furthermore, the method enables to discuss unknown active structures and tectonic style inland area during Quaternary. Methodology and concept proposed in this study give practical survey method of late Quaternary 3-dimensional uplift characteristics to evaluate the long-term stability of host rock for geological disposal of high-level radioactive waste. By applying this method to Quaternary research, new insights on the Quaternary tectonic movement may be given.

Acknowledgement

We would like to express our sincere thanks to Prof. Kazuhiro Tanaka of Yamaguchi University for his useful discussion and advice. Also we are grateful to Dr. Kenzo Kiho of Central Research Institute of Electric Power Industry for his critical reading of our manuscript.

Reference (* in Japanese with English abstract, ** in Japanese)

Chappell, J., (1994), *Upper Quaternary sea level coral terraces, oxygen isotopes and deep sea temperatures*, Journal of Geography, vol.103, pp.828-840.

Dury, G. H., (1959), *The face of earth*. Penguin Books, Harmondsworth, 225p.

Hataya R., (2006), *Study on the estimation method of uplift during the late Quaternary by using river terrace (2)*, CRIEPI Report, N05016, 30p (*).

Hataya, R., M. Yanagida, M. Sato, and T. Sasaki, (2005), *Recognition of the marine oxygen Isotope stage 6 fluvial terrace in Kawasaki Basin, Miyagi Prefecture, and its significance*. Quaternary Research, vol.44, pp.155-167 (*).

Hayakawa T., K. Hirose and M. Noguchi, (1985), *Development of fluvial terraces along upperstream of Hoki River, Tochigi prefecture, Japan*. Bulletin of the college of Education, Ibaraki University, Natural Science, vol. 34, pp.1-20 (*).

Kaizuka, S., (1977), *Nihon no Chikei*, 234p, Iwanami Shoten (**).

Koike, K., (1968), *Geomorphological developments of North Abukuma Mountains*. Komazawa Geography, vol.4&5(merger), pp.109-126 (*).

Koike, K. and T. Suzuki, (2000), Kinugawa lowland. Kaizuka S., Koike, K., Endo. K., Yamasaki, H. and Suzuki, T. eds., *Regional Geomorphology of Japan Islands*, vol. 4 Geomorphology of Kanto and Izu-Ogasawara, pp.172-183, University of Tokyo Press (**).

Koike, K. and H. Machida, (2001), *Atlas of Quaternary marine terraces in Japanese Islands*, 122p, University of Tokyo Press (**).

Machida, H. and Arai F. (2003) *Atlas of tephra in and around Japan*, 336p, University of Tokyo Press (**).

Ouchi, Y., (1973), *River terraces and their displacements along the Hirose River, Miyagi Prefecture*. Annals of the Tohoku Geographical Association, vol.25, pp.84-90 (*).

The Research Group for Active Faults of Japan, (1991), *Active fault in Japan*, 438p, University of Tokyo Press (*).

Yoshiyama, A. and M. Yanagida, (1995), *Uplift rate estimated from relative heights of fluvial terraces surfaces and valley bottoms*. *Journal of Geography*, vol.104, pp.809-826 (*).

EXAMINATION OF EARTHQUAKE GROUND MOTION IN THE DEEP UNDERGROUND ENVIRONMENT OF JAPAN

J. Goto¹, H. Tsuchi¹, M. Mashimo²

¹Nuclear Waste Management Organization of Japan (NUMO)

²Tokyo Electric Power Services Co., Ltd. (TEPSCO)

Abstract

Among the possible impacts of earthquakes on the geological disposal system, ground motion is not included in the criteria for selecting a candidate repository site because, in general, ground motion deep underground is considered to be smaller than at the surface. Also, after backfilling/closure, the repository moves together with the surrounding rock. We have carried out a detailed examination of earthquake ground motion deep underground using extensive data from recent observation networks to support the above assumption. As a result, it has been reconfirmed that earthquake ground motion deep underground is relatively smaller than at the surface. Through detailed analysis of data, we have identified the following important parameters for evaluating earthquake ground motion deep underground: depth and velocity distribution of the rock formations of interest, the intensity of the short period component of earthquakes and incident angle of seismic waves to the rock formations.

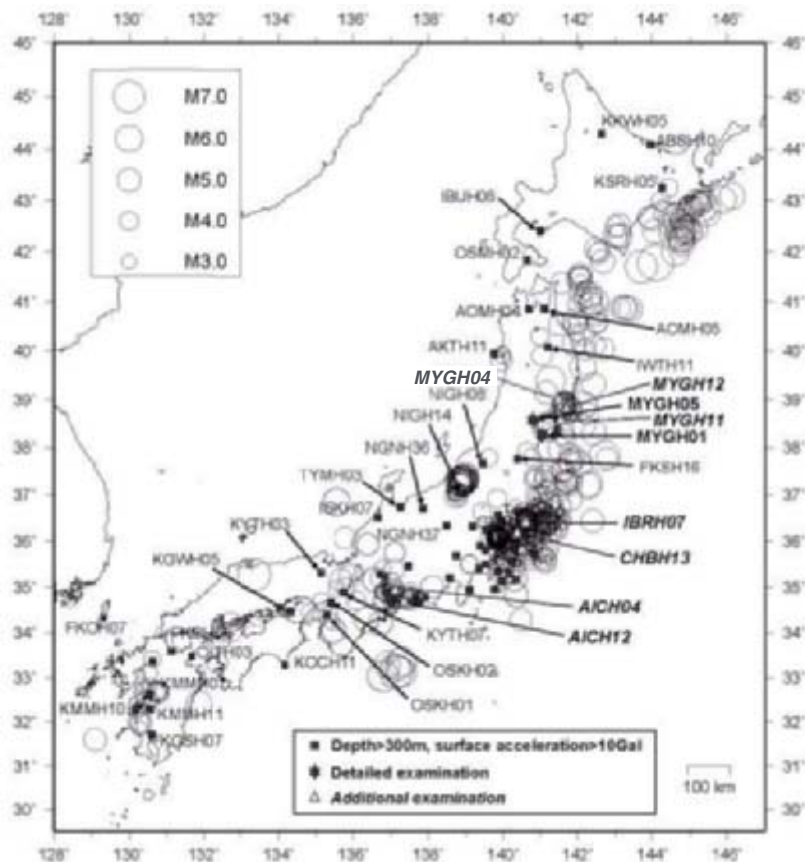
Introduction

NUMO – the Nuclear Waste Management Organization of Japan – was established in October 2000 on the basis of the Specified Radioactive Waste Final Disposal Act (the Act) promulgated in June 2000. In this Act, NUMO is given the clearly defined remit to develop a project for the safe disposal of vitrified high-level radioactive waste. In October 2001, NUMO presented a stepwise programme for selecting a repository site through Literature Surveys based on existing literature information, Preliminary Investigations involving surface-based field testing and, finally, Detailed Investigations with excavation of shafts and tunnels. A call was sent out for volunteers as potential areas for the Literature Surveys to all 3 239 municipalities in Japan in December 2002. The call was accompanied by a document on the Siting Factors used for selecting the sites for Preliminary Investigations, with explicit specification of exclusion criteria and other favorable factors (NUMO, 2002). A technical report (NUMO, 2004) was also published which provides the scientific background for the Siting Factors based on recent technical input from, for example, JNC (2000) and JSCE (2001). In parallel with these activities, NUMO has been carrying out research and development programmes to establish and improve its technical basis for siting and constructing a deep repository.

Japan is located in a subduction/convergent zone of several continental and oceanic plates and is one of the most tectonically active areas in the world. The possible impacts of earthquakes on the geological disposal system are displacement/deformation of geological formations due to faulting, earthquake ground motion, and changes in groundwater flow and hydrochemical properties. Of these, earthquake ground motion is not included in the Siting Factors for the reason that the ground motion deep underground is generally smaller than at the surface (e.g. JNC, 2000) and the safety of a deep

repository during operations can be assured by appropriate earthquake-resistant design; after backfilling and closure, the repository moves together with the surrounding rock. This assumption is based on relatively limited data on the deep underground compiled up to the 1990s. Considerable development of the earthquake observation networks in recent years has provided an abundance of reliable data on the deep underground environment. Technologies for the analysis and evaluation of earthquake ground motion have also been improved in the area of seismic hazard prevention and nuclear safety assessment in recent years (e.g. Headquarters for Earthquake Research Promotion, 2001 and Nuclear Safety Commission, 2006). We therefore conducted a detailed examination of ground motion in the deep underground environment by comparing it with motion at the surface, and by conducting an analytical study which assumes the repository to be a construction project with many open spaces. This paper presents the results of the former study.

Figure 1. Location of sites and earthquakes for examination



Examination and results

Examination of general trends using a nation wide published database

On its home page, National Research Institute for Earth Science and Disaster Prevention (NIED) provides acceleration data collected using a nation wide Digital Strong-Motion Seismograph Network (KiK-net). For the initial examination, we selected 69 sites where the depths of seismometers are greater than 300 m and used 861 earthquake data for which the maximum acceleration is more than 10 Gal (Figure 1). The correlation between the ratio of maximum acceleration underground and at the surface, hereafter the “maximum acceleration ratio (underground/surface)”, and parameters such as

seismometer depth, depth of hypocenter, distance from hypocenter, seismic rock properties (seismic wave velocities and specific period) were examined. The trend of the ratio of the response spectrum underground to that at the surface, hereafter “response spectral ratio (underground/surface)”, is also examined for seven sites where more than thirty earthquakes have been recorded and the rock properties are well described.

In most cases, the maximum acceleration ratio (underground/surface) is less than 1, indicating that the maximum acceleration underground is smaller than at the surface (Figure 2). The horizontal maximum acceleration ratio (underground/surface) decreases with increasing distance from the hypocenter, implying that the further away earthquakes are, the closer to vertical the seismic waves arrive and the more amplified the ground motion is in the rock formations. The response spectral ratios for both horizontal and vertical movement underground are smaller than at the surface. The ratio increases towards the longer period side, indicating that the longer period component is less amplified in the rock formations (Figure 3).

Figure 2. Maximum acceleration ratio (underground/surface) relative to distance from the hypocenter

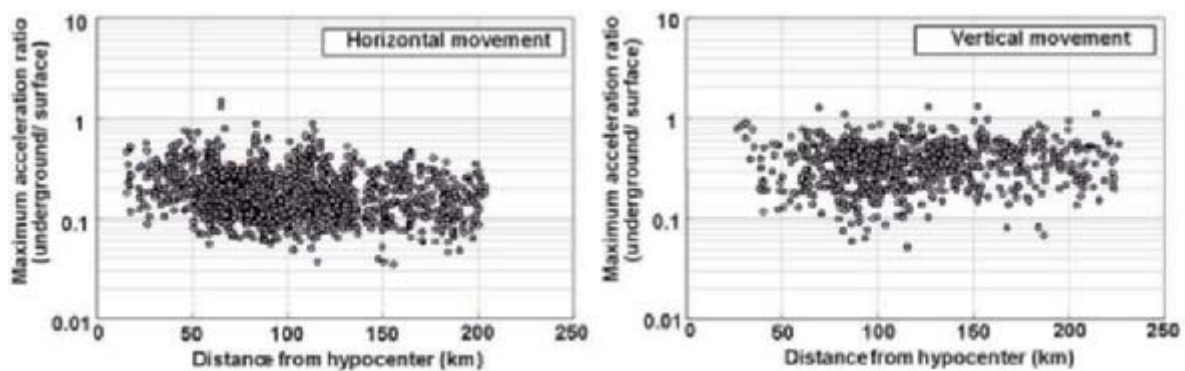
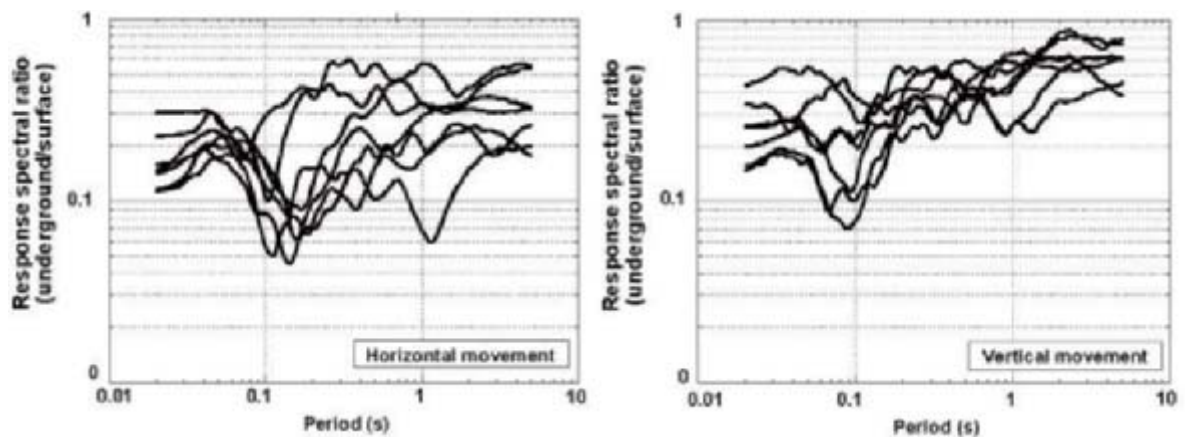


Figure 3. Response spectral ratio (underground/surface)



Detailed examination of cases where the maximum acceleration underground exceeds that at the surface

A detailed examination was carried out to understand the reason for an increase in the maximum acceleration ratio (underground/surface). One of the sites, MYGH 01, where the maximum acceleration underground exceeds that at the surface, was characterised in detail by comparing it with

an adjacent “normal” site, MYGH 05, which does not show such an increase in earthquake ground motion. The correlation between the maximum acceleration ratio (underground/surface) and parameters such as distance from hypocenter, depth of hypocenter and magnitude was investigated, and wave pattern and response spectral ratios were examined for each site. The relationship between maximum acceleration ratio (underground/surface) and velocity and incident angle of the seismic wave was also investigated. The incident angle was derived by constructing a rock formation model and using Snell’s law.

At MYGH 01, the following characteristics have been identified. Earthquakes with large maximum acceleration ratios typically have a shorter distance to the hypocenter, a smaller magnitude, a more abundant short period component of the response spectral ratio and pulse-like wave patterns compared to others (see the left side of Figures 4 to 6). The shear wave velocity of 3 260 m/s at the depth of the seismometer is equivalent to that of the seismic bedrock. The incident angles of earthquakes are distributed over a wide range (Figure 7, left). Earthquakes which have larger maximum acceleration ratios (underground/surface) tend to be concentrated at an incident angle around 60° from the vertical.

At MYGH 05, on the other hand, the following characteristics are found. The maximum acceleration ratio (underground/surface) is almost constant irrespective of hypocenter distance, hypocenter depth and earthquake magnitude, and a pulse-like wave pattern is rare (see the right side of Figures 4 to 6). The shear wave velocity of 690 m/s at the depth of the seismometer is very small compared to the seismic bedrock. The incident angle of the seismic waves is close to vertical and a correlation with the maximum acceleration ratio (underground/surface) is not obvious (Figure 7, right).

Figure 4. Maximum acceleration ratio (underground/surface) relative to distance from the hypocenter

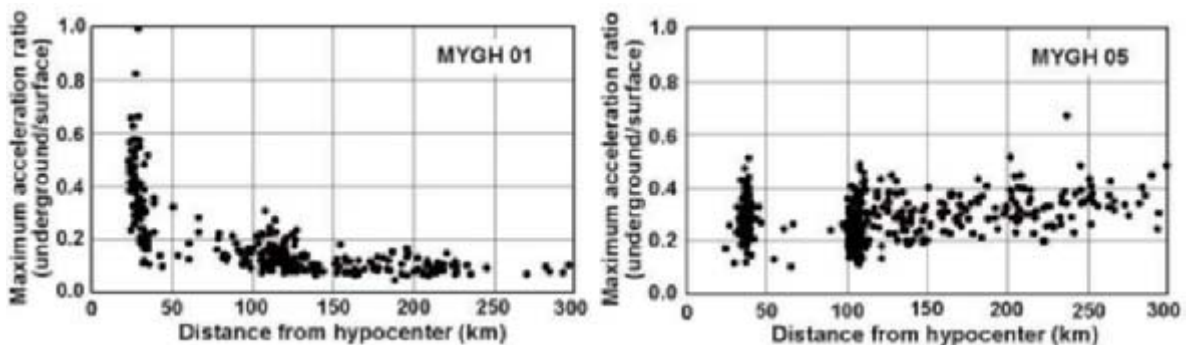


Figure 5. Response spectral ratio (underground/surface)

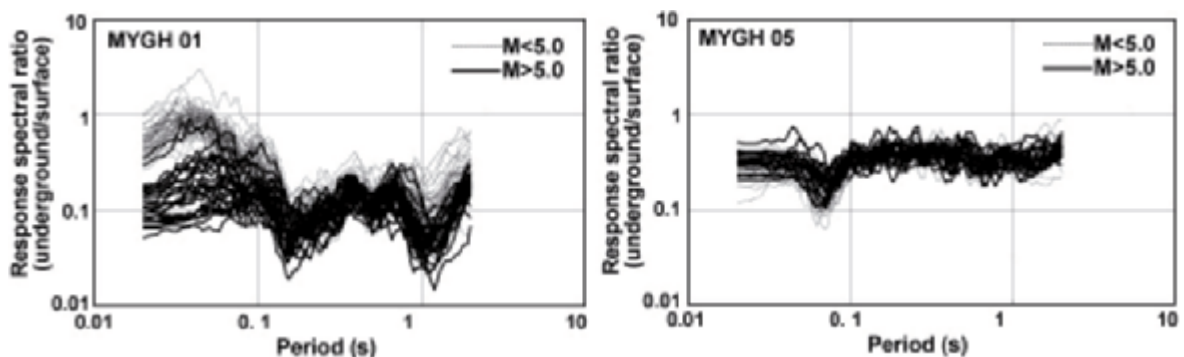


Figure 6. Seismic waves of a small earthquake at the surface and underground

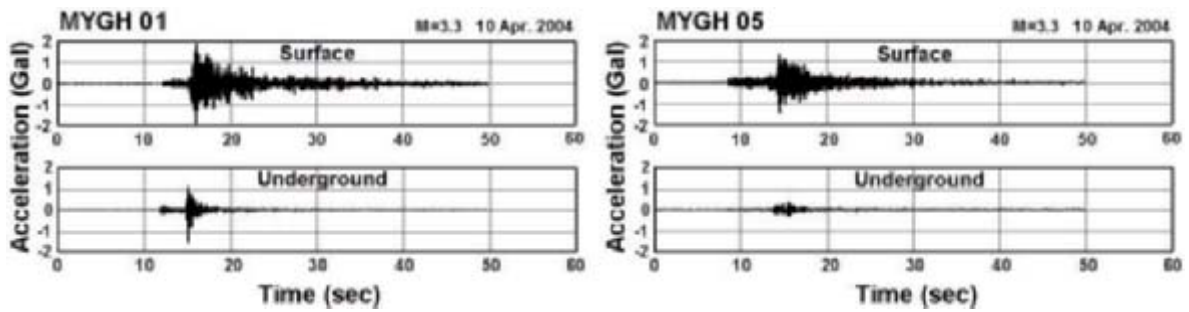
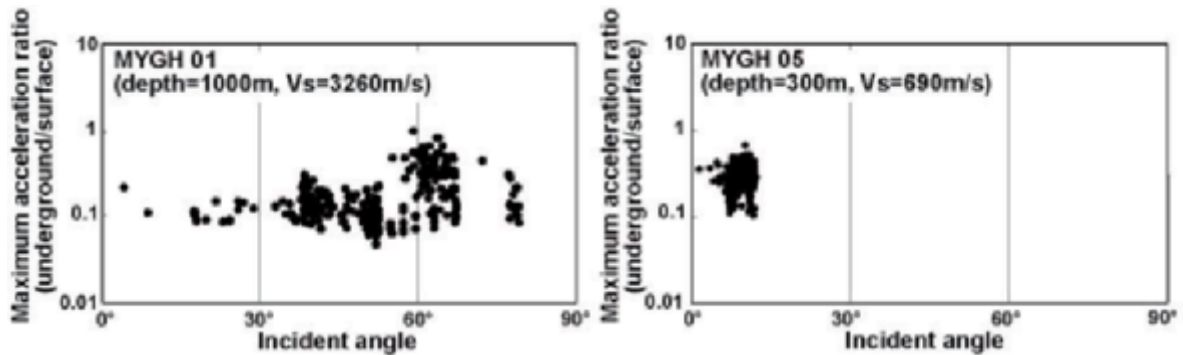


Figure 7. Maximum acceleration ratio (underground/surface) relative to incident angle



Based on these findings, the cause of the increase in the maximum acceleration ratio (underground/surface) is hypothesized to be as follows. At a site where a seismometer is located in deep rock formations with a shear wave velocity equivalent to that of the seismic bedrock, and when an earthquake with an abundant short period component comes in at a high incident angle to the vertical, the short period component wave may be decayed by reflection and dispersion before it reaches the surface, resulting in a higher maximum acceleration ratio (underground/surface) compared to cases with a lower incident angle.

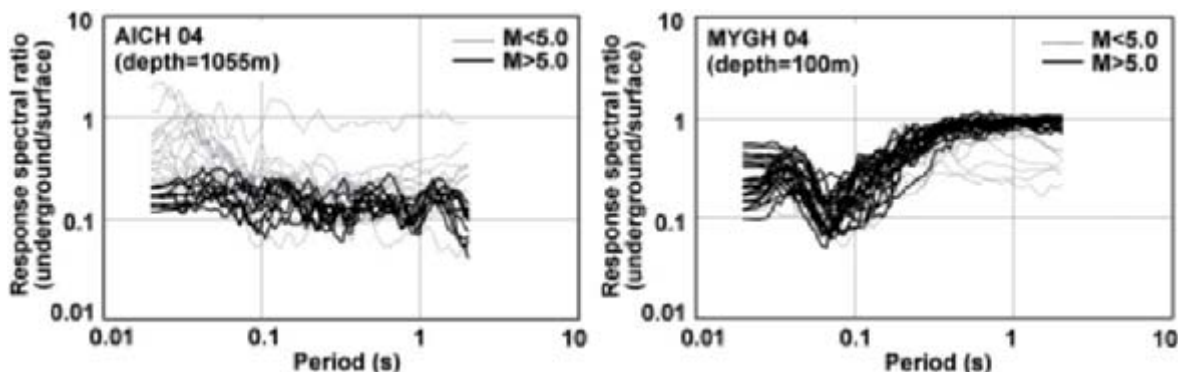
Verification of the hypothesis regarding the higher maximum acceleration ratio (underground /surface)

To verify the above hypothesis, an additional examination of the earthquake data from the KiK-net was carried out. Of the nation wide observation stations, two groups of sites were selected to assess the effect of different seismometer depths. One is a group of four sites, AICH 04, AICH 12, CHBH 13 and IBRH 07 (Figure 1) where the depths of the seismometers are greater than 400 m, the shear wave velocities are greater than 2.5 km/s equivalent to the seismic bedrock, and the maximum acceleration ratio (underground/surface) is high. The other group of the three sites, MYGH 04, MYGH 11 and MYGH 12 (Figure 1) which is close to MYGH 01 described in the previous section, and has seismometers at relatively shallow depths between 100-200 m from the surface but with shear wave velocities greater than 2.5 km/s. Both the maximum acceleration ratio (underground/surface) and the response spectral ratio (underground/surface) were compared with seismometer depth, period of ground motion and earthquake magnitude. The incident angles of the earthquakes were also calculated and compared with the maximum acceleration ratio (underground/surface). In addition, the relationship between incident angle and amplification in the rock formations (transmission function)

was investigated. Theoretical transmission functions were derived by constructing rock formation models and using a one-dimensional wave transmission analysis.

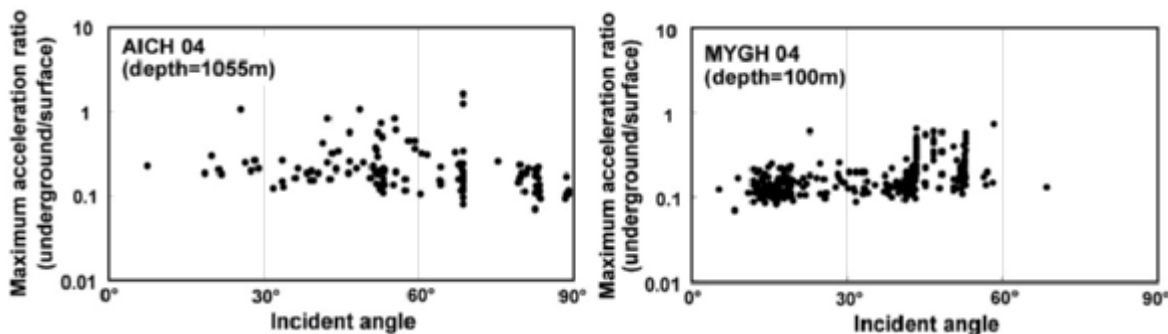
At all four sites with deep seismometers, it was confirmed that the response spectral ratio (underground/surface) is close to 1 at the short period side for earthquakes with a magnitude less than 5. Figure 8 (left) shows the case of AICH 04 as an example. On the other hand, at all three sites with shallow seismometers, the response spectral ratio (underground/surface) does not show any difference between larger and smaller earthquakes, and is generally at around 0.5. Figure 8 (right) shows the case of MYGH 04 as an example.

Figure 8. Response spectral ratio (underground/surface) for different seismometer depths



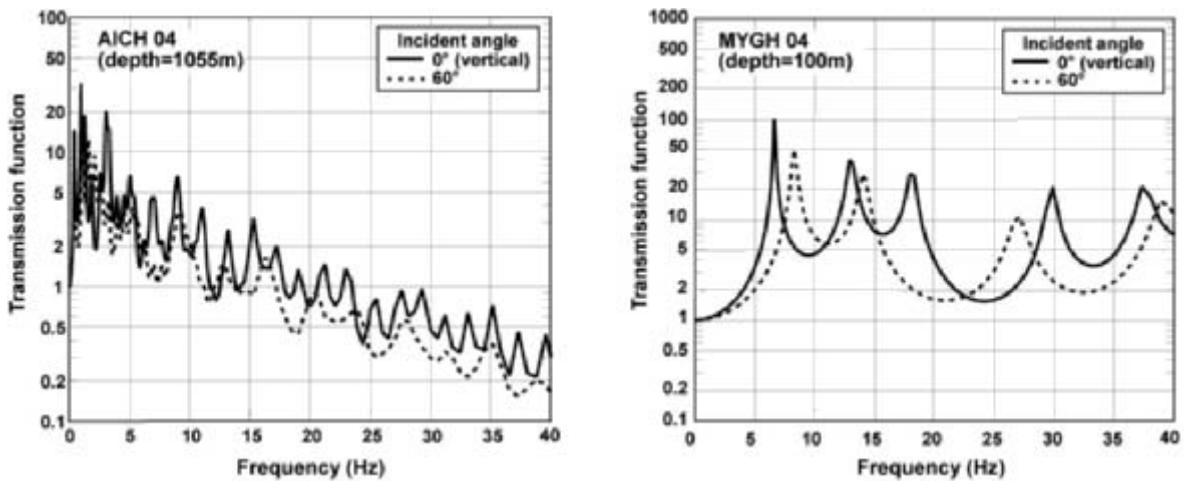
With respect to the incident angles of earthquakes, these tend to be distributed over a wide range irrespective of seismometer depth, and the angles for which the maximum acceleration ratio (underground/surface) is high are different at each site. Figure 9 shows the cases of AICH 04 and MYGH 04 as examples from the two groups.

Figure 9. Maximum acceleration ratio (underground/surface) relative to incident angle



From the analytical examination of the relationship between incident angle and transmission function, the following results are obtained. At the four sites with deep seismometers, the transmission function decreases with increasing frequency and becomes less than 1, indicating a larger decay of the shorter period component in the rock formation. It is noted that the transmission function at an incident angle of 60° is generally smaller than for vertical incidence at all four sites. Figure 10 (left) shows the case of AICH 04 as an example. At the three sites with shallow seismometer depth, the decay in the shorter period is small, indicated by a transmission function larger than 1. The difference in the incident angle is not obvious for all three sites. Figure 10 (right) shows the case of MYGH 04 as an example.

Figure 10. One-dimensional wave motion analysis for different insert angles



The hypothesis is consistent with the results of examinations using data from other sites and with model analyses, thus supporting its validity.

Conclusions

Recent nation-wide earthquake data were examined to characterize ground motion deep underground. The results are summarized as follows. (1) The general understanding that earthquake ground motion (maximum acceleration and response spectra) deep underground is relatively smaller than at the surface is reconfirmed. (2) At a site where the shear wave velocity of the rock formation is equivalent to that in the seismic bedrock, the incident angles will be distributed widely and ground motion deep underground relative to the surface may be larger for a certain incident angle range, depending on the type of earthquake. (3) At a site where the rock formation of interest is deep and has a high shear wave velocity, when an earthquake with a predominantly shorter period component occurs, the shorter component may be more decayed through transmission, resulting in relatively larger ground motion underground than at the surface. (4) At a site where the rock formation of interest is deep and has a high shear wave velocity, when an earthquake with a predominantly shorter period component occurs close to the site and the incident angle is high from the vertical, ground motion deep underground will be relatively larger than at the surface. (5) Based on (2) to (4) above, the important parameters for evaluating earthquake ground motion deep underground are considered to be depth and velocity distribution of the rock formations of interest, the intensity of the short period component of the earthquakes, and the incident angle of the seismic waves to the rock formations.

Acknowledgement

We thank the National Research Institute for Earth Science and Disaster Prevention (NIED) for providing us with extensive and detailed data for this study.

References

JNC, (2000), *H12: Project to Establish the Scientific and Technical Basis for HLW Disposal in Japan*, Project Overview Report, 2nd Progress Report on Research and Development for the Geological Disposal of HLW in Japan, JNC Technical Report TN1410 2000-001, Japan Nuclear Cycle Development Institute, Tokai-mura, Japan.

JSCE, (2001), *Geological Factors to be Considered in the Selection of Preliminary Investigation Areas for HLW Disposal*, Sub-Committee on the Underground Environment, Civil Engineering Committee of the Nuclear Power Facilities, Japan Society of Civil Engineers (in Japanese).

NUMO, (2002), *Information Package for Open Solicitation of Volunteers for Areas to Explore the Feasibility of Constructing a Final Repository for High-Level Radioactive Waste*, 3, Siting Factors for the Selection of Preliminary Investigation Areas, Nuclear Waste Management Organization of Japan, Tokyo, Japan.

NUMO, (2004), *Evaluating Site Suitability for a HLW Repository, Scientific Background and Practical Application of NUMO's Siting Factors*, NUMO-TR-04-04, Nuclear Waste Management Organization of Japan, Tokyo, Japan.

Headquarters for Earthquake Research Promotion, (2001), *A Methods of Evaluating Strong Ground Motion Assuming the Northern and Middle Part of Itoigawa-Shizuoka Tectonic Line Fault Zone as a Seismic Source Fault (Interim Report)*, Subcommittee for Evaluation of Strong Ground Motion, Earthquake Research Committee, Headquarters for Earthquake Research Promotion (in Japanese).

Nuclear Safety Commission, (2006), *A Guideline for Assessment of Earthquake-resistant Design for Light Water Reactors for Power Generation*, Nuclear Safety Commission (in Japanese).

FREQUENCY OF FAULT OCCURRENCE AT SHALLOW DEPTHS DURING PLIO- PLEISTOCENE AND ESTIMATION OF THE INCIDENCE OF NEW FAULTS

H. Shiratsuchi¹, S. Yoshida²
¹TEPCO, ²CRIEPI; Japan

Abstract

It is required that buried high-level radioactive wastes should not be broken directly by faulting in the future. Although a disposal site will be selected in an area where no active faults are present, the possibility of new fault occurrence in the site has to be evaluated. The probability of new fault occurrence is estimated from the frequency of faults which exist in Pliocene and Pleistocene strata distributed beneath 3 large plains in Japan, where a large number of seismic profiles and borehole data are obtained.

Estimation of the frequency of faults having occurred and/or reached at shallow depth during Plio-Pleistocene time.

The frequency of fault occurrence was estimated by counting the number of faults that exist in Plio-Pleistocene strata that are widely distributed in large plains in Japan. Three plains, Kanto, Nobi and Osaka Plains (Figure 1) are selected for this purpose because highly precise geological profiles, which were prepared from numerous geological drillings and geophysical investigations, are available in them.

Figure 1. Location of Three Plains

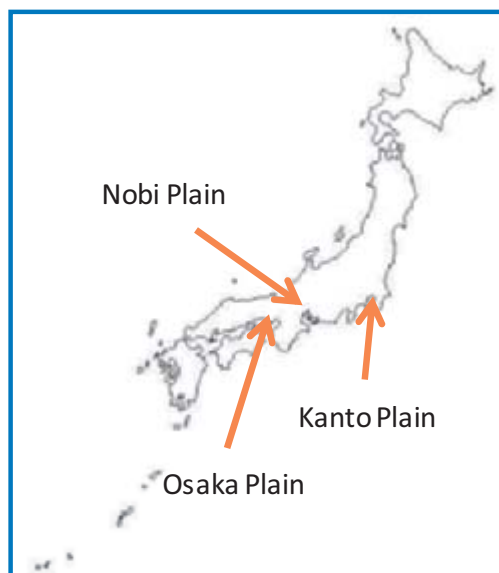
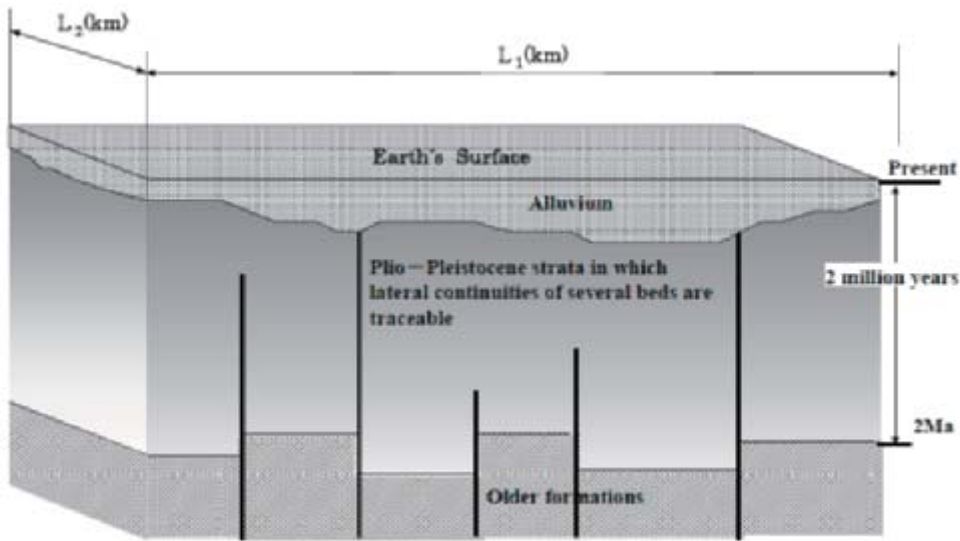


Figure 2. Method of estimation of the fault frequency per unit time and unit area



Formations older than Pliocene were excluded from this study because they have such complicated structures as folding, minor faulting, tilting, and so on. As is shown in Figure 2, five faults have occurred during 2 million years within the area ($L_1 \times L_2$) and consequently the fault frequency is estimated to be [5 faults per 2 million years and per ($L_1 \times L_2$)]

As is shown in Table 1, the frequencies of fault in the Kanto, Nobi and Osaka plains were estimated to be extremely infrequent at between 0.0008 faults to 0.0401 faults per 0.1 m.y. and per 10 km^2 .

Table 1. Fault Frequencies (Number of faults/0.1m.y/10km²)

The study area	Reference	Number of faults	Area (km ²)	Geological age (Ma)	Fault frequencies
Kanto Plain	"The Report of Geological Structure Investigation of Tokyo Bay," JGS, 1984	7	350	2.20	0.0091
	"The Report of Geological Structure Investigation in Kanto Plain (The Western Part of Chiba Prefecture)," JGS, 2001	2	400	2.20	0.0023
	"The Report of Geological Structure Investigation in Chiba Prefecture" JGS, 2001				
Nobi Plain	"The Report of Geological Structure Investigation in Nobi Plain," 2001	1	250	5.2	0.0008
	"Geological Cross Sections in Nobi Plain," JGS, 1987	1	400	0.78- 0.80	0.0032- 0.0031
	"Geology of The Southern Part of Nagoya," GSJ, 1986	1	195	0.25- 0.35	0.0205- 0.0147
Osaka Plain	"Geological Cross Sections in Osaka Plain," JGS, 1998	3	576	0.13	0.0401

Estimation of the incidence of new faults occurring at shallow depths

We checked the relationship between earthquake frequency and fault frequency. Table 2 shows the number of earthquakes in the past 75 years in the 3 plains, and shows calculated earthquake frequencies for 0.1 m.y. Earthquakes are caused by faulting. The fault frequencies in Table 1 and the earthquake frequencies in Table 2 differ largely. It is inferred from this evidence that almost all faults earthquakes-generated do not reach shallow depths.

Table 2. **Records of earthquake frequency in the study area**

Items	Kanto Plain	Nobi Plain	Osaka Plain
Total of earthquakes larger than magnitude 3 in the past 75 years	91	92	25
Area (km ²)	2,520	1,575	1,215
Frequency of earthquakes larger than magnitude 3 (number of earthquakes / 0.1m.y/ 10km ²)	478	774	294

We investigated the relationship between depth of hypocenters and scale of faults, using the Uzu and Matsuda formulae shown in Table 3. As is shown in Figure 3, the earthquake data of Tokyo Bay during the past 22 years were used for the study. Figure 4 shows the relationship between the depths of hypocenter and the earthquakes larger than magnitude 3.

Earthquakes larger than magnitude 3 have occurred 16 times in total during the past 22 years. From the relationship between the depth of hypocenter and the scale of a fault that is obtained from the magnitude of an earthquake, it is concluded that the upper limit of all faults that generated earthquakes is deeper than 1km. In other words, it can be said that the faults related to the 16 earthquakes did not reach near the ground surface. As has been shown, from the relationship between the depth of hypocenter and the scale of earthquake, it is obvious that the probability that earthquake-generating faults reach near the ground surface is extremely small. This is the reason, why a large difference is present between the frequency of earthquake occurrence and the frequency of fault occurrence near the ground surface.

Conclusion

The study also reviewed new methods using existing materials in order to grasp an overall understanding of the frequency of the existence of faults near the earth's surface at a depth shallower than 1km or less. The areas studied are not particular in seismicity, fault activity and geological structure. Therefore, the frequency of fault occurrence obtained from this study probably represents a typical value for the frequency of fault occurrence distributed near the earth's surface throughout Japan.

The crustal movements in the Japanese Islands are fundamentally controlled by plate motions. The plate motions around the Japanese Islands have been almost stable and constant since about 10 Ma and will make no large change for the coming 100 000 years. Accordingly, we can certainly expect that the overall status of tectonic stress in the vicinity of the Japanese Islands will change little; the frequency of new fault occurrences in the shallow depths will be as small as the above estimation during the next 100 000 years or more.

Table 3: Earthquake magnitudes and fault scales

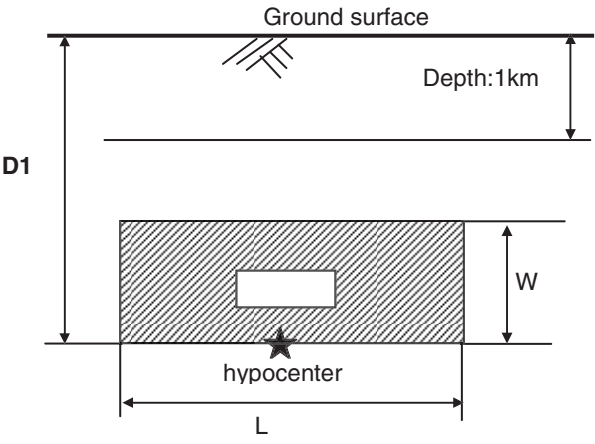
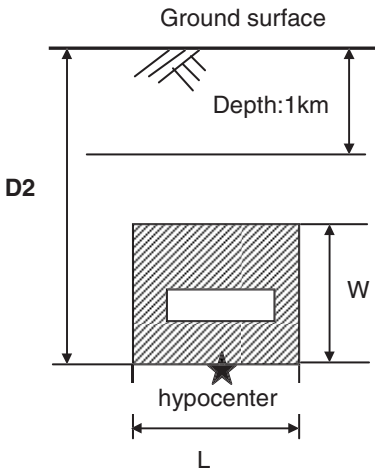
Magnitude	The formulae proposed by Uzu				The formulae proposed by Matsuda	
	Fault area (S:km ²) logS=1.0M-3.9	<i>Fault length</i> (L:km) logL=0.5M-1.8	Fault width (W:km) W=S/L	Critical depth of hypo-center (D1:km) (D1=W+1)	<i>Fault length</i> (L:km) logL=0.6M-2.9	Critical depth of hypo-center (D2:km) (D2=L+1)
3.0	0.13	0.50	0.26	1.3	0.080	1.08
3.5	0.40	0.89	0.45	1.5	0.16	1.16
4.0	1.3	1.6	0.81	1.8	0.32	1.32
4.5	4.0	2.8	1.4	2.4	0.63	1.63
5.0	13	5.0	2.6	3.6	1.3	2.3
5.5	40	8.9	4.5	5.5	2.5	3.5
6.0	130	16	8.1	9.1	5.0	6.0
6.5	400	28	14	15	10	11
Remarks						
	<p>D1,D2: Faults having generated earthquakes with hypocenters shallower than D may reach depths shallower than 1km</p>					

Figure 3. Epicenter map in study area (The Tokyo Bay)

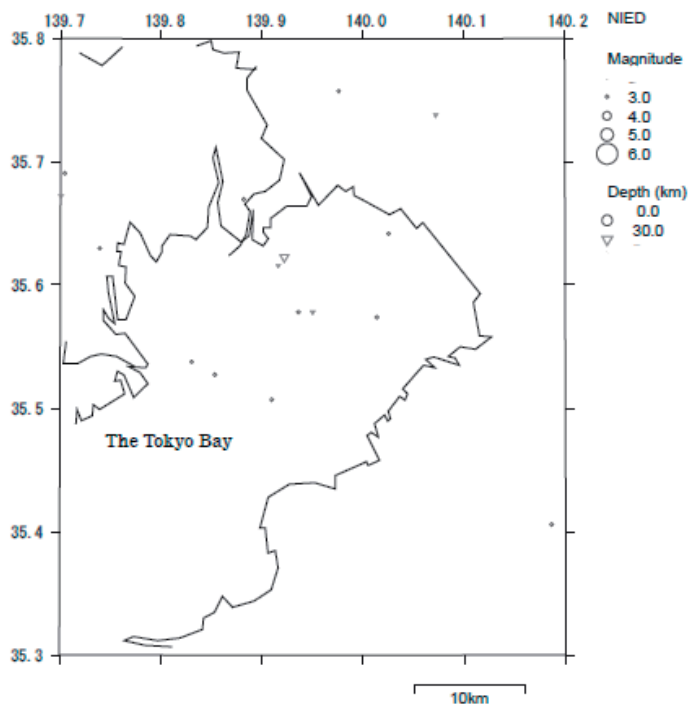
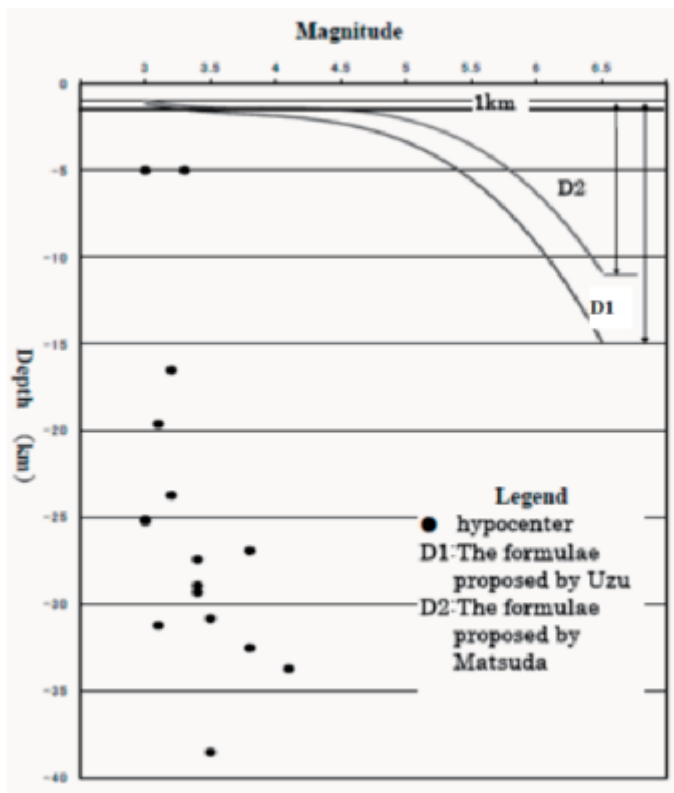


Figure 4. Relationship between depth of hypocenter and magnitude of earthquake



THE ROLE OF THE GEOSPHERE IN POSIVA'S SAFETY CASE

N. Marcos¹, P. Hellä², M. Snellman¹, M. Nykyri³, B. Pastina¹, M. Vähänen⁴, K. Koskinen⁴
¹Saanio & Riekkola Oy, ²Pöyry Environment Oy, ³Safram Oy, ⁴Posiva Oy; Finland

Abstract

Posiva Oy is developing a safety case for the construction licence application of the Finnish spent nuclear fuel repository. Following the selection of Olkiluoto for the site and the extension of the site characterization, the knowledge of site-specific properties is taken progressively into account in the assessment of the repository system.

Posiva's safety case is organised as a portfolio composed of ten main reports, as follows. The "Site" report, the "Repository Design" report, the "Evolution of Site and Repository", the "Characteristics of Spent Fuel", "Canister Design", the "Process" report and the following three reports addressing the safety and regulatory compliance: "Biosphere Assessment", "Radionuclide Transport" (safety assessment) and "Complementary Evaluations of Safety" (e.g. natural analogues). The "Summary" report draws together the key findings and arguments of the safety case.

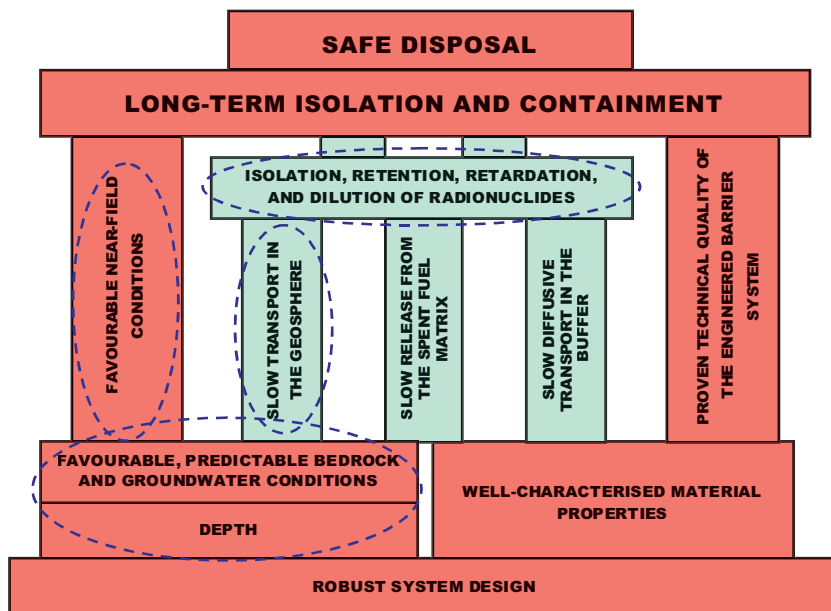
Posiva's safety concept is primarily based on the long-term isolation and containment of the spent fuel in copper canisters (Figure 1). In this concept, the key functions of the geosphere are to provide favourable and predictable conditions for the engineered barrier system, to isolate it against processes taking place in the proximity of the ground surface and to lower the probability of inadvertent human intrusion. The geosphere also limits and retards the inflow and release of harmful substances to and from the repository. Characteristics of the Olkiluoto bedrock supporting the safety include low flow rate of groundwater deep in the bedrock, groundwater salinity at acceptable level, neutral to slightly alkaline pH, low content of organics, reducing geochemical conditions deep in the bedrock, pH and redox buffering capacity, e.g. consumption of oxygen, and rock mechanical stability including a low probability of post-glacial movements. Evolution of these favourable properties under disturbance of the construction and over the time frames reaching at least several hundreds of thousands of years with changing climate are key issues in compiling the safety case. Most relevant to canister integrity are the functionality of buffer, especially under the potential infiltration of diluted glacial meltwater and in case of rock shear movements, in particular during post-glacial periods.

Introduction

The selection of the Olkiluoto site for construction of the Finnish spent fuel repository was preceded of intensive investigations to characterize and compare the geological features of four candidate sites (Anttila *et al.*, 1999a-d). Common to all the sites were the type of rock (hard crystalline rock), the relatively layered groundwater system, and the resilience of the groundwater systems to the natural perturbation(s) produced during the last glacial cycle(s). Being the characteristics of the geosphere at all sites similar at this level, Olkiluoto was mostly selected on the basis of public acceptance. The geosphere of the pristine Olkiluoto site (i.e. before construction) offered most of the

requirements supporting safety, that is, low flow rate of deep groundwater, reducing geochemical conditions, and neutral-to-slightly alkaline pH. The construction of the underground research facility ONKALO represents on one hand a major perturbation of the natural system and, on the other hand, the best way to check what was partly assumed in preliminary surface and borehole-based investigations and to gather new information about the site at depth. New information is being gathered to adjust geochemical and groundwater flow models in updated site reports. The geological (including geochemical, geomechanical, and hydrological) data derived from these investigations is periodically updated and incorporated in the reports of the Safety Case portfolio.

Figure 1. Outline of the safety concept for a KBS-3 type repository for spent fuel in crystalline bedrock (Posiva 2006; adapted from Vieno & Ikonen, 2005). The major role or functions of the geosphere are encircled



The geosphere in the safety case

The site and the repository design

The geological features of the site (deformation zones and hydrology) serves as a basis for the site-specific repository design, and the repository layout is based mainly on the principle of avoiding water-conductive features and large structures that could reactivate in case of future earthquakes. Water-conductive features can be of different sizes and they are to be avoided as they may serve as a path for the entering of harmful substances or for the transport of radionuclides towards the biosphere. Recently a host-rock classification system was set up using Olkiluoto data (Hagros, 2006) and following this work a programme on rock classification criteria (RSC) is being developed at Posiva (TKS, 2006). Part of this programme consists of identifying structures that might reactivate during future earthquakes and thus damage the engineered barrier system. Thus the repository design makes use of geosphere data taking into account criteria aiming at the long-term safety, altogether with other data (e.g. geomechanics) addressing to the stability of the geosphere at the site as a whole. Knowledge of in situ stresses is important to assess the probability of EDZ formation, spalling and thermal spalling. Thus, in situ stresses orientation and magnitude have a large impact on the detailed repository

layout. The depth of the repository is selected taking into account the chemistry of the groundwater as for favourable reducing conditions. The levels of salinity and sulphate, sulphide and methane contents are adequate or low enough only up to certain depth.

The site, the evolution of site and repository, and processes

The starting point for the description of the evolution of site and repository is the site report, and whenever possible, the repository design report, as well as the process report. The most important processes relating the evolution are external processes that may affect the repository at depth (e.g. climate-related processes) and internal processes inherent to the geosphere such as those related to groundwater flow and geochemistry. The characteristics of the site, its geological and geographical situation, and the design of the repository can be used to rank the importance of the process to be taken into account in the description of the evolution of site and repository. The different groundwater types at Olkiluoto are layered in a fashion common to several sites in Finland and Sweden (see e.g. Andersson *et al.*, 2006 and references therein). The range of groundwater compositions varies from fresh to brackish and saline groundwater at increasing depth. The presence of relatively high methane concentrations in groundwater increasing with depth is a characteristic feature of the Olkiluoto site and a strong indicator of the reducing environment. The pH conditions in the deep aquifer system at Olkiluoto are well buffered by the presence of abundant carbonate and clay minerals. This is also true for the reducing redox conditions, which are buffered by the presence of iron sulphides and microbially-mediated redox processes.

The site and the radionuclide transport (safety assessment)

In the radionuclide transport analysis, the formulation of the calculation cases is based – among other – on such geosphere related features that are presented in the site report, evolution report and process report. The goal is to cover all meaningful features, events and processes by the calculation cases while keeping the number of calculation cases rather low. In order to achieve the goal, it is necessary to simplify the cases and to make them less realistic. The resulting broadly defined cases may look like having lost their site-specificity, although the site properties have affected the cases. Similar principle is applied to the selection of the input data of the calculation cases. There are other driving forces for the calculation cases like the regulatory guideline YVL 8.4 (STUK, 2001), the properties of spent fuel, the properties of canister, and the design and operation of the repository.

The site data are not straightforwardly applied in calculation cases. It can be said that the data used in calculation cases are derived from real data measured at the site, e.g. temperature, transmissivity, hydraulic conductivity, position of hydrostructural features, groundwater chemistry. There is a chain of different interpretations between the acquired raw data and the final input parameter values forwarded into the transport models. Along the flow modelling, which feeds to the transport models, uses heavily interpreted site information.

In the geosphere-transport analyses of radionuclides, matrix diffusion and sorption in the rock matrix are so far the only processes assumed to retard and disperse radionuclides.

The site and complementary evaluations

Data supporting the buffering capacity of the geosphere at the site come from hydrogeochemical and palaeohydrogeological studies. The layering of the different groundwater types and their mixed interfaces seems to recover quite fast from (or resist being affected by) disturbances related to glaciation, like infiltration of meltwater. Palaeohydrogeological arguments provide convincing support for expectations concerning long-term flow system evolution, as the current groundwater chemistry is

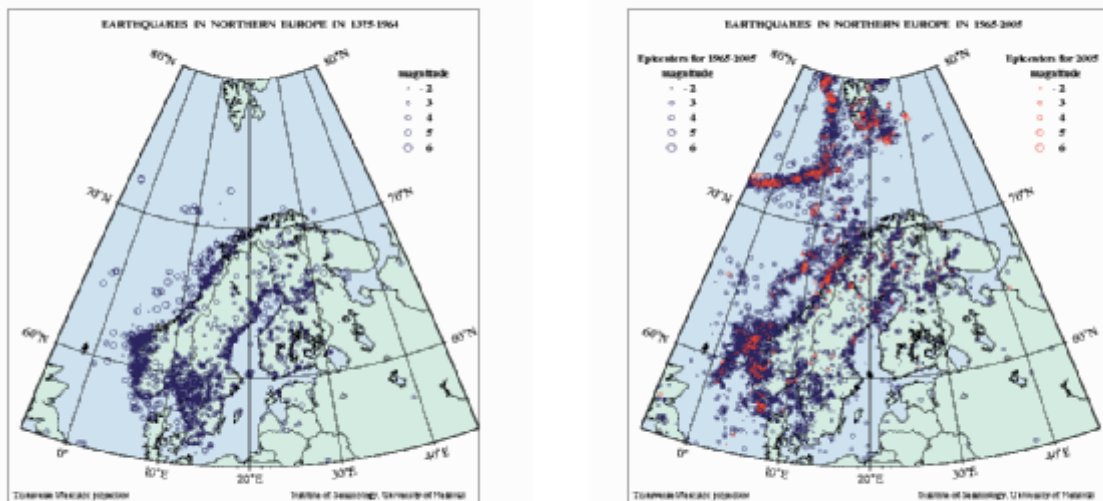
the result from flow, transport and water rock interactions driven by the past and current climate (Laakasoharju *et al.*, 2005, Posiva 2005, Pitkänen *et al.*, 2004). The location of the site in the Fennoscandian shield and especially in Finland is advantageous with respect to the stability of the geosphere (Figure 2). Earthquakes magnitudes in Finland have never reached 5 on the Richter scale (e.g. Mäntyniemi & Ahjos, 1990, Ahjos & Uski, 1992), the latest dating from the 1880s (Mäntyniemi, 2005). La Pointe and Hermansson (2002) studied the displacements of fractures with respect to future seismicity for Olkiluoto considering earthquakes of magnitudes (M_L) of 5.5 up to 7-8, and estimated the probability for canister failure due a rock displacement exceeding 10 cm to be 0.0041% i.e. the expected number of failed canisters is 0.12 (out of 3 000) during a 100 000 year period. The estimate is based on the simulations giving that in case of earthquake the canister failure probability is 0.0021 (i.e. 6 canisters out of 3 000) and the probability of a damaging earthquake is 0.02. These arguments serve to build confidence in the buffering capacity and long-term stability of the geosphere at the Olkiluoto site. The absence of natural resources at Olkiluoto is also a complementary line of evidence for the long-term safety of the site.

Figure 2. Earthquakes in Northern Europe in 1375-1964 (to the left) and in 1965-2005 (to the right). Note that the density and magnitude of earthquakes in Finland is lower than in other sites.

Figures can be found in the website of the University of Helsinki in the addresses:

<http://www.seismo.Helsinki.fi/bulletin/list/catalog/histomap.html> (left)

<http://www.seismo.Helsinki.fi/bulletin/list/catalog/instrumap.html> (right)



Other data supporting the safety of geological disposal

Descriptive, semi and fully quantitative data from other geological environments than the site itself can be used to support safety. These may come from the study of natural analogues and also from the measurements of natural radionuclide fluxes and concentrations. For example, in the IAEA Coordinated Research Project (CRP) entitled Natural Safety Indicators (Concentrations and Fluxes) (IAEA, 2005) Finland and many other countries contributed to assess the long-term safety of the geological disposal of radioactive waste by means of additional safety indicators based on the observation of natural systems. Experiences from Finland show that the geosphere, nearly at any investigated site (e.g. Pitkänen *et al.*, 2003, Kaija *et al.*, 2003) can act as an effective chemical and physical barrier limiting the movement of element to and from the repository.

Conclusions

The geosphere in the safety assessment vs. the geosphere in the safety case

The broader concept of the Safety Case, as explained above, allows the use of the geosphere and geosphere related data a more multidimensional way to address the safety of a geological repository than the concept of Safety Assessment alone. Numerical and descriptive geosphere data previously only supporting the results of performance or safety assessment are now integrated in the Safety Case since the very beginning and are included directly or indirectly in most of the reports included in the Safety Case portfolio.

References:

Ahjos T. and M. Uski, (1992), *Earthquakes in northern Europe in 1375-1989*. Tectonophysics, 207, 1–23.

Andersson J., H. Ahokas, J. Hudson, L. Koskinen, A. Luukkonen J. Löfman V. Keto P. Pitkänen J. Mattila, A.T.K. Ikonen and M. Ylä-Mella, (2006), *Olkiluoto Site Description 2006*. Posiva Oy, Olkiluoto, Finland. Report POSIVA 2007-03.

Anttila P., H. Ahokas, K. Front, H. Hinkkanen, E. Johansson, S. Paulamäki, R. Riekkola, J. Saari, P. Saksa, M. Snellman, L. Wikström and A. Öhberg, (1999a), *Final disposal of spent nuclear fuel in Finnish bedrock – Hästholmen site report*. Posiva Oy, Helsinki, Finland. Report POSIVA 99-08.

Anttila P., Ahokas H., Front K., Heikkinen E., Hinkkanen H., Johansson E., Paulamäki S., Riekkola R., Saari J., Saksa P., Snellman M., Wikström L., Öhberg A. 1999b. Final disposal of spent nuclear fuel in Finnish bedrock – Kivetty site report. Posiva Oy, Helsinki, Finland. Report POSIVA 99-09.

Anttila P., H. Ahokas, K. Front, H. Hinkkanen, E. Johansson, S. Paulamäki, R. Riekkola J. Saari, P. Saksa, M. Snellman, L. Wikström and A. Öhberg, (1999c), *Final disposal of spent nuclear fuel in Finnish bedrock – Olkiluoto site report*. Posiva Oy, Helsinki, Finland. Report POSIVA 99-10.

Anttila P., H. Ahokas, K. Front, H. Hinkkanen, E. Johansson, S. Paulamäki, R. Riekkola, J. Saari, P. Saksa, M. Snellman, L. Wikström and A. Öhberg, (1999d), *Final disposal of spent nuclear fuel in Finnish bedrock – Romuvaara site report*. Posiva Oy, Helsinki, Finland. Report POSIVA 99-11.

IAEA, (2005), *Natural activity concentrations and fluxes as indicator for the safety assessment of radioactive waste disposal – Results of a coordinated research project*. IAEA-TECDOC-1464.

Hagros A., (2006), *Host Rock Classification (HRC) system for nuclear waste disposal in crystalline bedrock*. Publications of the Department of Geology D8, University of Helsinki.

Kaija J., K. Rasilainen and R. Blomqvist, (2003), *IAEA coordinated Research Project, The Use of Selected Safety Indicators (Concentrations, Fluxes) in the Assessment of Radioactive Waste Disposal*, Report 6, Site Specific Natural Geochemical Concentrations and Fluxes at the Palmottu U-Th mineralisation (Finland) for Use as Indicators of Nuclear Waste Repository Safety. YST-114, Geological Survey of Finland, Nuclear Waste Disposal Research, GSF, Espoo, Finland.

Laaksoharju M., P. Pitkänen, J-O. Selroos and M. Mäntynen, (2005), *Potentials and Limitations of the Use of Geohistory for the Understanding of Current Features and Conditions and Possible Future Evolutions*. OECD/NEOEC/NEA International project on approaches and methods for integrating

geologic information in the safety-case (AMIGO) 2nd Workshop on: *Linkage of geoscientific argument and evidence in supporting the safety case*, Toronto – Canada, 20-22 September 2005.

La Pointe P. and J. Hermansson, (2002), *Estimation of rock movements due to future earthquakes at four Finnish candidate repository sites*. Posiva Oy, Helsinki, Finland. Posiva report POSIVA 2002-02.

Mäntyniemi P. and T. Ahjos, (1990), *A catalog of Finnish earthquakes in 1610-1990*. Geophysica, 26(2), 17-35.

Mäntyniemi P., (2005), *A Tale of two earthquakes in the Gulf of Bothnia, Northern Europe in 1880s*. Geophysica, 41(1-2), 73-91.

Pitkänen P., J. Löfman, A. Luukkonen and S. Partamies, (2003), *IAEA coordinated Research Project, The Use of Selected Safety Indicators (Concentrations, Fluxes) in the Assessment of Radioactive Waste Disposal*, Report 7, Site Specific Natural Geochemical Concentrations and Fluxes at Four Repository Investigation Sites in Finland for Use as Indicators of Nuclear Waste Repository Safety. YST-115, Geological Survey of Finland, Nuclear Waste Disposal Research, GSF, Espoo, Finland.

Pitkänen, P., S. Partamies and A. Luukkonen, (2004), *Hydrogeochemical interpretation of baseline groundwater conditions at the Olkiluoto site*. Posiva Oy, Eurajoki, Finland. Posiva Report POSIVA 2003-07.

Posiva, (2005), *Olkiluoto Site Description 2004*. Posiva Oy, Olkiluoto, Finland. Posiva Oy, Olkiluoto, Finland. Posiva Report POSIVA 2005-03.

Posiva, (2006), *Nuclear waste management of the Olkiluoto and Loviisa power plants: Programme for research, development and technical design for 2007-2009*. Posiva Oy, Olkiluoto, Finland. POSIVA TKS-2006.

STUK, (2001), *Long-term safety of disposal of spent nuclear fuel*. Radiation and Nuclear Safety Authority (STUK). Guide YVL 8.4.

UNDERSTANDING THE CHARACTERISTICS OF LONG-TERM SPATIO-TEMPORAL VARIATION IN VOLCANISM AND THE CONTINUITY OF THE RELATED PHENOMENA FOR ESTIMATING REGIONS OF NEW VOLCANO DEVELOPMENT

H. Kondo

Central Research Institute of Electric Power Industry, Japan

Abstract

The basic policy for evaluating volcanism for selecting sites for HLW (high-level radioactive waste) geological disposal is excluding regions of future volcanism in order to avoid magmatic intrusion or volcanic eruption regarded as external factors causing serious damage to the repository. For the purpose of evaluating regions of new volcano development in a subduction zone such as the Japanese Islands, it is essentially important to focus on the duration of the uneven and concentrated distribution of the past volcanism and the geologic processes causing such characteristics within a volcanic arc for as long period as possible to the present, in terms of the continuity of the present subduction conditions around the arc. The regions of future volcanism can be estimated by extrapolation based on plausible geological models in consideration of the trends or regularity deduced from the past volcanic activities. For the actual estimation, the duration of the uneven and concentrated distribution of the past volcanism to the present within the characteristics of long-term spatio-temporal variation in volcanism, and the continuity of the related phenomena indicated by topographical, geological and geophysical data observable at the present time should be confirmed through the correlation between them.

Introduction

Paleozoic to Cenozoic formations in the Japanese Islands, consisting of a variety of sedimentary, igneous and metamorphic rocks, show a zonal arrangement extending along the island arc. Granitic rocks, the predominant rock type of plutonic rocks occupying around 10% of the total area of Japan (Murata and Kano, 1995), are typical of crystalline rocks and widely distributed forming a framework of the main body of the Japanese Islands. They were formed mainly through Cretaceous (to Paleogene) magmatism as a continental arc being active before the period of the opening of the Japan Sea back-arc basin. After the end of the opening of the back-arc basins (Japan Sea, Kurile Basin, Shikoku Basin, etc.) at around 15 Ma (Jolivet *et al.*, 1994), basic framework of the plate system around the Japanese Islands has been fixed. Under such reorganised plate tectonic regime, rock bodies including the above-mentioned granitic rocks formed in earlier stages have suffered from new stage volcanism (magmatic intrusion or volcanic eruption) in regions of back-arc side of the volcanic front of various ages in the arc-trench system lasting to the present.

Within the scope of understanding the past volcanism and the related phenomena, which have occurred in this arc-trench system, it is important to exclude regions of future volcanism in order to avoid magmatic intrusion or volcanic eruption regarded as external factors causing serious damage to the repository for selecting sites for HLW (high-level radioactive waste) geological disposal in Japan.

Estimation of regions of new volcano development will be accomplished by establishing plausible geological models using available data such as spatio-temporal patterns in volcanism combining with the related topographical, geological and geophysical data. In terms of establishing geological models, recent research revealed a lot of useful information about uneven and concentrated distribution of volcanism, characterized by volcanic clusters and gaps, and the related phenomena lasting for at least several millions of years in subduction zone of the Japanese Islands (Kondo *et al.*, 1998, 2004; Tamura *et al.*, 2002; Hasegawa and Nakajima, 2004).

In this presentation, the basic framework of an empirical approach to the methodology of the evaluation of regions of new volcano development for selecting sites for HLW geological disposal will be introduced with special emphasis on the correlation between the spatio-temporal patterns within the characteristics of long-term variation in volcanism and the continuity of the related phenomena indicated by the available topographical, geological and geophysical data in the arc-trench system of the Japanese Islands lasting to the present. This study was financially supported by the Nuclear Waste Management Organization of Japan.

Premises of discussion and timeframe for the evaluation of future volcanism in the Japanese Islands

In a subduction zone such as the Japanese Islands, volcano distribution and the basic processes of magmatic generation and ascent strongly reflect subduction conditions, essentially controlled by the movement modes (e.g. movement rate, direction, inclination of subduction surface) of the oceanic plate. Therefore, the duration of subduction conditions can be one of the preconditions for evaluating future volcanism around the target area. Basic framework of the plate system around the Japanese Islands has been fixed since the cessation of the opening of the back-arc basins at around 15 Ma (Jolivet *et al.*, 1994), although there have been slight changes in the movements of the oceanic plates (the Pacific and the Philippine Plates) since then (Pollitz, 1986; Kamata and Kodama, 1999).

The report entitled “Guidelines on Research and Development Relating to Geological Disposal of HLW in Japan”, published in 1997 by Advisory Committee on Nuclear Fuel Cycle Backend Policy, Atomic Energy Commission of Japan, stated the following view on the projected timescale of the future geological events. It is possible to evaluate the extent and pattern of natural phenomena for the next one hundred thousand years, based on analyzing and interpreting the regularity and continuity of the phenomena for the past several hundreds of thousands of years. This view is supported by the information about the stability of the above-mentioned plate tectonic regime and also the continuity of the stress conditions in and around the Japanese Islands. In accordance with this view, a period of around one hundred thousand years has been adopted as the projected timescale for evaluating future geological events for HLW geological disposal (JNC, 1999; JSCE, 2001; NUMO, 2004), although a timescale for repository safety assessment has not yet stipulated in Japan.

A lifetime of a volcano of a volcanic arc such as the Japanese Islands is several hundreds of thousands of years on average (Kaneoka and Ida, 1997). During the next one hundred thousand years as the projected timescale for evaluating future geological events for HLW geological disposal, a possibility of the generation of new volcano as a new magma plumbing system in the target area, not only a possibility of the migration of magma to the repository from each existing volcano (a magma plumbing system) around the target area during its lifetime, should be considered because the timescale for evaluation is long enough as compared with a lifetime of a volcano. For the purpose of evaluating new volcano development and the changes in the position of magma activity in a region, the information about spatio-temporal variation of volcanism for the period of over the past 10^5 - 10^6 years (order of the average lifetime of a volcano) is indispensable. Investigation of the past volcanism

for as long period as possible in terms of the continuity of the present subduction conditions around the volcanic arc enables us to evaluate regions of future volcanism with much confidence.

Current information useful for the evaluation of regions of new volcano development in terms of HLW geological disposal

For the purpose of evaluating regions of new volcano development, it is essentially important to focus on the duration of the uneven and concentrated distribution of the past volcanism and the geologic processes causing such characteristics within a volcanic arc for as long period as possible to the present, in terms of the continuity of the present subduction conditions around the arc. The regions of future volcanism can be estimated by extrapolation based on plausible geological models in consideration of the trends or regularity deduced from the past volcanic activities.

Presence of the volcanic front

Volcanism occurring within the Japanese Islands under constant subduction conditions is essentially characterized by uneven and concentrated distribution. In the Japanese Islands, the ocean trench-side distribution of volcanoes of various ages is defined as the volcanic front. The generation of magma in a subduction zone in general is controlled by both decompression melting process within the upward flow portion of the convection from the deep mantle within the mantle wedge induced by oceanic plate subduction, and dehydration process of subducting slab and the affected underlying hydrous layer of the mantle wedge (Tatsumi, 1995; Iwamori, 1998; Takahashi, 2000; Kawakatsu, 2002). The volcanic front is a boundary line dividing into two regions, implying whether or not the region meets the condition of magmatic generation and ascent, although the cause of the volcanic front has not been settled definitely. Exceptionally, the volcanic front is understood as a boundary line between the regions of alkali-basalt monogenetic volcanism not related to subduction processes, and that of no volcanism where the subducting oceanic plate (the Philippine Sea Plate) has been covering its magma source, in the Chugoku District, the western part of Honshu (Uto, 1995; Kimura *et al.*, 2005).

In any case, the rate of migration of the volcanic front since the late Miocene can be estimated to be several km per million years or under, i.e. the volcanic front has been stable on the order of several millions of years, based on available literature (Yoshida *et al.*, 1995; Uto, 1995, etc.). Therefore, it is extremely unlikely that new igneous activity will commence on the ocean trench side away from the present volcanic front in the next hundred thousand years or so (JSCE, 2001).

Characteristics of uneven distribution of volcanism on the back-arc side of the volcanic front

As for uneven and concentrated distribution of volcanism on the back-arc side of the volcanic front in the Japanese Islands, the examination of the spatio-temporal distribution of Quaternary volcanoes revealed that the Quaternary volcanism is unevenly distributed in particular regions where new volcano has formed repeatedly (JNC, 1999). In the Northeast Japan Arc, east-west trending 'branches' showing regions of volcanic cluster at intervals of 50-100 km, with the fields of rare volcanism adjacent to the north and south of each 'branch' on its back-arc side, reflect regular intervals of magmatism along the arc which has been under constant subduction conditions since the cessation of the back-arc opening at 14 Ma (Kondo *et al.*, 1998, 2004). The evolution of the thermal structure (cooling process) within the mantle wedge since the cessation of the back-arc opening has resulted in a tendency for the distribution of volcanism during the late Miocene to Quaternary to become localized and concentrated more specific areas (Kondo *et al.*, 2004).

Within the scope of discussion on the Quaternary volcanism in the Northeast Japan Arc, the correlation of regions of volcanic cluster and the related phenomena indicated by such indexes as topographic highs (including elevated basements), local negative Bouguer gravity anomalies (indicative of the thickening of the crust), and low-velocity anomalies in the images of seismic tomography (interpreted as hot regions) of the mantle wedge were pointed out (Tamura *et al.*, 2002; Hasegawa and Nakajima, 2004). Regular intervals of volcanism and the related phenomena indicated by topographical, geological and geophysical data along the arc reflect convection-controlled, heterogeneous thermal structures within the mantle wedge along the Northeast Japan Arc (Tamura *et al.*, 2002; Hasegawa and Nakajima, 2004).

Consequently, in a volcanic arc under constant subduction conditions, it is likely that the elucidation of the correlation between uneven and concentrated distribution of the past volcanism to the present and the related phenomena indicated by topographical, geological and geophysical data, provides useful information in order to estimate the regions where new volcano will form around the target area. Through such a correlation, the duration of the uneven and concentrated distribution within the characteristics of long-term variation in volcanism and the continuity of the related phenomena observable at the present time should be confirmed.

Tohoku case as a basic example

The results of a case study of the correlation between uneven and concentrated distribution of the past volcanism to the present and the related phenomena under constant subduction conditions in the Northeast Japan Arc are described below as a basic example in terms of abundance of available data and characteristics of volcanic clusters and gaps.

Plausible geological model for the evaluation of regions of future volcanism

On the back-arc side of the volcanic front in the Northeast Japan Arc, a typical volcanic arc undergoing constant subduction, a geological model for evaluating regions of future volcanism can be established in consideration of at least the following three kinds of key phenomena inferred from current available literature (Tamura *et al.*, 2002; Hasegawa and Nakajima, 2004; Kondo *et al.*, 1998, 2004, etc.): (1) hot regions capable of supplying magma to the crust, where the thickness of the upwelling mantle flow (partially molten) is larger enough to become sufficient melt contents to cause repeated ascent of magma to the crust, are distributed in specific regions within the mantle wedge with east-west trending patterns arranged along the arc; (2) volcanism occurring within specific regions in the form of volcanic cluster accompanied by its uplifted basements and crustal thickening have been caused by repeated injection or underplating of magmas derived from the hot regions in the mantle to the crust; and (3) there is a tendency for the distribution of volcanism to become localized and concentrated into more specific areas in the form of clusters since 14 Ma.

These phenomena have been possibly caused by the presence of convection-controlled heterogeneous thermal structures and their evolution within the mantle wedge along the arc under long-term constant subduction conditions. This model is supported by spatio-temporal patterns in volcanism and the related topographical, geological and geophysical data.

Result of the correlation between uneven and concentrated distribution of the past volcanism to the present and the related phenomena

From the viewpoint of the estimation of regions of new volcano development on the basis of such model, the duration of the uneven and concentrated distribution of the past volcanism to the present within the characteristics of long-term spatio-temporal variation in volcanism, and the continuity of

the related phenomena indicated by topographical, geological and geophysical data observable at the present time were confirmed through the correlation between them. The correlation was carried out in an area of long. 139° 30′-142° 00′, lat. 38° 40′-41° 40′, which was fixed so that it includes typical Quaternary volcanic clusters and gaps in the northern part of Tohoku of the Northeast Japan Arc.

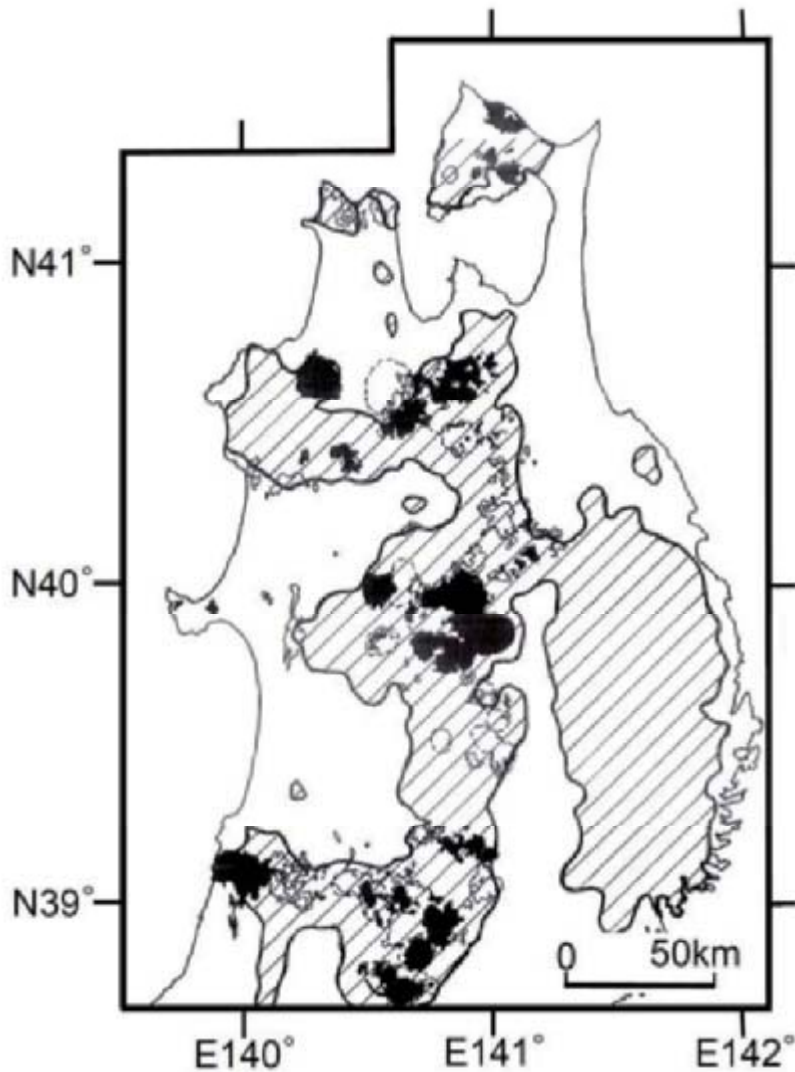
Since the cessation of the opening of the Japan Sea back-arc basin at 14 Ma, sedimentary basins widely developed in the back-arc region indicating regional subsidence due to lithospheric cooling (Sato, 1992, 1994), whereas volcanism occurred in specific regions characterized by both a “trunk” with a north-south trend in the volcanic front region and ‘branches’ with east-west trends in the back-arc region in the Northeast Japan Arc (Kondo *et al.*, 1998, 2004). Moreover, the distribution of volcanism tended to become localized and concentrated into more specific areas as mentioned before. For the purpose of the above-mentioned correlation, accumulative distribution maps of igneous rocks, within several kinds of fixed periods of time from a certain point after 14 Ma to the present were illustrated using available literature. The comparison between accumulative distribution maps of volcanism for different periods of time to the present revealed that the shorter the period is fixed, the more conspicuous the characteristics of the distribution of volcanic cluster become, volcanic cluster in the 2-0 Ma period is the most conspicuous.

However, the accumulative distribution pattern of volcanism in the 2-0 Ma period is not the best consistent with the patterns of the related phenomena indicated by topographical, geological and geophysical data observable at the present time. In the survey area, the accumulative distribution pattern of volcanism since 5 Ma can be much correlated with both the distribution pattern of mountainous regions that include east-west trending warping (indicating differential uplift related to volcanism) on the contour map showing the distribution of summit level of topography, and that of hot regions indicated by low-velocity anomalies on the map showing the distribution of S-wave velocity perturbations along the core zone of the mantle wedge, using tentative thresholds after several trial and error of qualitative correlation (Figures 1 and 2). The coincidence of distribution patterns between volcanism since 5 Ma and the related phenomena observable at the present time indicates that the time frame of the continuity of these phenomena is estimated to be the order of several millions of years. In order to specify possible regions of future volcanism, optimal thresholds of the correlation should be fixed appropriately, through the information of key phenomena obtained by more detailed investigation focusing on the region around the target area.

Flow chart showing basic procedure for evaluating regions of future volcanism

Based on the results of this case study in Tohoku, a flow chart showing basic procedure for evaluating regions of future volcanism is developed from more generalized viewpoints (Figure 3). Within the time range fixed in consideration of constant subduction conditions, the investigation of spatio-temporal patterns in the past volcanism among volcanoes or volcanic units around the target area provides fundamental information for evaluating future volcanism in terms of the determination of meaningful trends or regularity in volcanism. The viewpoint of the investigation of crustal structure and movement indicating (or controlling) concentration of volcanism is extremely variable as it is dependent on the conditions of magmatic generation and ascent in relation to tectonic settings: e.g. volcanism initiated by crustal melting associated with graben formation along a major tectonic line (Kamata and Kodama, 1999) and volcanism posterior to basement subsidence forming a sedimentary basin indicative of crustal erosion due to the convective coupling between the ductile lower crust and the upper mantle induced by mantle diapiric upwelling in the back-arc region (Nakada *et al.*, 1997).

Figure 1. Map showing the correlation between the distribution of igneous rocks since 5 Ma and the range of mountainous regions, the elevation of which is more than 500 meters above (the hatched area with oblique lines). The distribution of igneous rocks is extracted from the following literature: Editorial Committee for Civil Engineering Geological Maps of Tohoku District (1988), Hata *et al.*, (1972, 1984), Kamata *et al.*, (1991), Ozawa *et al.*, (1988, 1993), Ozawa and Suda (1978, 1980), Tsushima (1964), and Yoshida *et al.*, (1984). It is compiled from the viewpoint of volcanic central facies (Ohguchi *et al.*, 1989; Kondo *et al.*, 1998, 2004) in consideration of the location where magmatism occurred *in situ* or in close proximity. Distributions of igneous rocks for two periods, 5-2 and 2-0 Ma are differentiated. The caldera outline is extracted from Yoshida *et al.*, (1999). The contour line is extracted from a distribution map of summit level of topography with a 10 km mesh, based on “Digital Map 50m Grid (Elevation)” published by the Geographical Survey Institute of Japan (2001). Note that the region of the Kitakami Mountains on the ocean trench side of the volcanic front is not considered here, because it is clear that the Kitakami Mountains have been formed by warping, not related to the agency of volcanism (Koike *et al.*, 2005)



Distribution of igneous rocks




2-0 Ma			Caldera outline
5-2 Ma			

Figure 2. Map showing the correlation between the distribution of igneous rocks since 5 Ma and the range of S-wave low-velocity anomalies within the mantle wedge, the velocity perturbation of which is less than -4% (the hatched area with vertical lines). The base map of seismic tomography data is showing the projection of the distribution of S-wave velocity perturbations along the core of the inclined low-velocity zone shallower than ~150 km within the mantle wedge sub-parallel to the subducting slab (the Pacific Plate). The data are provided by Prof. A. Hasegawa and Dr. J. Nakajima with their permission, the same as those used in (Hasegawa and Nakajima, 2004). The rest of the legend is the same as that for Figure 1

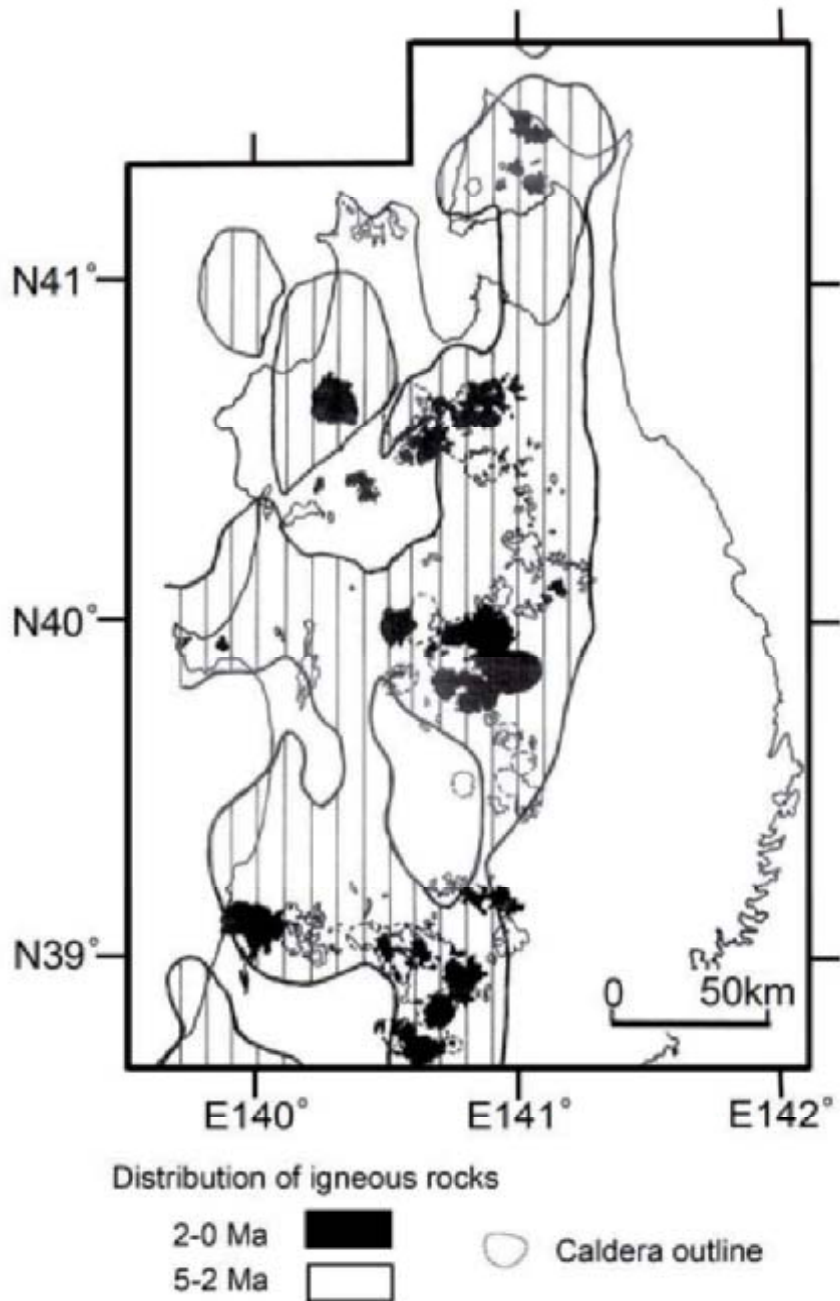
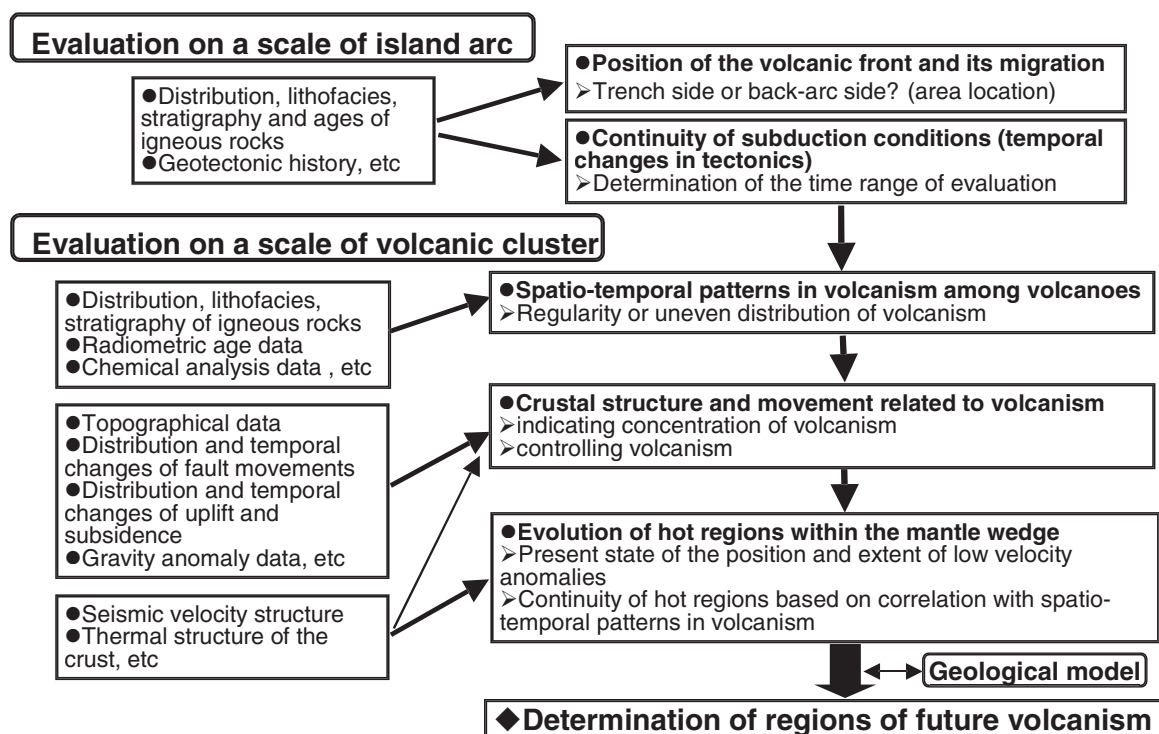


Figure 3. Flow chart showing basic procedure for evaluating regions of future volcanism



References

Advisory Committee on Nuclear Fuel Cycle Backend Policy, Atomic Energy Commission of Japan, (1997), *Guidelines on Research and Development Relating to Geological Disposal of High-Level Radioactive Waste in Japan*. (in Japanese)

Editorial Committee for Civil Engineering Geological Maps of Tohoku District (ed.), (1988), *Civil Engineering Geological Maps of Tohoku District at 1: 200,000 scale*. Tokyo: Japan Institute of Construction Engineering. (in Japanese)

Geographical Survey Institute of Japan, (2001), *Digital Map 50 m Grid (Elevation)* (CD-ROM).

Hasegawa, A. and J. Nakajima, (2004), Geophysical constraints on slab subduction and arc magmatism, In: Sparks, R. S. J. and C. J. Hawkesworth (eds.). *The State of the Planet: Frontiers and Challenges in Geophysics*. Geophysical Monograph Series, **150**. Washington, D. C.: American Geophysical Union, 81-94.

Hata, M., K. Tsushima, Y. Suda and Y. Ono, (1972), *Geological Map of Japan 1:200,000, Hakodate and Shiriyazaki*. Tsukuba: Geological Survey of Japan.

Hata, M., F. Uemura and T. Hiroshima. 1984. *Geological Map of Japan 1:200,000, Hakodate and Oshima-Oshima*. Tsukuba: Geological Survey of Japan.

Iwamori, H., (1998), Transportation of H₂O and melting in subduction zones. *Earth and Planetary Science Letters*, **160**, 65-80.

JNC (Japan Nuclear Cycle Development Institute), (1999), *Project to Establish the Scientific and Technical Basis for High-Level Radioactive Waste Disposal in Japan: Second Progress Report on Research and Development for the Geological Disposal of High-Level Radioactive Waste in Japan*. JNC TN1400 99-020 (Japanese version), JNC TN1410 2000-001 (English version).

Jolivet, L., K. Tamaki and M. Fournier, (1994), Japan Sea, opening history and mechanism: A synthesis. *Journal of Geophysical Research*, **99**(B11), 22237-22259.

JSCE (Japan Society of Civil Engineers), (2001), *Geological Disposal and the Geological Environment: Geological Factors to be Considered in the Selection of Preliminary Investigation Areas for High-Level Radioactive Waste Disposal*. Sub-Committee on the Underground Environment, Civil Engineering Committee of the Nuclear Power Facilities. (in Japanese)

Kamata, H. and K. Kodama, (1999), Volcanic history and tectonics of the Southwest Japan Arc. *The Island arc*, **8**, 393-403.

Kamata, K., M. Hata, K. Kubo and T. Sakamoto, (1991), *Geological Map of Japan 1:200,000, Hachinohe*. Tsukuba: Geological Survey of Japan.

Kaneoka, I. And Y. Ida (eds.), (1997), *Volcanoes and Magma*. Tokyo: University of Tokyo Press. (in Japanese)

Kawakatsu, H (ed.), (2002), *Earth Dynamics and Tomography*. New Development of Earth Science, **1**. Tokyo: Asakura Publishing (Earthquake Research Institute, University of Tokyo ed.). (in Japanese)

Kimura, J., R. J. Stern and T. Yoshida, (2005), Reinitiation of subduction and magmatic responses in SW Japan during Neogene time. *Geological Society of America Bulletin*, **117**, 969-986.

Koike, K., T. Tamura, K. Chinzei and T. Miyagi (eds.), (2005), *Geomorphology of Tohoku Region*. Regional Geomorphology of the Japanese Islands, **3**. Tokyo: University of Tokyo Press. (in Japanese)

Kondo, H., K. Kaneko and K. Tanaka, (1998), Characterization of spatial and temporal distribution of volcanoes since 14 Ma in the Northeast Japan arc. *Bulletin of the Volcanological Society of Japan*, **43**, 173-180.

Kondo, H., K. Tanaka, Y. Mizuochi and A. Ninomiya, (2004), Long-term changes in distribution and chemistry of middle Miocene to Quaternary volcanism in the Chokai-Kurikoma area across the Northeast Japan Arc. *The Island arc*, **13**, 18-46.

Murata, Y. and K. Kano, (1995), The areas of the geologic units comprising the Japanese Islands, calculated by using the Geological Map of Japan 1: 1,000,000, 3rd Edition, CD-ROM Version. *Chishitsu News*, no. 493, 26-29. (in Japanese)

Nakada, M., T. Yanagi and S. Maeda, (1997), Lower crustal erosion induced by mantle diapiric upwelling: Constraints from sedimentary basin formation followed by voluminous basalt volcanism in northwest Kyushu, Japan. *Earth and Planetary Science Letters*, **146**, 415-429.

NUMO (Nuclear Waste Management Organization of Japan), (2004), *Evaluating Site Suitability for a HLW Repository: Scientific Background and Practical Application of NUMO's Siting Factors*. NUMO-TR-04-02 (Japanese version), NUMO-TR-04-04 (English version).

- Ohguchi, T., T. Yoshida and K. Okami, (1989), Historical change of the Neogene and Quaternary volcanic field in the Northeast Honshu arc, Japan. *Memoirs of the Geological Society of Japan*, no. 32, 431-455. (in Japanese with English abstract)
- Ozawa, A., T. Hiroshima, M. Komazawa and Y. Suda, (1988), *Geological Map of Japan 1:200,000, Shinjo and Sakata*. Tsukuba: Geological Survey of Japan.
- Ozawa, A., K. Mimura and T. Hiroshima, (1993), *Geological Map of Japan 1:200,000, Aomori (2nd ed.)*. Tsukuba: Geological Survey of Japan.
- Ozawa, A. and Y. Suda, (1978), *Geological Map of Japan 1:200,000, Hirosaki and Fukaura*. Tsukuba: Geological Survey of Japan.
- Ozawa, A. and Y. Suda. (1980), *Geological Map of Japan 1:200,000, Akita and Oga*. Tsukuba: Geological Survey of Japan.
- Pollitz, F. R., (1986), Pliocene change in Pacific plate motion. *Nature*, **320**, 738-741.
- Sato, H., (1992), Late Cenozoic tectonic evolution of the central part of northern Honshu, Japan. *Bulletin of the Geological Survey of Japan*, **43**, 119-139. (in Japanese with English abstract)
- Sato, H., (1994), The relationship between late Cenozoic tectonic events and stress field and basin development in northeast Japan. *Journal of Geophysical Research*, **99**(B11), 22261-22274.
- Takahashi, M., (2000), *Island Arc, Magma and Tectonics*. Tokyo: University of Tokyo Press. (in Japanese)
- Tamura, Y., Y. Tatsumi, D. Zhao, Y. Kido and H. Shukuno, (2002), Hot fingers in the mantle wedge: new insights into magma genesis in subduction zones. *Earth and Planetary Science Letters*, **197**, 105-106.
- Tatsumi Y., (1995), *Subduction Zone Magmatism - A Contribution to Whole Mantle Dynamics*. Tokyo: University of Tokyo Press. (in Japanese)
- Tsushima, K., (1964), *Geological Map of Japan 1:200,000, Noheji*. Tsukuba: Geological Survey of Japan.
- Uto, K., (1995), Volcanoes and age determination: now and future of K-Ar and $^{40}\text{Ar}/^{39}\text{Ar}$ dating. *Bulletin of the Volcanological Society of Japan*, **40**, S27-S46. (in Japanese with English abstract)
- Yoshida, T., K. Aizawa, Y. Nagahashi, H. Sato, T. Ohguchi, J. Kimura and H. Ohira, (1999), Geological history and formation of late Cenozoic calderas in the stage of island arc volcanism in Northeast Honshu arc. *Earth Monthly*, extra issue, no. 27, 123-129. (in Japanese)
- Yoshida, T., T. Ohguchi and T. Abe, (1995), Structure and evolution of source area of Cenozoic volcanic rocks in Northeast Honshu arc. *Memoirs of the Geological Society of Japan*, no. 44, 263-308. (in Japanese with English abstract)
- Yoshida, T., A. Ozawa, M. Katada and J. Nakai, (1984), *Geological Map of Japan 1:200,000, Morioka*. Tsukuba: Geological Survey of Japan.

NUMERICAL ASSESSMENT OF THE INFLUENCE OF TOPOGRAPHIC AND CLIMATIC PERTURBATIONS ON GROUNDWATER FLOW CONDITIONS

H. Saegusa¹, K-I. Yasue¹, H. Onoe¹, T. Moriya², K. Nakano¹

¹Japan Atomic Energy Agency, ²Nittetsu Mining Co., Ltd.; Japan

Abstract

Establishment of comprehensive techniques for investigation, analysis and assessment of the stability of deep geological environments for time periods exceeding several 100 000 years is important for the geological disposal of nuclear wastes. The purpose of this study is to provide a method to evaluate the effects of future topographic and climatic perturbations on groundwater flow conditions, such as hydraulic gradient, velocity distribution, flow paths and lengths.

Simulations of landform development and groundwater flow have been carried out in the Tono area. The Tono area, located in Central Japan, has typical uplift rate of Japanese inland areas and abundant data on the geology, hydrogeology and hydrochemistry have been obtained in this area. The regional scale, tens of kilometers square, has been selected for the simulations in order to evaluate the effects of topographic changes on groundwater flow conditions within an entire groundwater flow system, from recharge area to discharge area. The period selected for the landform development simulation is from the present to approximately 120 000 years into the future and is based on past global climatic cycles ranging from extremely warm to glacial periods. The input dataset for the landform development simulation is based on a literature survey of topics such as uplift and erosion rates. Topographic conditions predicted by landform development simulations have been used as the upper boundary in the groundwater flow simulation models. A cold period was selected for the groundwater flow simulation in order to evaluate the effect of a major climatic perturbation, as well as that of changed topography.

Results of the simulations show the influence of the topographic and climatic perturbations on hydraulic gradient and groundwater velocity. In particular, the influence on hydraulic gradient downstream of the faults normal to the major direction of groundwater flow is much smaller than in the area upstream of the faults.

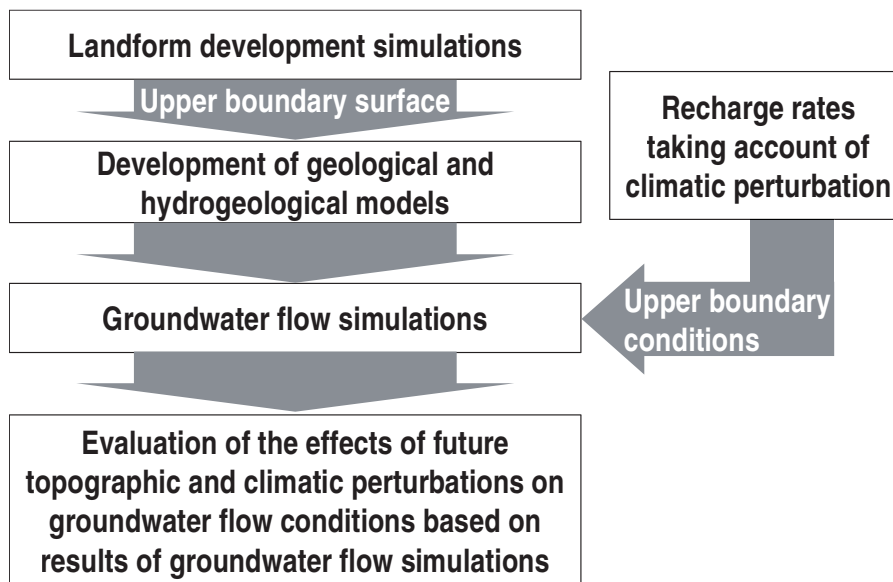
Through this study, it has been confirmed that the method of combining simulations of landform development with groundwater flow is useful for the evaluation of effects of topographic and climatic perturbations on groundwater flow conditions. In future studies, field investigations to obtain site-specific data regarding topographic and climatic changes and hydrogeological characterization of faults will be carried out in order to confirm the appropriateness of the general hypotheses and the input parameters used in the simulations in this study. For example, future studies could include pollen analysis for paleoclimate studies and terrace investigations on uplift rates.

Introduction

Establishment of comprehensive techniques for investigation, analysis and assessment of the stability of deep geological environments for time periods exceeding several 100 000 years is important for the geological disposal of nuclear wastes. Simulations of landform development and groundwater flow have been carried out in the Tono area in order to provide a method to evaluate the effects of long term topographic and climatic changes on groundwater flow conditions. The Tono area is located in Central Japan and has an uplift rate typical of the Japanese inland. Abundant data on the geology, hydrogeology and hydrochemistry are available from investigations during the Regional Hydrogeological Study (RHS) project [1-3] and the Mizunami Underground Research Laboratory (MIU) project [2-5] carried out by Japan Atomic Energy Agency (JAEA).

This study has been carried out based on the workflow shown in Figure 1. Future topographic conditions in the Tono area have been predicted based on landform development simulations [6]. The topography predicted by landform development simulations have been used as the upper boundary in the geological and hydrogeological models. Groundwater flow simulations have been carried out based on the hydrogeological models in order to evaluate the effects of topographic and climatic perturbations on groundwater flow conditions. In the groundwater flow simulation, climatic perturbations have also been taken into account with respect to the upper boundary conditions.

Figure 1. **Workflow of the study**



Overview of the study area

The Toki River basin has been selected as the study area (Figure 2). The local scale area shown on the figure is where the RHS project and the MIU project have been carried out. The study area is located around the boundary between the Mino Highland and Mikawa Highland (Figure 2). The Kiso River flowing through the northern part of the study area forms a deep antecedent valley. The Toki River flows from east to west in the central part of the study area.

The sedimentary Neogene Mizunami group unconformably overlies the Paleozoic Mino sedimentary complex, the Upper Mesozoic Nohi rhyolites and granites (Figure 3). The Neogene Seto group, consisted of weakly consolidated deposits, unconformably overlies the Mizunami group. Unconsolidated terrace and alluvial deposits are distributed along the mainstream and branches of the river. The study area is dominated by active faults with northeast and northwest strikes. The NE faults are the Byobuyama, Enasan and Kasahara faults, the NW faults are the Ako and Hanadate faults (Figure 3). The inactive Tsukiyoshi fault, traverses the central part of the study area. Granites and the Mizunami group are displaced by the fault.

Figure 2. Study area (Reference the A-A' line to Figure 9)

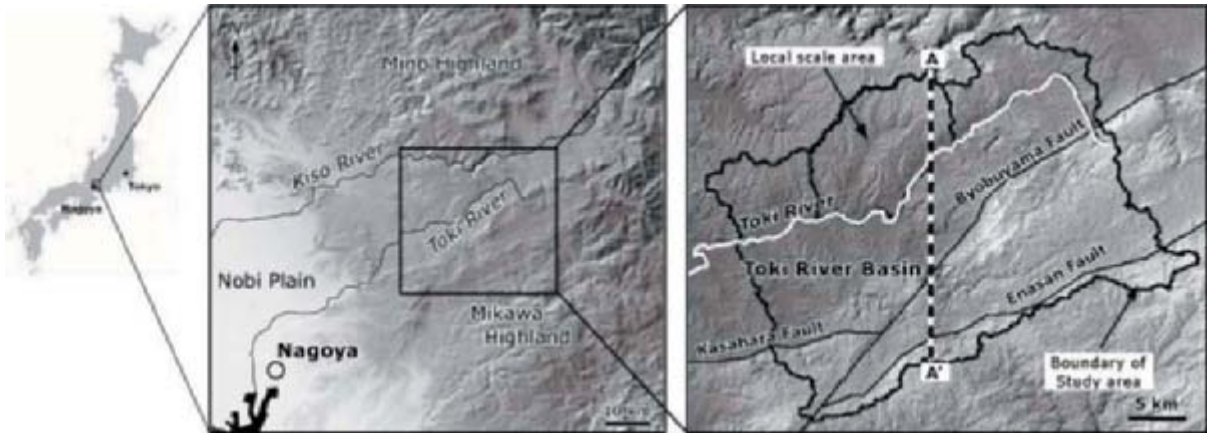
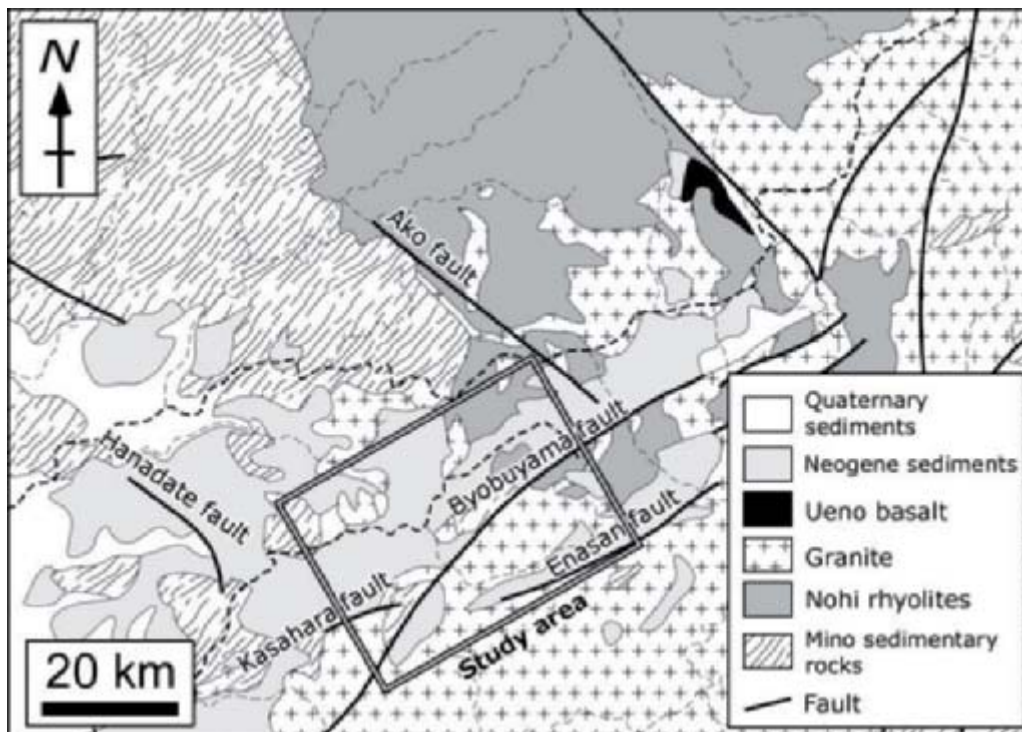


Figure 3. Geological map (modified from Geological Survey of Japan, 1992⁷⁾)



Landform development simulation

Simulation methodology

The landform development simulation is aimed at predicting approximately 100 000-years of landform development in an actual drainage basin. Landform development is roughly categorized as occurring in hill slope, channel, and sea domains (Figure 4). The simulation programme for landform development of an inland area used different diffusion equations for the hill slope and channel domains. The hill slope domain is dominated by creep of weathered materials. Therefore, an equation to determine flux of material is a basic requirement for the simulation. The simulation programme for the hill slope domain applied the following equation [8] to calculate flux by a diffusion phenomenon dependant on gradient.

$$\partial u / \partial t = k \partial^2 u / \partial x^2$$

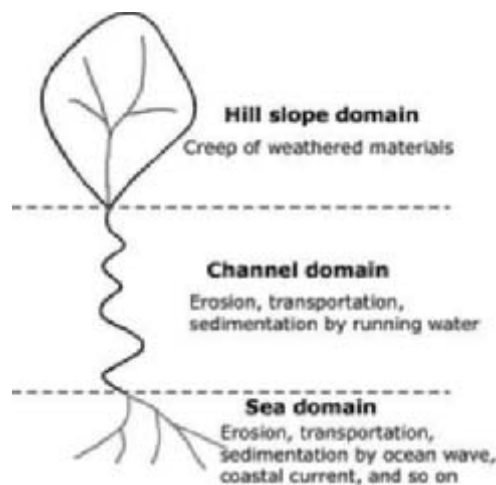
where u is height at time t and position x , k is the diffusion coefficient.

The channel domain is dominated by running water and its role in erosion, transportation, and sedimentation. The simulation programme for the channel domain applied the following equation⁶⁾ to calculate landforms having straight and concave segments.

$$\partial u / \partial t = k e^{r x} (\partial^2 u / \partial x^2)$$

where r is the coefficient that determines concavity of a longitudinal river profile.

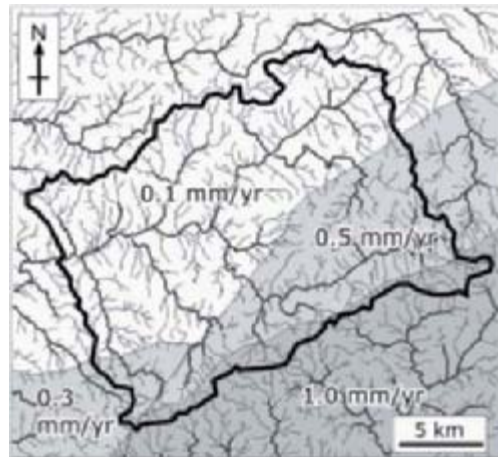
Figure 4. Mass transport and mass movement in landform system



Input parameters

The period for the landform development simulation is from the present to approximately 120 000 years into the future, based on past global climatic cycles with extremely warm and cold periods. Warm periods are assumed to occur from 0 to 30 000 years and from 60 000 to 120 000 years into the future. On the other hand, a cold period is assumed from 30 000 to 60 000 years into the future. The lithologic character is divided into two types; alluvium and bedrock. A digital elevation model with a 10 meter mesh is used for the simulation. Two uplift cases, G1 and J1, were modeled. For the G1 case, it is assumed that the entire area uplifts at 0.3 mm/yr uniformly. For the J1 case, it is assumed that uplift rate is different for each fault block (Figure 5).

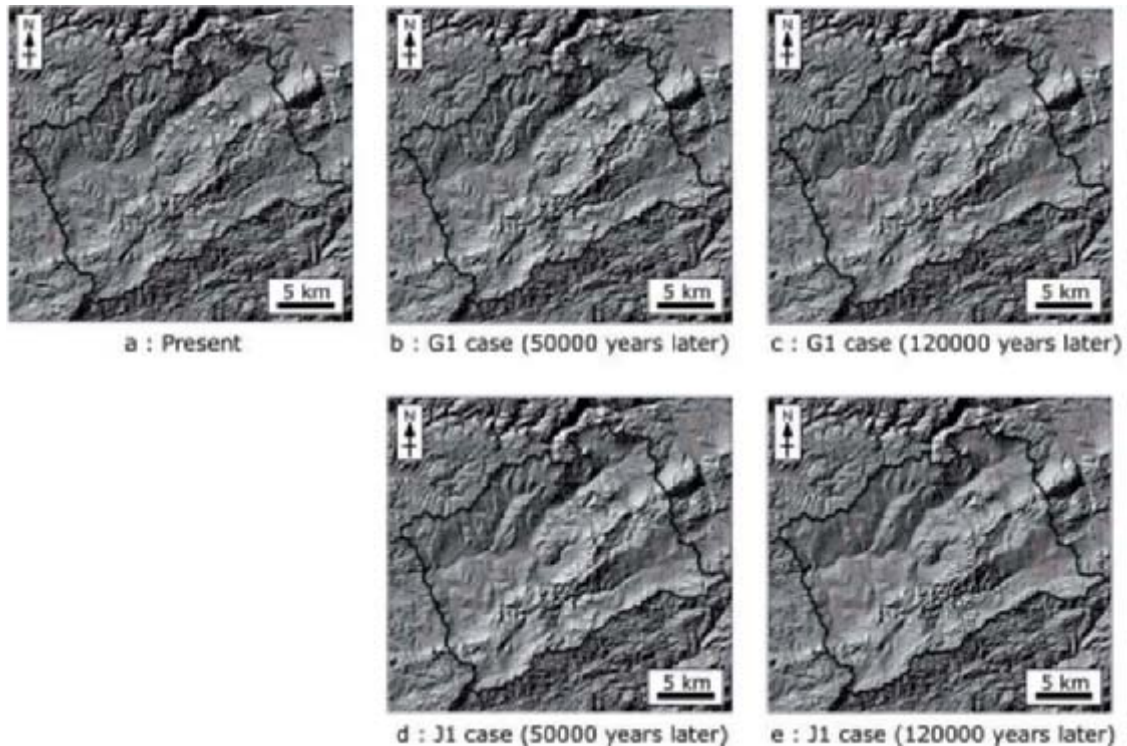
Figure 5. Uplift rate map for J1 case of the simulation



Results of the landform development simulation

There are some problems with the simulation results. For example, topographic change with high resolution cannot be simulated, and overall the landforms become more subdued due to erosion. However, the simulation results generally show the development of landforms consistent with current topographical knowledge, e.g. enhanced erosion because of high relief energy (Figure 6). The maximum erosion after about 120 000 years, for the G1 and J1 cases are about 140 meters and about 200 meters, respectively. The simulated absolute value does not show actual quantity of landform development because many of the input parameters for these simulations are hypothetical.

Figure 6. Results of landform development simulation



Groundwater flow simulation

The time 50 000 years into the future (a cold period in the landform development simulation) has been selected as the time for the groundwater flow simulations in order to evaluate the effect of a major climatic perturbation, as well as major topographic change. The time 120 000 years into the future (warm period) has also been selected to evaluate the effect of topographic perturbations. In the warm period, the climatic condition was assumed to be same as present climatic condition.

Hydrogeological modeling and groundwater flow simulations were carried out using the newly developed software system (GEOMASS system; geological modelling analysis and simulation software system) [9-10]. The GEOMASS system has been developed by JAEA for integration of the results of 3-D geological modeling using a commercial system (EarthVision®), with automatic 3-D grid generation and groundwater flow simulation using the proprietary code (Frac-Affinity), which is based on the finite difference method.

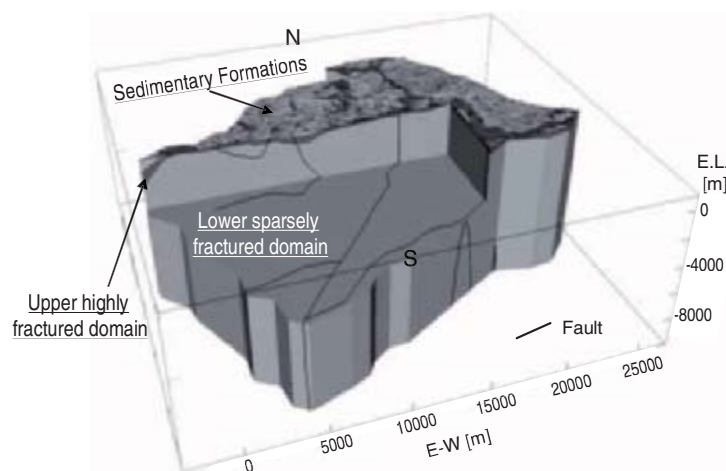
Development of hydrogeological models

The topographic conditions predicted by the landform development simulation have been used as the upper boundary surface in the geological and hydrogeological models. The topographic conditions, lithological units and geological structures, all of which are considered to have a great effect on groundwater flow, are spatially represented in the geological model. Therefore, the geological model serves as a template for the hydrogeological and the geochemical models. The follows were modeled:

- Topographic conditions.
- Sedimentary formations.
- Geological structures such as an upper highly fractured domain and a lower sparsely fractured domain in granite.
- Faults [Byobuyama fault, Enasan fault and Kasahara fault (Figure 2)].

Geometries of the boundary surface of selected lithological units and structures were modeled independently at first. Then, a 3-D geological model was constructed combining the 3-D tectonic structure model and the geological sequence, as shown in Figure 7.

Figure 7. **Geological model**



In the geological modelling, the lithological units and structures were classified from a hydrogeological point of view. Hydraulic conductivities in each lithological unit were assumed to be homogeneous and were assigned geometric mean values from the results of long interval hydraulic testing [1,2,3,5], as shown in Table 1.

Table 1. **Hydraulic parameters of the hydrogeological model**

Unit	Hydraulic Conductivity (m/s)
Sedimentary Formations	Horizontal: 1.0E-05 Vertical: 1.0E-07
Upper highly fractured domain	4.0E-07
Lower sparsely fractured domain	3.2E-08
Faults (Byobuyama Fault, Enasan Fault and Kasahara Fault)	Normal to fault: 1.0E-11 Parallel to fault: 7.0E-06

All faults were modeled with hydraulic anisotropy (hydraulic conductivity parallel to fault plane higher than hydraulic conductivity normal to fault) based on the hydraulic characteristic of the Tsukiyoshi fault [1,2,3,5] and large scale faults located around the study area.

Groundwater flow simulation cases

Groundwater flow simulations cases are summarised in Table 2. It is considered that recharge rate in a cold period will decrease due to decrease in precipitation. However, there is a large uncertainty in estimation of recharge rate during a cold period. In particular, large uncertainty exists in the estimation of evapotranspiration. Hence, three recharge rates were assigned (25%, 50% and 75% of present recharge) to evaluate the effect of climatic perturbations in this study. A 3-D steady state groundwater flow simulation with saturated and unsaturated conditions has been carried out.

Table 2. **Groundwater flow simulation case**

Simulation Case	Case of the Landform development simulation	Time of groundwater flow simulation	Recharge rate
Regional_t000	Present		Measured value
G1Regional_t050_025	G1 Case	50,000 years into future	25 % of recharge rate at present
G1Regional_t050_050			50 % of recharge rate at present
G1Regional_t050_075			75% of recharge rate at present
G1Regional_t120		120,000 years into future	Same as recharge rate at present
J1Regional_t050_025	J1 Case	50,000 years into future	25 % of recharge rate at present
J1Regional_t050_050			50 % of recharge rate at present
J1Regional_t050_075			75% of recharge rate at present
J1Regional_t120		120,000 years into future	Same as recharge rate at present

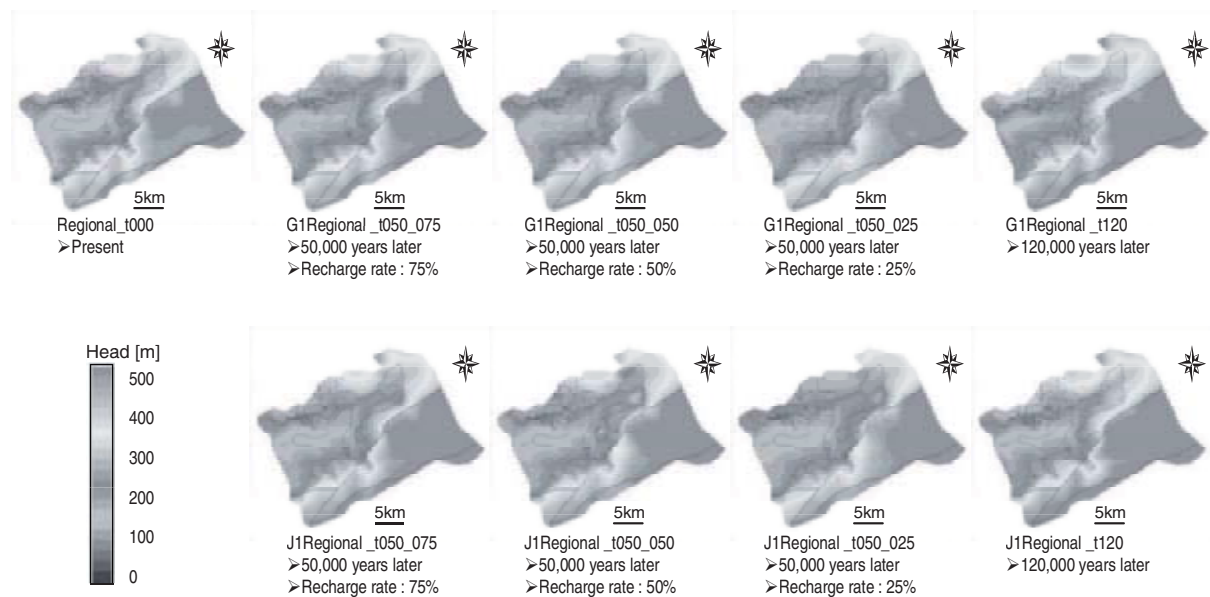
Boundary conditions

A constant recharge rate boundary was set at the upper boundary. Since side boundaries of the study area were located at the boundary of a large river basin, no-flow boundary conditions were selected. A constant head boundary was set for the part of the model at the Toki River. A no-flow boundary condition was set at the bottom boundary.

Results of groundwater flow simulation

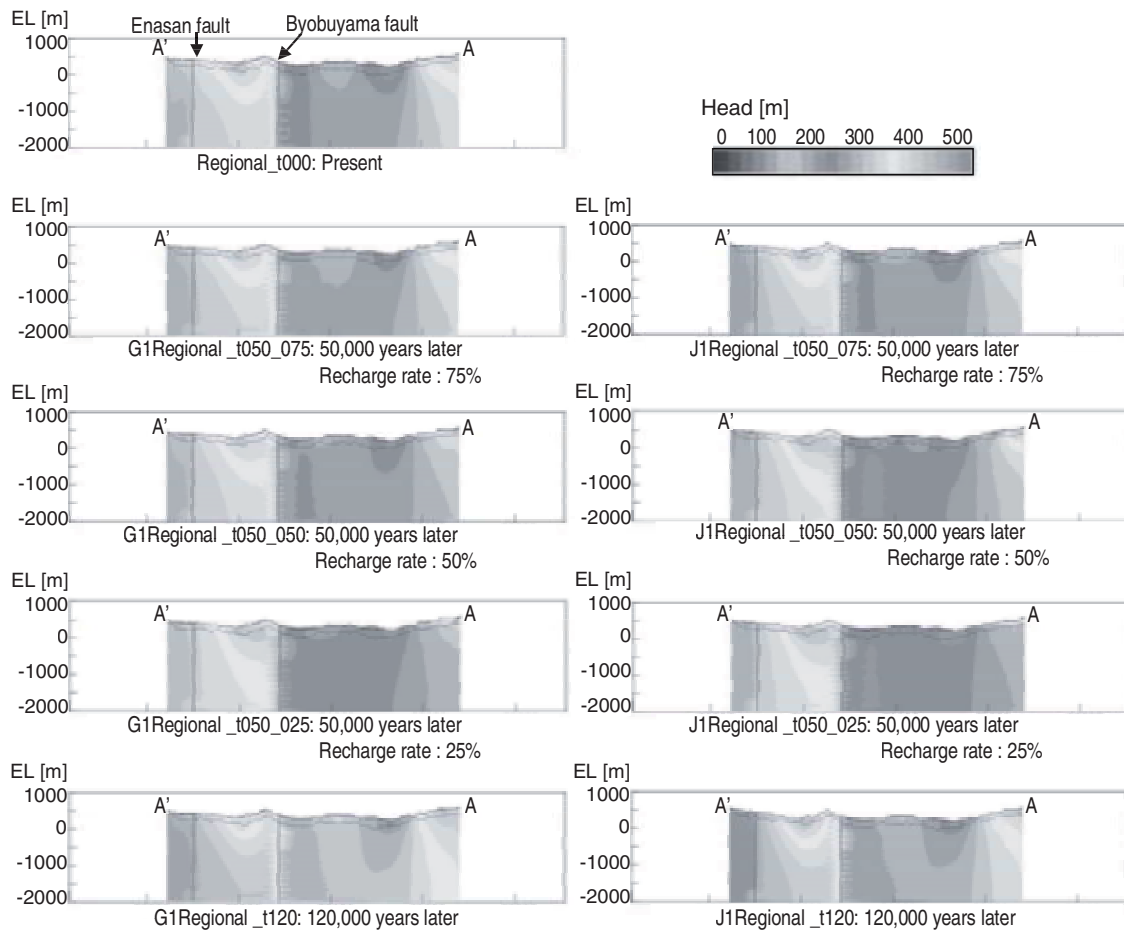
Head distributions on the horizontal plane at E.L. 100m and the cross-section along line A-A' shown in Figure 2 were compared to evaluate the effects of future topographic and climatic perturbations on groundwater flow conditions (Figures 8 and 9).

Figure 8. Head distributions on horizontal plane at E.L. 100m



Based on the groundwater flow simulations during the cold period, drawdown of water table is recognized. The drawdown is especially large in the recharge area. The recharge areas almost coincide with the mountainous area with high uplift rates. The drawdown is caused by decrease in recharge rate. Hydraulic gradients from recharge area to discharge area also decrease due to decrease in recharge rate. In particular, decrease in the hydraulic gradient occurred in the area between the northern recharge area (“A” in Figure 9) and the Byobuyama fault. On the other hand, decrease in hydraulic gradient is not significant in the area between the Byobuyama and Enasan faults. This tendency is observed for both cases, G1 and J1.

Figure 9. Head distributions on cross-sections along the A-A' line in Figure 2



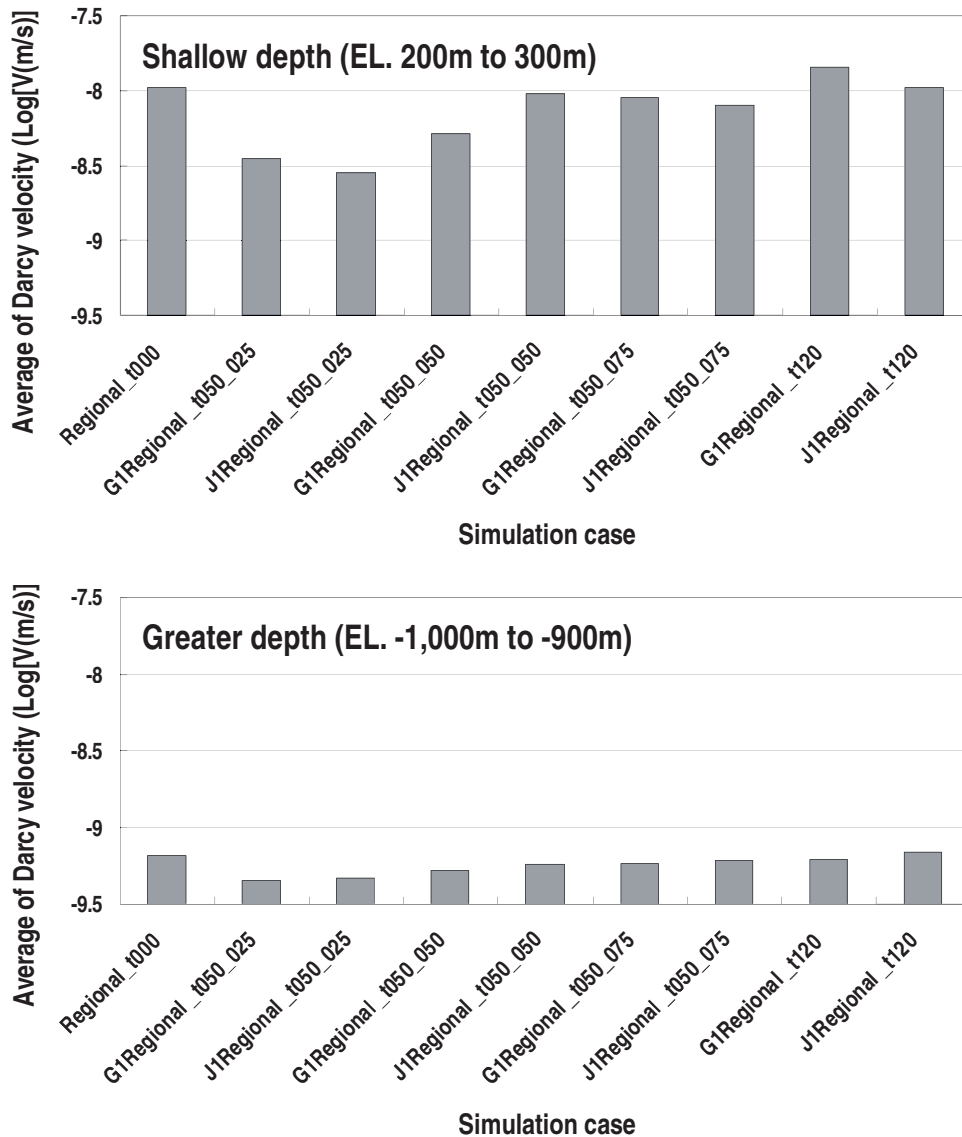
The water table in the recharge areas rises considerably at 120 000 years into the future. The effect of the rising water table in the recharge area on the hydraulic gradient in the area between the Byobuyama and Enasan faults is not significant. The rise of the water table in the G1 and J1 cases is different in the recharge areas. However, the effect of the difference on the hydraulic gradient in the area between the Byobuyama and Enasan faults is also not significant.

The reason considered for these results is that there are anisotropic faults normal to the major direction of groundwater flow and the faults limit the effect of the changing water table on the hydraulic gradient downstream of the fault.

Also, it is found that the influence of topographic and climatic perturbations on hydraulic gradient gradually decrease with depth.

The average Darcy velocities in 100 m vertical intervals were compared. Figure 10 shows the average Darcy velocity at shallow (EL. 200 m to 300 m) and at greater depths (EL. - 1 000 to - 900 m). Variations of the simulated Darcy velocities at shallow depth are much larger than at greater depth. The magnitude of the Darcy velocity at shallow depths is also larger than at greater depths.

Figure 10. Average of Darcy velocities



Conclusion and future study

In this study, the effects of long term changes to topographical relief on the results of groundwater flow simulations have been evaluated. Consequently, it has been confirmed that the method combining simulations of landform development and groundwater flow is useful for the evaluation of effects of topographic and climatic perturbations on groundwater flow conditions.

In future studies, field investigations to obtain site-specific data regarding topographic and climatic perturbations and hydrogeological characterisation of a fault will be carried out in order to confirm appropriateness of the general hypotheses and input parameters used in the simulations carried out in this study. For example, investigations such as pollen analysis for paleoclimate studies and terrace investigations to assess uplift rates are possible.

Acknowledgement

This study was carried out with the technical support and discussion of Dr. Michio Nogami of the Nihon University, Mr. Tomoji Sanga of the Nikko Exploration & Development Co., LTD, Dr. Kaoru Inaba of the Takenaka Cooperation, and Dr. Glen McCrank. The authors gratefully acknowledge them.

References

1. Japan Nuclear Cycle Development Institute, (2000), *Regional Hydrogeological Study Project. Results from 1992-1999 Period*, JNC TN7400 2000-014.
2. Japan Nuclear Cycle Development Institute, (2005), *H17: Development and management of the technical knowledge base for the geological disposal of HLW, Supporting Report 1: Geoscience study*, JNC TN1400 2005-014.
3. Ota, K., T. Sato, S. Takeuchi, T. Iwatsuki, K. Amano, H. Saegusa, T. Matsuoka and H. Onoe, (2005), *Technical expertise gained from the surface-based investigations at the Tono area*, Japan Nuclear Cycle Development Institute, JNC TN7400 2005-023.
4. Japan Nuclear Cycle Development Institute, (2003), *Master Plan of the Mizunami Underground Research Laboratory Project*, JNC TN7410 2003-001.
5. Saegusa, H., Y. Seno, S. Nakama, T. Tsuruta, T. Iwatsuki, K. Amano, R. Takeuchi, T. Matsuoka, H. Onoe, T. Mizuno, T. Ohyama, K. Hama, T. Sato, M. Kuji, H. Kuroda, T. Semba, M. Uchida, K. Sugihara and M. Sakamaki, (2007), *Final Report on the Surface-based Investigation (Phase I) at the Mizunami Underground Laboratory Project*, Japan Atomic Energy Agency, JAEA-Research 2007-043.
6. Nogami, M., O. Fujiwara and T. Sanga, (2002), *Simulation of a small drainage basin during the future of 120 000 years.*, Trans. Jap. Geomorph. Union, 24. pp.105-106.
7. Geological survey of Japan, (1992), *1:1,000,000 Geological Map of Japan Third Edition*
8. Hirano, M., *A mathematical model of slope development*. Jour. Geosci., Osaka City Univ., 11, pp.13-52.
9. White, J.M., P.J. Humm, N. Todaka, S. Takeuchi and K. Oyamada, (1998), *GEOMASS: Geological Modelling Analysis And Simulation Software for the characterization of fractured hard rock environments*, Proc. the third Äspö International Seminar, Oskarshamn, June 10-12 1998, SKB Technical Report, TR-98-10,233-242.
10. Saegusa, H., J.M. White, P. Robinson and J. Guimerà, (2006), *Development of a System for Integrated Geological Modelling and Groundwater Flow Simulation*, Proceedings of the 11th International High-Level Radioactive Waste Management Conference, April 30 – May 4, 2006, Las Vegas, NV, USA, pp.330-337.

IMPACTS OF NATURAL EVENTS AND PROCESSES ON GROUNDWATER FLOW CONDITIONS: A CASE STUDY IN THE HORONOBE AREA, HOKKAIDO, NORTHERN JAPAN

T. Niizato, K-I. Yasue, H. Kurikami
Japan Atomic Energy Agency, Japan

Abstract

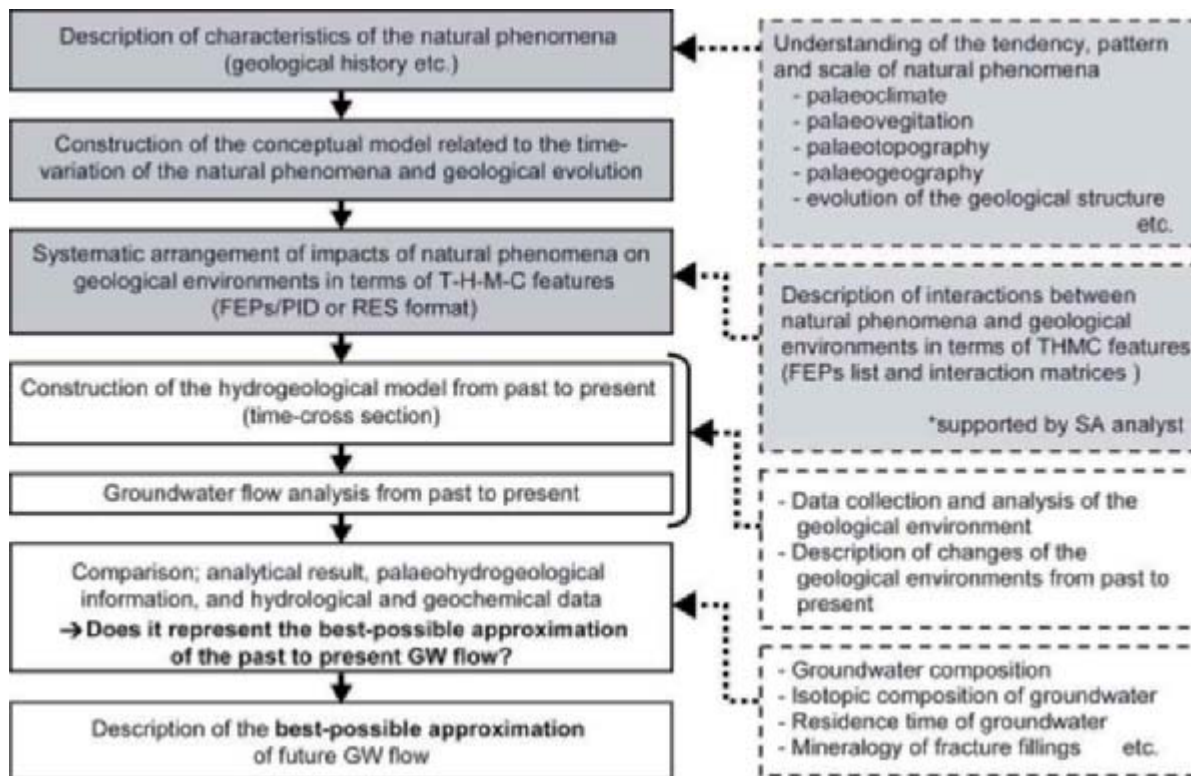
In order to assess the long-term stability of the geological environments for over several hundred thousand years, it is important to consider the influence of natural events and processes, such as uplift, subsidence, denudation and climate change, on the geological environments, especially in an active region such as Japan. This study presents a conceptual model related to the future natural events and processes which have potential impacts on the groundwater flow conditions in the Horonobe area, Hokkaido, northern Japan on the basis of the neotectonics, palaeogeography, palaeoclimate, historical development of landform, and present state of groundwater flow conditions. We conclude that it is important to consider interactions among natural events and processes on the describing of the best-possible approximation of the time-variation of geological environment.

Introduction

In research and development for geological disposal of high-level radioactive waste, it is important to establish comprehensive investigation and analysis technique of describing future evolutions of the geological environment in consideration of influence of the natural events and processes. Prediction methods of geological environments are roughly classified into four categories: 1) prediction by extrapolation, 2) prediction by analogy (e.g. natural analogue), 3) prediction by probability, and 4) prediction by numerical simulation (e.g. Kusunose and Koide, 2001). In any method, the studying the past to the present is fundamental approach to reach to a best-possible approximation of the future geological environments.

This paper provides a conceptual model related to the future natural events and processes which have potential impacts on the groundwater flow conditions in the Horonobe area, Hokkaido, northern Japan on the basis of the tectonics, palaeogeography, palaeoclimate, historical development of landform, and present state of groundwater flow condition. It also suggests the interaction matrices of the natural events and processes. The items included in the matrices are important for the description of the future geological environments in the area situated in the coast and sedimentary basin, such as the Horonobe area. The range of this study in the sequence of tasks for the description of the future groundwater flow conditions is shown in Figure 1. The approach employed in this study is based on the framework of palaeo-hydrogeological study proposed by Chapman and McEwen (1992) and Yusa *et al.* (1992).

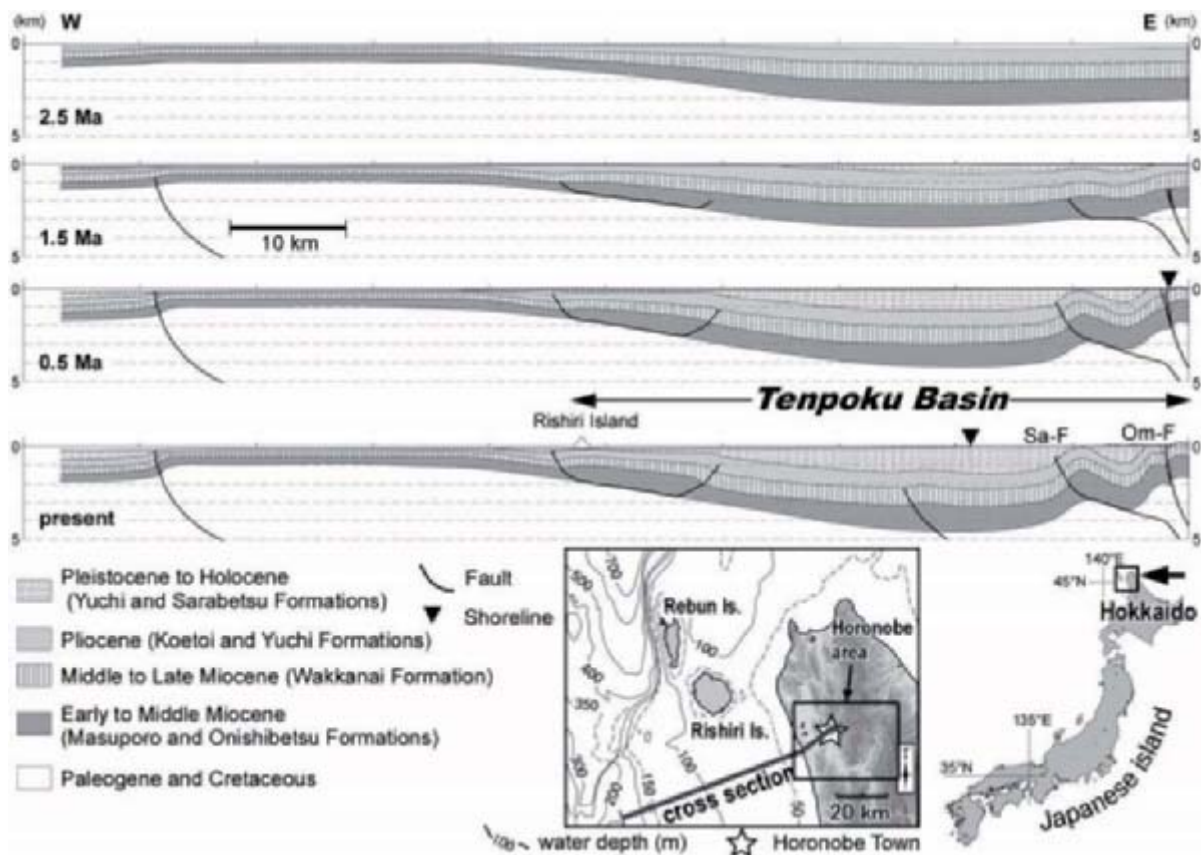
Figure 1. A framework of the study on the long-term stability of the geological environments in and around the Horonobe area. The tasks in grey boxes indicate the range of this study.



Outline of geology

The Horonobe area is situated in the eastern part of the Tenpoku Basin, and its geology is dominated by the Neogene to Quarternary sedimentary sequences, that is, Onishibetsu (alternating beds of conglomerate, sandstone, and mudstone, intercalated with coal seams), Masuporo (alternating beds of conglomerate, sandstone, and mudstone), Wakkanai (diatomaceous and siliceous shale), Koetoi (diatomaceous and siliceous mudstone), Yuchi (sandstone), and Sarabetsu Formations (alternating beds of conglomerate, sandstone, and mudstone, intercalated with coal seams) in ascending order. These formations are unconformably overlain by terrace deposits, alluvium, and lagoonal deposits (unconsolidated deposits of gravel, sand, and mud). The growth structures of the fold-and-thrust belt of northern Hokkaido indicated by seismic reflection profiles suggest that the ongoing EW compressive tectonics (neotectonics) in the western part of the Horonobe area has begun in Late Pliocene time (Figure 2).

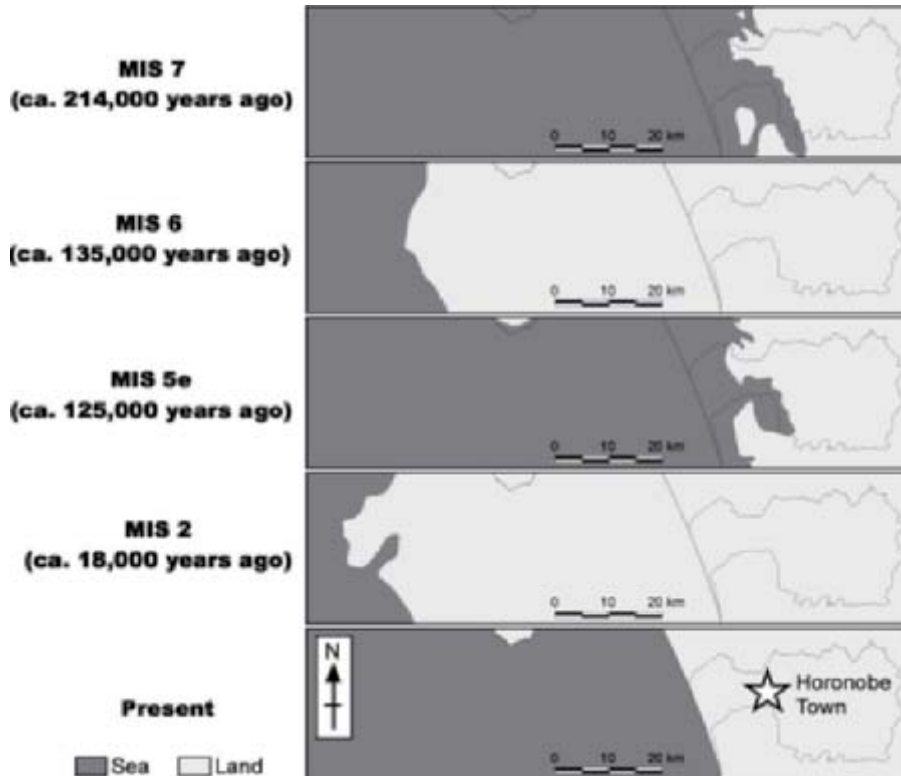
Figure 2. Geological evolution in the Horonobe area since Late Pliocene, Partly modified from Niizato *et al.* (2007). The shaded relief map is after geographical survey institute (2001). Sa-F: Sarobetsu fault zone, Om-F: Omagari fault.



Based on the time-stratigraphy and sedimentary analysis, the development of the structures has resulted in westward migration of the depositional area in the Tenpoku Basin (Yasue *et al.*, 2005). In addition, the distribution of hypocenters for micro-earthquake, active structures, and the Quaternary sediments indicates that present-day activity has been localized with the western part of the Horonobe area.

The Horonobe area has widespread distribution of the marine terrace deposits, which are correlated to the marine oxygen isotope stage (MIS) 7 through 5e. Figure 3 shows the palaeogeography in the area from MIS7 to the present on the basis of the formative age and distribution of the deposits, global-scale sea-level change, and sea-floor topography. The former shorelines of interglacial stages (e.g. MIS5e) have proceeded ca. 12 km away from that of the present on the landward. On the other hand, the former shorelines of glacial stages (e.g. MIS2) have proceeded ca. 50 km away from the present shorelines on the seaward. The great migration of the shoreline caused by glacial-interglacial cycles is attributed to the gentle slope of sea-floor topography.

Figure 3. Palaeogeography from MIS7 to the present in and around the Horonobe area, Partly modified from Niizato *et al.* (2007). The age of each MIS stage is after Koike and Machida (2001).



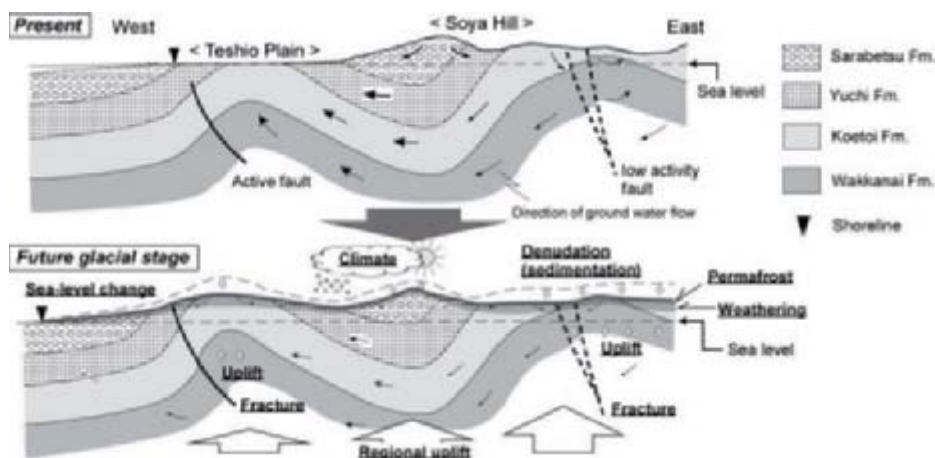
Additionally, we can point out a few natural events and processes which have potential impacts on the groundwater flow conditions. The main phenomena are as follows:

- Distribution of the fossil periglacial wedges suggests that northern Hokkaido was located in the northern margin of the discontinuous permafrost zone during the maximum cold stage of the Last Glacial Age (MIS2; Miura and Hirakawa, 1995).
- The relationship between geology and geomorphology (hill morphology, drainage pattern, etc.) suggests that geomorphic processes are different in each geological formation (Ota, *et al.*, 2007).
- A change in porosity due to burial process will also change hydraulic conductivity and transport properties of formations. This time-dependent phenomena will proceed in time frame of ten thousand to one million years.

Conceptual model for future geological evolution and geological environments

Consequently, natural events and processes which have potential impacts on groundwater flow conditions in the Horonobe area are summarised in Figure 4. The figure represents the situation in the present and future glacial stage with some exaggerations on the basis of the tectonics, palaeogeography, palaeoclimate, historical development of landform, and present-state of groundwater flow conditions in the area. Also, it assumed that the future natural events and processes will behave much as it did in past and does in the present (the past is the key to the future).

Figure 4. **A conceptual model for natural phenomena That have potential impacts on groundwater flow conditions in the Horonobe area, partly modified from Niizato *et al.* (2007)**



The groundwater flow conditions (direction and flux) in the present are taken and simplified from Kurikami *et al.* (2006). The conditions in the future glacial stage are conceptually drawn in consideration of impacts of future natural events and processes on the groundwater flow conditions in the present. The events and processes with underline in the Figure 4 (lower figure) are important ones for the description of the best-possible approximation of the future groundwater flow conditions. For example, the development of the permafrost will prevent meteoric water from infiltrating to the underground, and then the recharge rate of groundwater will be decreased dramatically. Figure 4 further explains certain types of interactions between natural phenomena. For example, a relative sea-level change is attributed not only to climate change but also to local uplift due to fault movement in the coastal area (see left-hand side on Figure 4). Moreover, a change of base-level of erosion due to sea-level change causes a change of sedimentation and denudation area. As mentioned above, the interactions of natural events and processes impact on geological environments.

The interaction matrices of natural events and processes

All of the geological evolutions, and potential impacts of natural events and processes on the geological environments in the Horonobe area are summarised in Figure 5a and 5b in the form of interaction matrices. These are the current integration and will be updated during the investigation, as additional data and analytical results are obtained.

Figure 5a. **Overview of the Interaction Matrices of Natural Events and Processes in the Horonobe Area. See Figure 5b for Details of the Items Enclosed by Heavy Solid Line.**

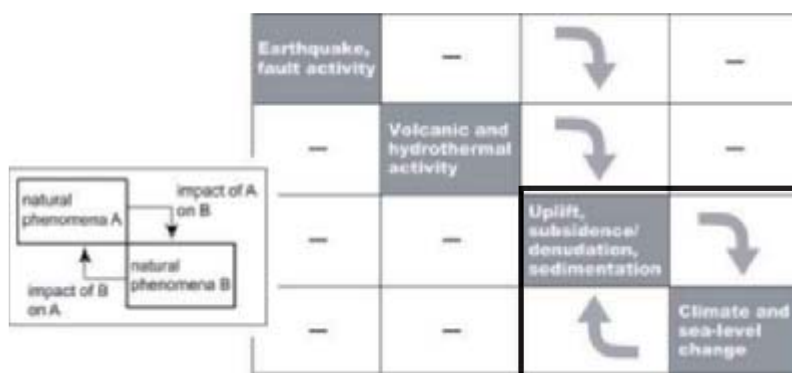
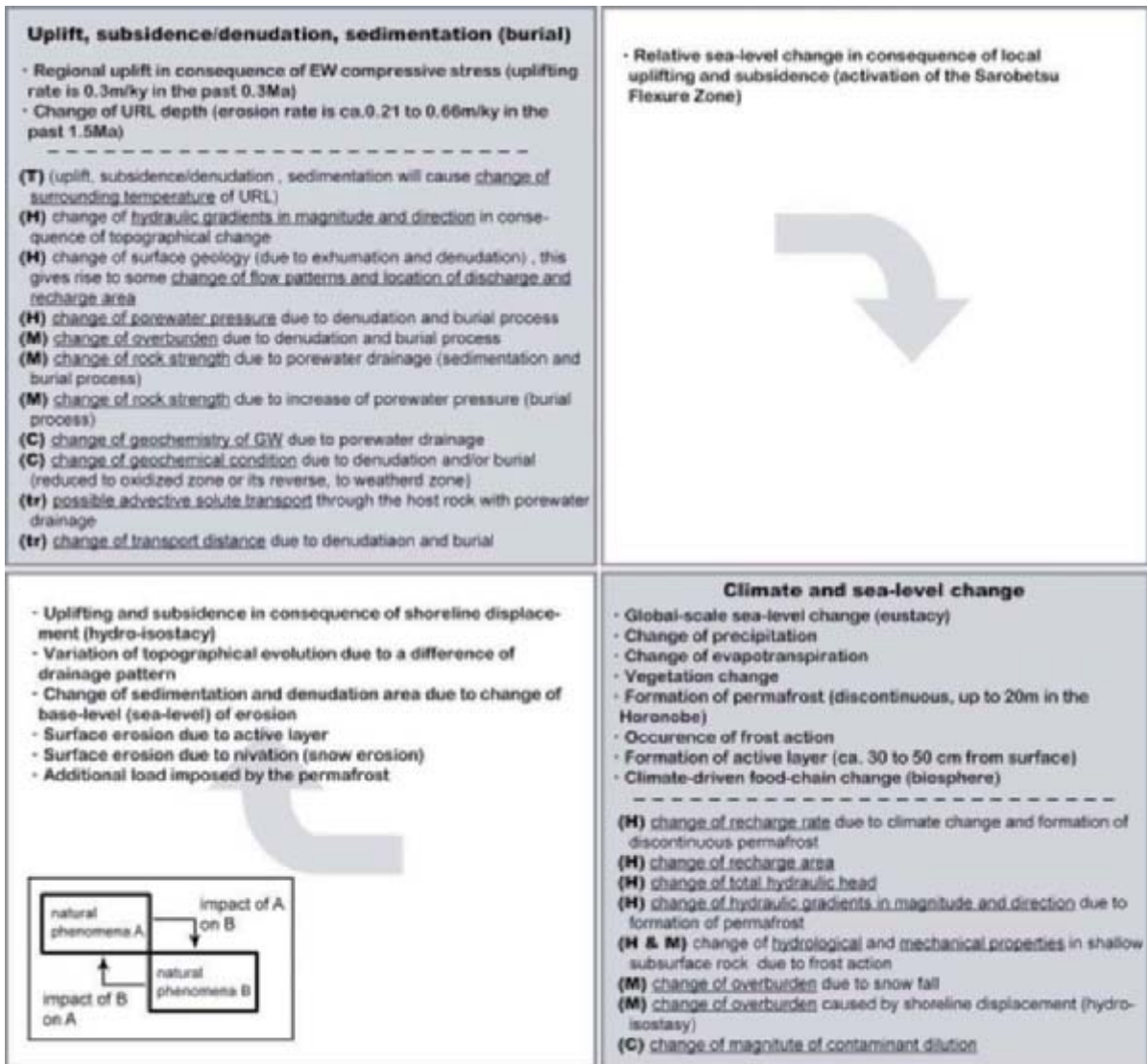


Figure 5b. Details of natural events and processes, Their impacts on geological environments, and interactions of them related to the future evolution of the geological environments, especially for uplift/subsidence, Denudation/sedimentation, and climate and sea-level change, in the Horonobe area.



Bold face: natural phenomena, Regular face: impacts of natural phenomena (underline: **(T)** Thermal, **(H)** Hydrological, **(M)** Mechanical, **(C)** Chemical, **(tr)** transport property) on geological environments.

Conclusion

So far we have outlined the geological evolutions, impacts of natural events and processes on the geological environments, and the interaction of it in the case of the Horonobe area. We conclude that it is important to consider interactions of natural events and processes. If not so, we assume that it is impossible to assess the impacts of natural events and processes on the geological environments, and long-term evolution and stability of it in an appropriate manner.

Acknowledgement

We are grateful to Professor K. Hirakawa of Hokkaido University for many helpful suggestions and encouragement during the course of this study.

References

Chapman, N.A. and T.J. McEwen, (1993), The application of palaeohydrogeological information to repository performance assessment. *In Paleohydrogeological methods and their applications. Proceedings of and NEA workshop, Paris (France), 9-11 November 1992*, OECD, Paris, pp.23-35.

Geographical Survey Institute, (2001), Digital Map 50 m Grid (Elevation) NIPPON-I.

Koike, K. and H. Machida, eds., (2001), *Atlas of Quaternary Marine Terraces in the Japanese Islands*. University of Tokyo Press, p.105 (with CD-ROM and attached map). (*in Japanese*)

Kurikami, H., T. Kunimaru, S. Yabuuchi, S. Seno, M. Shimo and S. Kumamoto, (2006), Hydrogeological model in Horonobe Underground Research Laboratory Project. *GeoProc2006 Advances on Coupled Thermo-Hydro-Mechanical-Chemical Processes in Geosystems and Engineering, Nanjing*, pp.584-589.

Kusunose, K., and H. Koide, (2001), Time frames and uncertainty in assessment of geoscientific environment. *Shigen-to-Sozai*, vol.117, pp.808-815. (*in Japanese with English abstract*)

Miura, H. and K. Hirakawa, (1995), Origin of fossil periglacial wedges in northern and eastern Hokkaido, Japan. *Journal of Geography*, vol.104, pp.189-224. (*in Japanese with English abstract*)

Niizato, T., H. Funaki and K. Yasue, (2007), Paleogeography and geological evolution since the Late Pliocene in and around the Horonobe area, northern Hokkaido. *Journal of Geological Society of Japan*, vol.113 (*Supplement*), pp.119-135. (*in Japanese*)

Ota, K., H. Abe, T. Yamaguchi, T. Kunimaru, E. Ishii, H. Kurikami, G. Tomura, K. Shibano, K. Hama, H. Matsui, T. Niizato, K. Takahashi, S. Niunoya, H. Ohara, K. Asamori, H. Morioka, H. Funaki, N. Shigeta and T. Fukushima, (2007), *Horonobe Underground Research Laboratory Project Synthesis of Phase I Investigations 2001-2005 Volume "Geoscientific Research"*. JAEA-Research 2007-044. (*in Japanese with English abstract*)

Yasue, K., E. Ishii and T. Niizato, (2005), Neotectonics of the Tenpoku Sedimentary Basin in northern Hokkaido, Japan: a case of Horonobe area. *In: Research on active faulting to mitigate seismic hazards: the state of the art. Abstracts of the HOKUDAN International Symposium on Active Faulting, Hokudan, Japan, January 17th-24th 2005*, pp.176-177.

Yusa, Y., K. Ishimaru, K. Ota and K. Umeda, (1993), Geological and geochemical indicators of paleohydrogeology in Tono uranium deposits, Japan. *In Paleohydrogeological methods and their applications. Proceedings of and NEA workshop, Paris (France), 9-11 November 1992*, OECD, Paris, pp.117-146.

GROUNDWATER FLOW PREDICTION METHOD IN CONSIDERATION OF LONG-TERM TOPOGRAPHIC CHANGES OF UPLIFT AND EROSION

T. Sasaki¹, T. Moritomo¹, H. Ikeda¹, T. Shiraishi², S. Sugi³

¹Japan Nuclear Fuel Limited, ²Shimizu Corporation, ³Dia Consultants Co., Ltd.; Japan

Abstract

When evaluating margin of safety of radioactive waste disposal, leakage and transfer of radioactive material into groundwater are important factors. The evaluation should be done for a long geologic period, such as tens of thousand to hundreds of thousand years, depending on the concentration and quantity of radioactive materials. It is essential to take climatic and topographic changes into consideration of the groundwater flow for such long-term prediction. We examined a method for a long-term prediction, and found it effective through its application to realistic example.

Purpose

Since 1992 in Japan, disposal of low level radioactive wastes generated by operation of nuclear power plant have been carried out at Rokkasho-mura, Aomori Prefecture. At the moment about 80 000 m³ of low level radioactive wastes are authorized to be buried at near-surface sites. On the other hand, methods of disposal for low level wastes not suitable for near-surface burial have been under investigation if they could be disposed at depths over several tens of meters in the ground where it is assumed to be safely isolated for a long-term (called sub-surface disposal).

In July 2007, the Nuclear Safety Commission disclosed a report, “Fundamental guidelines of safety regulation of low level radioactive waste (Interim report),” in which they pointed out that when evaluating long-term safety of disposal facilities, various uncertainties have to be taken into consideration. The report said that depending on the levels of uncertainties the evaluations should be classified, based on risk evaluation method, into likely scenario, unlikely scenario, and very unlikely scenario, and for each category tentative dose limit should be applied. Further, it emphasised that in likely scenario of sub-surface disposal, a suitable groundwater scenario should be considered taking effects of long-term geologic changes such as uplift, subsidence, sediment deposition, erosion, sea water level change etc. into consideration as well as climatic change from the viewpoints of isolating the waste materials from biosphere by deep burial.

There are few examples of groundwater scenario taking long-term effects of geologic and climatic changes, however. We therefore examined long-term (up to tens of thousand years) prediction of groundwater flow from topographic and climatic changes into consideration based on realistic examples and discuss the effectiveness of the method.

Examination procedures

Before starting assessment of examination procedures, it is necessary to see if the items of natural phenomena have possibilities of affecting the groundwater flow. On volcanic activities and faulting, the disposal site is quite unlikely to be affected is confirmed in principle. Next, the laws governing changes of uplift rate and of sea level, and erosional history are examined to predict topographic future. Lastly, based on the changes of topography and climate, groundwater flow in the future is estimated.

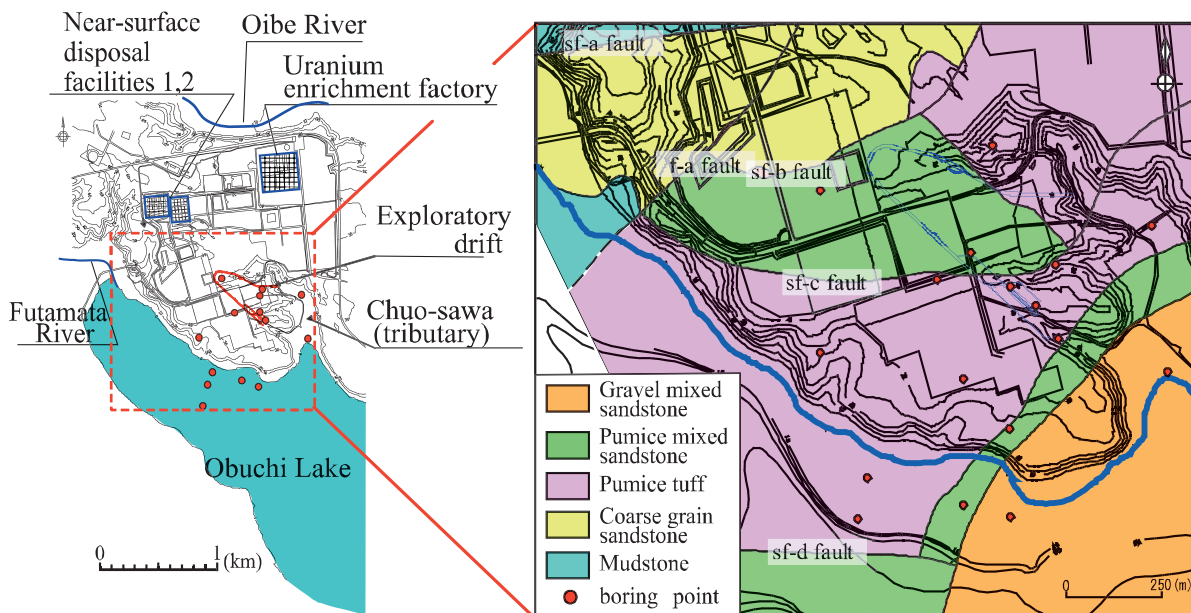
Outline of geology, groundwater, and climate of the area examined

Topography and Geology

The research area is situated on the Pacific side of southern Shimokita Peninsula, Aomori Prefecture. It is bounded in the north by Oibe River, and south by Futamata River and Obuchi Lake, and a plateau consisting of sea terraces about 30 to 60 m a.s.l.

Geology of the area is Miocene pumiceous tuff and pumice mixed sandstone (Takahoko Formation). The thickness of each bed is 10 to 50 m. It is overlain by about 10 m thick Quaternary terrace deposits and volcanic ash beds (Figure 1).

Figure 1. **Geologic map of research area (Horizontal slice EL.-80m)**



Takahoko Formation is dominated by low-angle fractures which are assumed to have been formed by unloading of overlying strata during uplift. Density of fracture distribution tends to become less from the ground surface to the depths. At depths below 50 m from the ground surface, numbers of fractures are about 0.3 to 1.3 per 10 m, somewhat depending on the type of rocks. As far as examined on the exploratory drift walls at depth below 50 m, 90 % of apparent lengths of the fractures tend to be shorter than 5 m.

Groundwater

Hydraulic conductivities of Takahoko Formation measured at bore holes are mostly in the order of 1×10^{-8} m/s \sim 1×10^{-9} m/s with slight differences among different rock types and depths. Flow porosities measured on boring cores by tracer test tend to be large at 11 to 57 % suggesting that the matrix of the basement rocks is porous easily allowing groundwater flow. Also, fractures seem to be not connected to each other because their densities are small, and it is judged that most of the groundwater flow occurs through matrix and scattered non-continuous fractures.

Water table is located within the Quaternary beds about 10 m thick overlying the terraces and its surface shape follows topography. Judged from topography and pore water pressure measurements, the groundwater recharged on the terraces is estimated to be discharged to the lakes and valleys of surrounding areas. Based on chemical analyses and resistivity data, stagnant high salinity fossil sea water seems to exist at depths deeper than 300 m. Therefore, the depths of infiltrated groundwater from the surface seem to be restricted about above 300 m depth. The flow velocity of the groundwater estimated from hydraulic conductivity, hydraulic gradient, and flow porosity is about 0.01 to 0.1 m per year.

Climate

Climate of the research area is as follows: Average annual atmospheric temperature about 10°C, annual precipitation about 1 300 mm, and average amount of recharge to the groundwater about 250 to 500 mm per year.

Volcanoes and active faults

The research area is situated close to the boundary of North American Plate and Pacific Plate. The subducting Pacific Plate produces volcanic front (eastern edge of distribution of volcanoes) on North American Plate on which the research area is situated. The research area is 20 km to the east of the volcanic front. The position of the volcanic front has not changed much in the last 2 000 000 years.

No active faults have been identified directly beneath the research area. Also there is no active fault that to extend to the research area.

From the above, the disposal site is unlikely to be directly influenced by volcanoes and active fault in the future.

Uplift rate

In all Shimokita Peninsula, marine terraces formed during last 700 000 years are distributed. The uplift rate is between 20 m per 100 000 years and 45 m per 100 000 years, and uplift rate at each area is estimated to be steady (Koike *et al.*, 2001). Also this area is under E-W stress field for the last 5 000 000 years.

In the southern part of Shimokita Peninsula within which the research area is located, six marine terraces (MIS11 \sim 5c) formed by uplift movements during the last 400 000 years are identified (Figure 2). Using elevations of old shorelines and relative sea level data of Chappell (1994), uplift rate of the area is estimated as shown in Figure 3. The calculated values are conformable to the present day topography; that is, they are large in high elevation areas and small in low-lying areas.

Figure 2: Classification of marine terraces in the southern part of Shimokita Peninsula

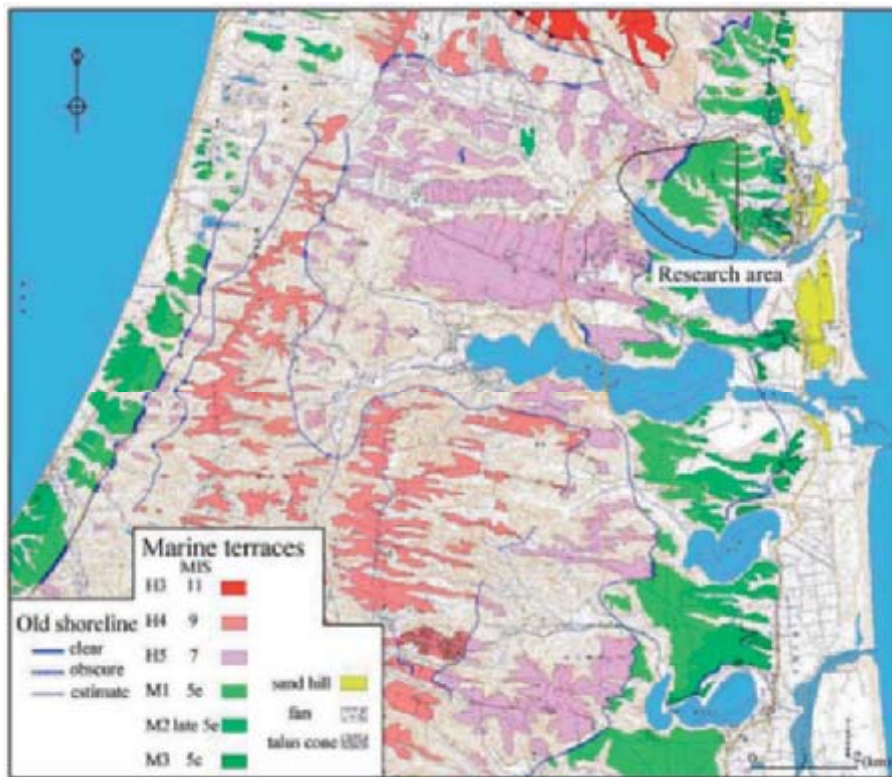
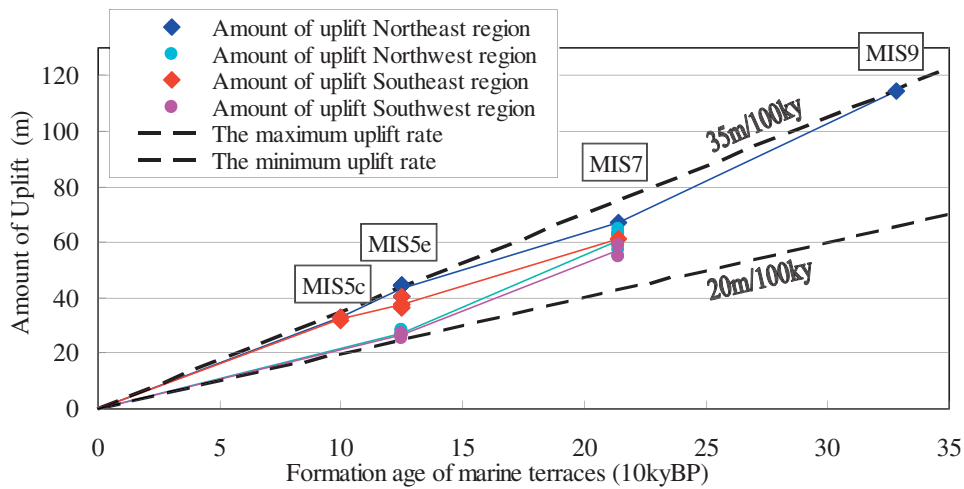


Figure 3. Uplift rate during last 330 000 years in the southern part of Shimokita Peninsula



Plot data are based on clear old shorelines (MIS9, MIS7, MIS5e and MIS5c) of six marine terraces (MIS11 ~ MIS5c).

From the above, predictions are made for the coming several hundreds of thousand years assuming that similar stress field and uplift rate would continue to work. The assumed uplift rate is 35 m per 100 000 years for the research area.

Climatic and sea level changes

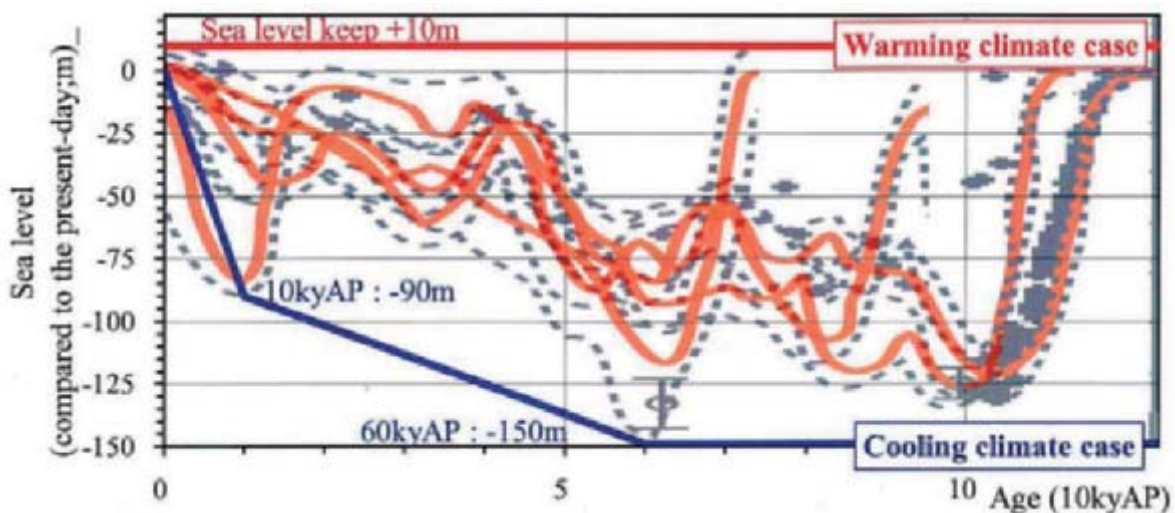
Climatic and sea level changes are claimed to occur due to changes of global air and seawater circulation pattern, and to wax and wane of continental ice sheet caused by changes of solar radiation which could result from change in solar activity or Earth's orbital element or both (e.g. Kumazawa *et al.*, 2002). Sea level changes for the last 450 000 years studied by oxygen isotope ratios such as ($\delta^{18}O$) revealed that the level may have fluctuated with cycles of 80 000 to 120 000 years between +10 m and -130 m as compared to the present level (Labeyrie *et al.*, 2002). Also from salt contents of bottom sediments, Rohling *et al.* (1998) reported that the sea level of the Red Sea about 440 000 yBP was lower than present-day level by $139 \text{ m} \pm 11 \text{ m}$. In addition, Chappell (1994) reported that the range of sea level change was estimated to be within +5 m~-130 m based on the data from sea terrace heights in Huon Peninsula, Papua New Guinea, where uplift rate was found to be exceptionally large.

According to Ishizaki *et al.* (2004), variations of sea water temperatures to the east of the research area deduced from alkenones during last 25 000 years are conformable with the data estimated in north Atlantic. Combined with elevation data of alluvial deposits in the area, the sea level and climatic changes of this area are conformable with global trend.

Climate and sea levels deduced on the cyclic nature of past records indicate a cooler temperature in the future than present-day, as the earth is near the apex of warm period at the moment. However, the amount of solar radiation calculated from earth's orbital element is similar to that of 400 000 years ago, and from this the warm period may last another 15 000 years according to a report (EPICA community members, 2004). Another hypothesis says that according to climate simulation taking the effect of greenhouse gas into it shows that warmer period may last for another 50 000 years (ANDRA, 2005).

As are shown above, there remain too many uncertainties as to the future climate and sea level changes. Here predictions are made for two cases; one for continuing warm period, and the other for cool temperature. As to the sea level, constant +10 m high level than present-day is assumed. For cooling climate cases, -90 m for 10 000 years and -150 m for 60 000 years from now is assumed, based on the case with fastest cooling change among 4 cycles in past 450 000 years (Figure 4).

Figure 4. Forecast sea level changes in the future



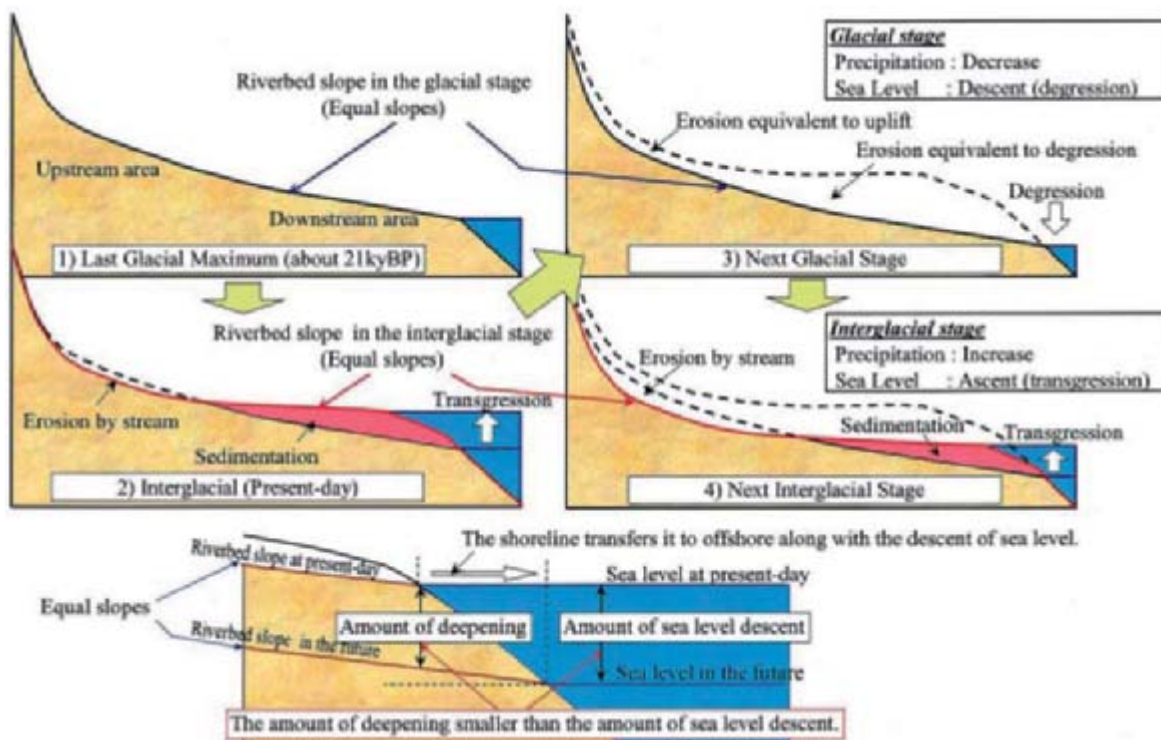
Prediction of future topography

To predict future topography of the research area, it is necessary to understand the erosion proceeds such as fluvial erosion, marine erosion, glacial erosion and wind erosion. However, the surface of the research area is covered by eolian deposits such as loess from China and volcanic ash deposits after the formation of terrace surfaces, and glacial erosion and wind erosion need not be considered. Therefore, for prediction in cooling model, only fluvial erosion related to the lowering of sea level is to be considered. For warming model, as sea level would rise, marine erosion and fluvial erosion are to be considered.

Fluvial erosion

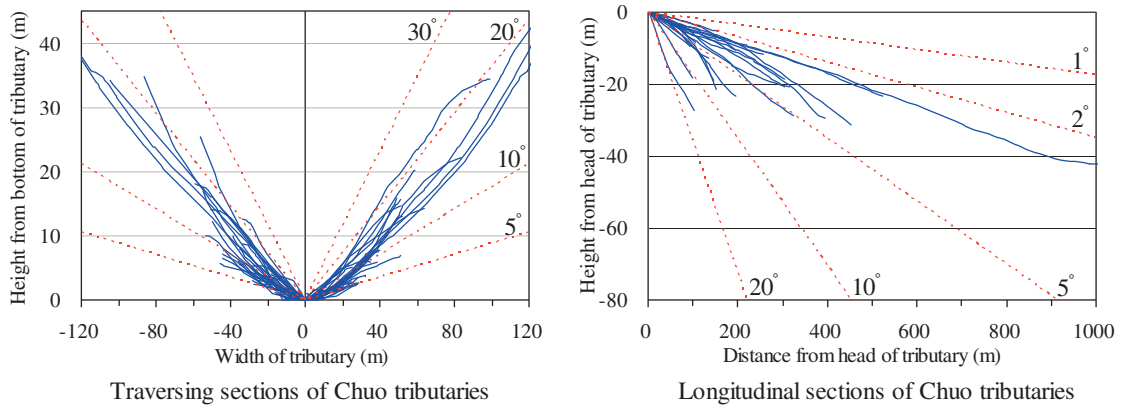
Longitudinal river section at the times of last glacial maximum and interglacial can be known from current riverbed shape, distribution of basal elevations of alluvial deposits, and distribution of fluvial terrace elevations. Therefore, it would be safe to conclude that future erosion would occur along this longitudinal shape. For the amount of deepening, Fujiwara *et al.* (1999) reported that under stable sea level it does not exceed uplift rate. Therefore, it would be safe to assume that the deepening is balanced with uplift rate. The method to estimate amount of fluvial erosion is shown in Figure 5.

Figure 5. Method of estimating fluvial erosion for research area



Erosion by small tributaries are estimated in comparison to erosional shapes on marine terraces at the times of MIS7 (peaked at about 210 000 yBP) and MIS5e (peaked at about 125 000 yBP) and rules of erosion was obtained. In Figure 6 is shown longitudinal and traversing sections of tributaries for different catchments of the research area. From this figure, it is clear that longitudinal and traversing sections show similar shape despite differences in the depths of the tributaries, ages of erosions, and geology. It shows that the erosion in tributaries progresses while holding longitudinal and traversing shapes constant with the major river as datum plane.

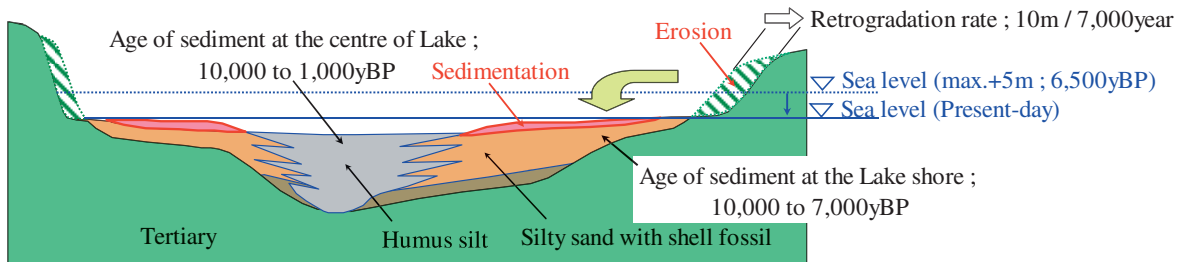
Figure 6. Similarities of longitudinal and traversing sections of tributaries for research area



Marine Erosion

Rate of marine erosion in the research area is estimated from the deposits in nearby Obuchi Lake. As is shown in Figure 7, humus silt is accumulating in the central part of the lake for the last 10 000 years, and no deposits have been supplied from lake shore or sea. On the other hand, sand mixed with silty material is found deposited on the lake shore. The topmost deposits are supplied from materials composing terraces. Therefore, topmost deposits are identified to have derived from eroded terrace materials during hypsithermal period. From the volume of the materials, marine erosion rate would be estimated. Assuming maximum erosional rate, the edges of the terraces are estimated to be eroded at a rate of 10 m per 7 000 years.

Figure 7. Amount of marine erosion as deduced from deposits of Obuchi Lake

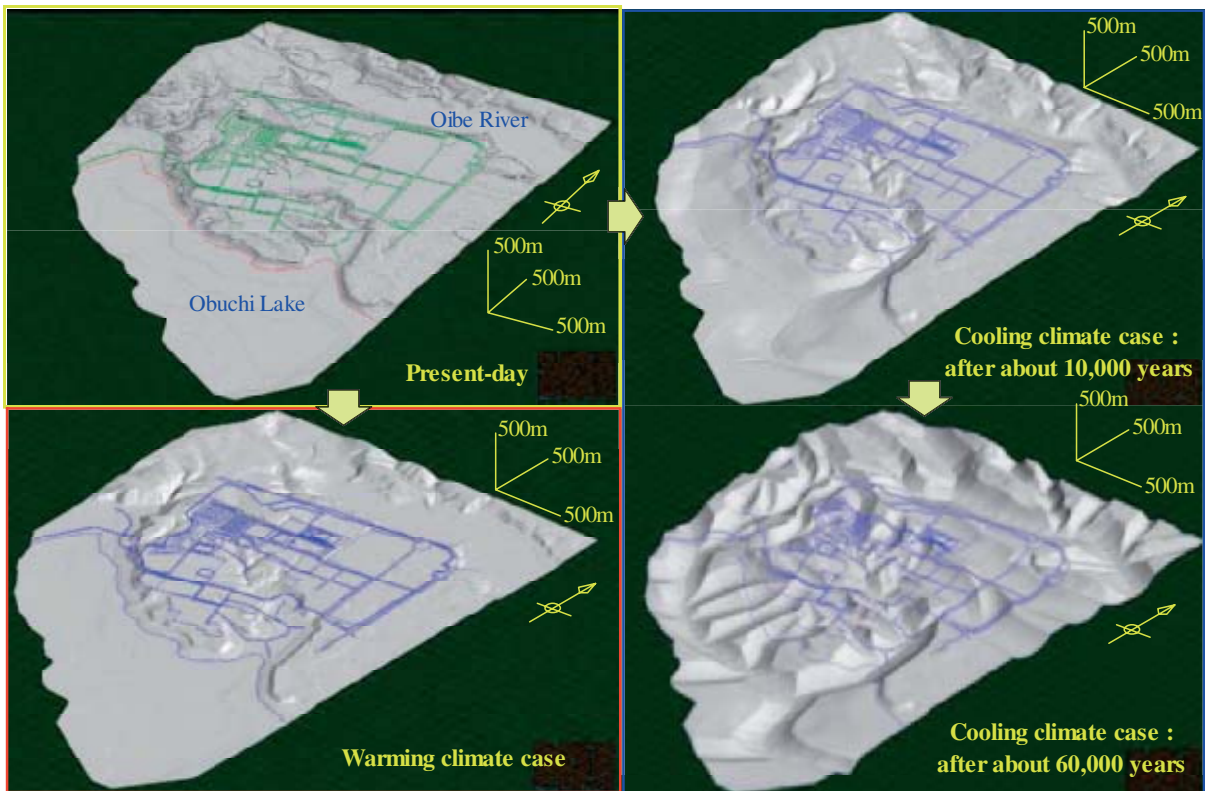


Prediction of topographic change

Upper left in Figure 8 present-day topography of the research area (2 km square) is shown, and upper right and lower right are shown those predicted for 10 000 and 60 000 years from now under cooling climate conditions, respectively. Lower left in Figure 8 is shown future topography under warming conditions. Based on those, future groundwater flow analysis models are produced.

Appropriateness of the future topographic model is judged using erosional rates of marine terraces. Observed erosional rates of marine terraces are about 30 % for MIS5e, which emerged from the sea about 125 000 years ago, while it is about 50% for MIS7, emerged about 214 000 years ago. Calculated erosional rates of future topographic model are found to be about 30 % and 50 % for the terraces corresponding to about 125 000 and 214 000 years, respectively, after emergence from the sea. The fact that those values match with observed values confirm the appropriateness of the model.

Figure 8. Bird's eye view of topographic model



Prediction of groundwater flow pattern

Analysis model and boundary conditions

Groundwater flow pattern in the future is analyzed using three dimensional FEM model. Two analyzed areas, one regional model of 20 km across and another medium-sized model of 10 km across have been chosen and influences of geology and geography as well as sea water-fresh water boundary are considered (Figure 9). The results show that groundwater of research area flows within a drainage area of about 2 km which is bounded by closest river and lake. Also it is clear that very little intermixing occurs between water at depths deeper than 300 m, where fine-grained sandstone and mudstone with lower hydraulic conductivity is distributed, and the water of shallower depths. From these results, further detailed analysis is carried out for a 2 km square area. The chosen area is bounded in the north, west, and south by drainage area consisting of rivers and a lake. The boundary is assumed to be impervious. The eastern boundary is assumed to be where flowing out occurs (hydraulic head value is fixed based on the regional model analysis). The base of the groundwater flow is also assumed to be impervious at depth of 300 m (Figure 10).

Hydraulic conductivity is assumed to be the same with that obtained from in situ permeability test of included fractures. To confirm the influence of fractures on groundwater flow, gross permeability for rocks with fractures and actual matrix is analytically examined. Specifically, density, dip and strike, and expanse of fractures are set at statistically matching values, and only positions of fractures are randomized in Monte Carlo method in preparing three dimensional groundwater flow analysis model. Through flowing of water and other materials to this model, parameters necessary to calculate gross hydraulic conductivity and gross flow rate are obtained.

Figure 9. Regional analysis model of groundwater flow

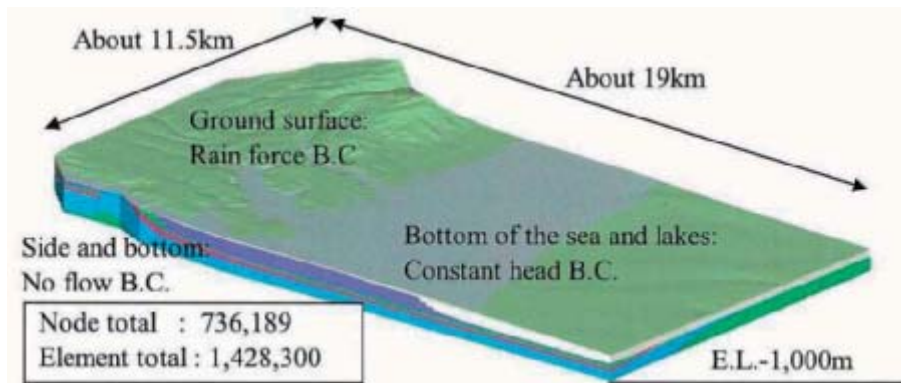
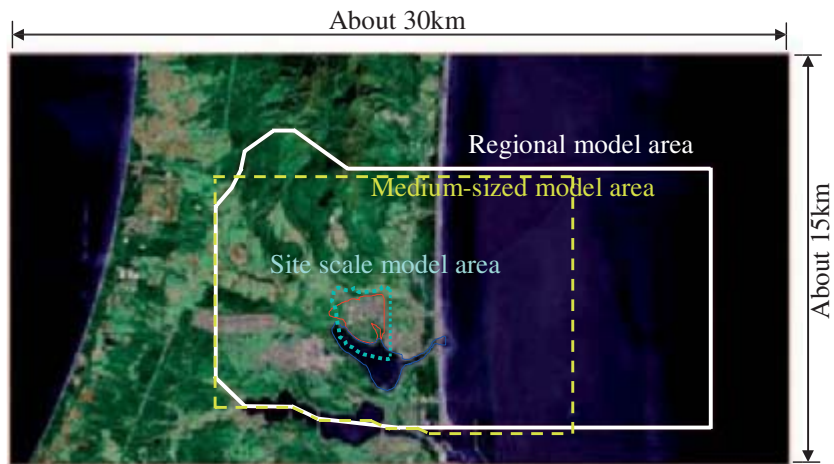
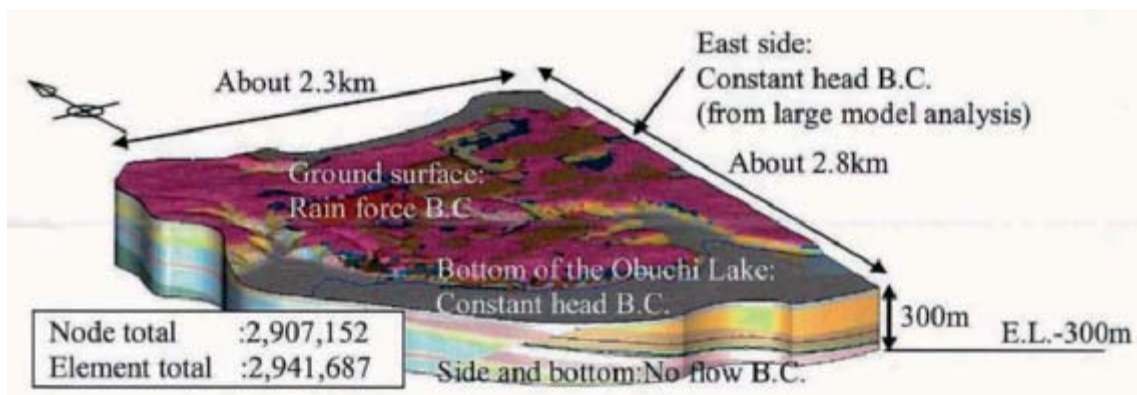


Figure 10. Groundwater flow analysis model (for an area detailed study is carried out)



Within the 2 km square of research area for groundwater flow analysis, drilling survey at 250 m grids has been carried out. Some three dimensional reflection seismic survey data are available, in addition to geologic observations on exploratory tunnel. Therefore, detailed geology of the area is well known. Also in situ permeability tests utilizing drill holes are carried out which reveal relationships between rock types and hydraulic conductivities, and state of weathering and depths. As a result of these data it becomes clear that hydrographic characteristics such as hydraulic conductivity, effective flow porosity should be set for each rock type (hydrogeological classification) for realistic modeling.

To the upper part of the model is given infiltrating precipitation. The rate of infiltration is given to conform, in average, calculated groundwater level to observed level. On the other hand, future rate of infiltration in glacial period may become less with the decrease of precipitation. Therefore, it is assumed that the brown discoloration shown in weathered rocks represents groundwater level at the glacial maximum period about 20 000 yBP with lowest temperature, and calculation of the amount of infiltration from analysis is carried out.

Confirmation of model

To confirm validity of the groundwater flow analysis model, calculated values of pore water pressure distribution, amount of spring water seeping into exploratory tunnel, and groundwater quality are compared to those of observed. The calculated pore water pressure distribution shows similar trend with that of observed. Thus, it is confirmed that hydrographic classification and relative hydraulic conductivity allotted to each rock type are properly modeled. Also, amount of groundwater discharge to drift is found to be matching between calculated and observed, confirming the validity of allocated hydraulic conductivity to the rocks near the tunnel, which in turn confirms the validity of the allocation of hydraulic conductivity and the model as a whole (Figure 11). In the meantime as to the water quality, groundwater collected from several boreholes are analyzed for oxygen/hydrogen isotopic ratios ($\delta^{18}O$, δD). Some groundwater show small isotopic ratios indicating that they originate at the time of prevailing low temperature during glacial maximum period of 10 000 to 20 000 yBP. Therefore, by using groundwater flow analysis, time required for the water to infiltrate from the ground surface to the depths can be calculated, and these in turn can be used to confirm validities of flow velocities of groundwater and effective flow porosities. It is confirmed that the calculated groundwater flow velocities give about one to twice as high velocities from actual cases (Figure 12).

Figure 11. Comparison of observed and calculated amounts of groundwater discharge

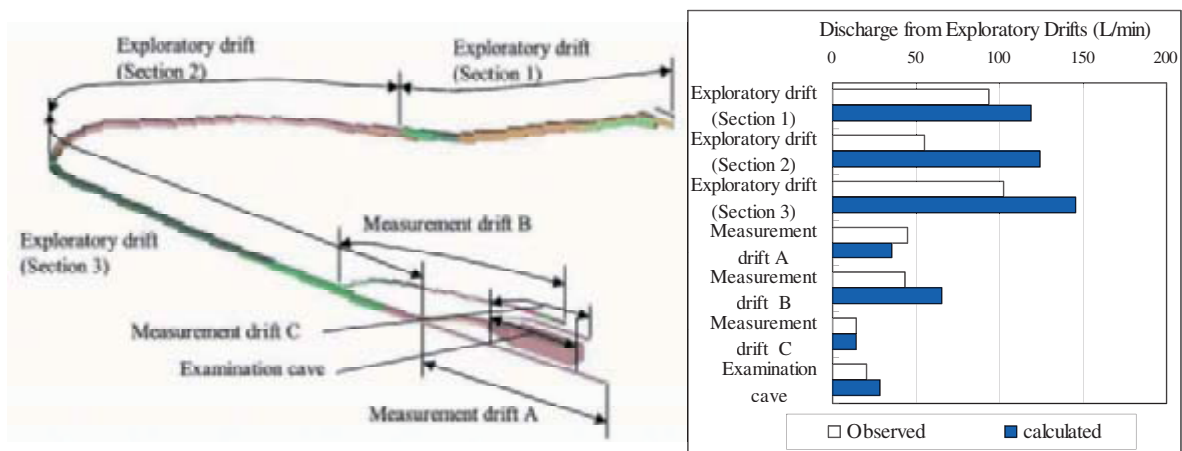
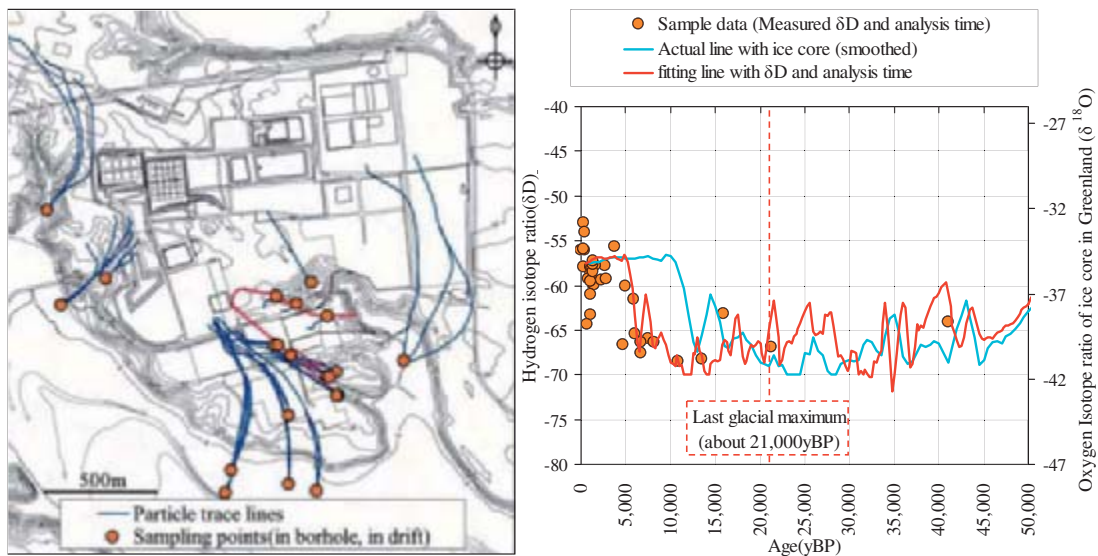


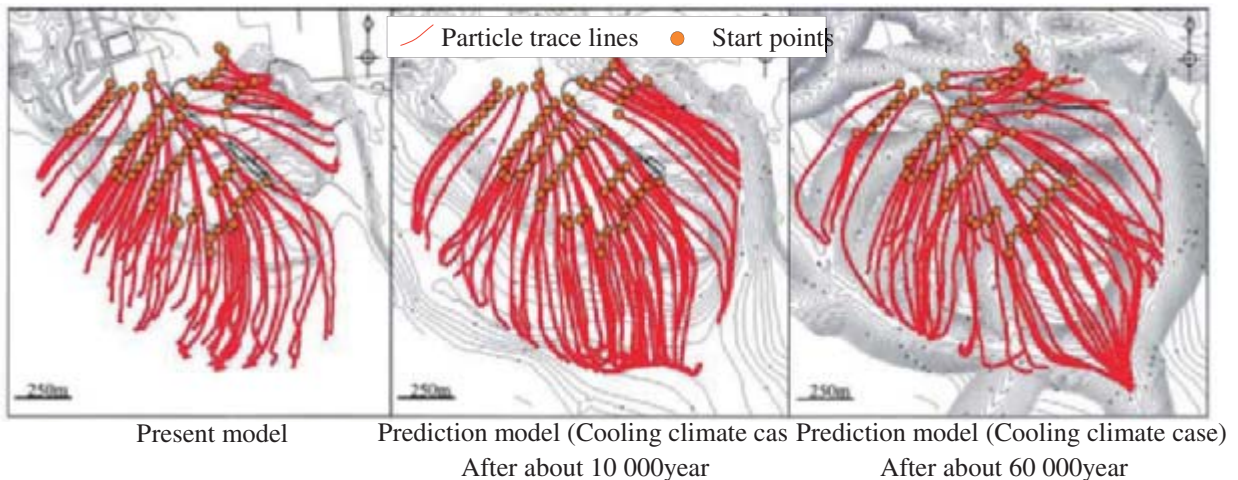
Figure 12. Comparison of general and analyzed trends in oxygen/hydrogen isotope ratios



Prediction of Groundwater flow

Using the confirmed model as described above groundwater flow analysis is carried out with consideration to future changes in topography, sea level, and precipitation and recharge rates. The results show that with changes to those, how groundwater flow rate and flow direction change (Figure 13).

Figure 14. Results of groundwater flow analyses in consideration of long-term topographic changes



Summary

Based on the predicted topographic changes for a period over several tens of thousand years, long-term prediction of groundwater flow is carried out. The prediction has carefully followed along current scientific knowledge, with the validity of the model confirmed along the way as far as possible. With the changes of topography, groundwater flow rate and its direction would change. This shows importance of similar examination along the same lines of this study as well as effectiveness of the method.

References

- ANDRA, (2005), *Dossier 2005 Argile*, Tome, Phenomenological evolution of a geological repository, 525p.
- Chappell, J., (1994), *Upper Quaternary sea levels, coral terraces, oxygen isotopes and deep-sea temperatures*. J. Geogr., 103, pp.828-840.
- EPICA community members, (2004), *Eight glacial cycles from an Antarctic ice core*, Nature, 429, 10, pp.623-628.
- Fujiwara, O., T. Sanga, H. Omori, (1999), *Distribution of erosional rate in Japan*. Technical Report of Japan Nuclear Cycle Development Institute, No.5, pp.85-93. (in Japanese)
- Ishizaki, Y., H. Kawahata, K. Okushi, (2004), *Paleoenvironmental changes over the past 30 000 years in the northwestern Pacific: based on a core from east of the Tsugaru Strait*, Abstract of papers, Annual General Meeting of Japan Geochemical Society (51st). pp.109. (in Japanese)
- Koike, K., H. Machida, (2001), *Atlas of Quaternary Marine Terraces in the Japanese Islands*, University of Tokyo Press. (in Japanese)
- Kumazawa, M., T. Ito, S. Yoshida, (2002), *Decoding the Earth's Evolution*, University of Tokyo Press, 504p. (in Japanese)
- Labeyrie, L., J. Cole, K. Alverson, T. Stocker, (2002), *The History of Climate Dynamics in the Late Quaternary*, Paleoclimate, Global Changes and the Future.
- Nuclear Safety Commission, (2007), *Fundamental guidelines of safety regulation of low level radioactive waste* (Interim report), 22p. (in Japanese)
- Rohling, E.J., M. Fenton, F.J. Jorissen, P. Bertrand, G. Ganssen, J.P. Caulet, (1998), *Magnitudes of sea-level lowstands of the past 500 000 years*, Nature, 394, 9, pp.162-165.

AN INTEGRATED APPROACH FOR DETECTING LATENT MAGMATIC ACTIVITY BENEATH NON-VOLCANIC REGIONS: AN EXAMPLE FROM THE CRYSTALLINE IIDE MOUNTAINS, NORTHEAST JAPAN

K. Umeda

Japan Atomic Energy Agency, Japan

In order to avoid future volcanic hazards at any given waste disposal site or something similar, it is indispensable to ascertain in advance the presence of latent magmatic activity in the deep underground. The Iide Mountains are located on the Japan Sea side of northeast Japan, and are mainly composed of Late Cretaceous to Paleogene crystalline rocks. Although no evidence of volcanism during the Pliocene and the Quaternary is known in and around the Iide Mountains, the region has long been recognized to be unusual in comparison to other “non-volcanic” regions, as indicated by the presence of high temperature hot springs. In order to examine whether or not the heat source for the hydrothermal activity originates from recent magmatic activity in this “non-volcanic” region, we carried out local seismic travel time tomography and wide-band magnetotelluric soundings and also determined the helium isotopes content in gas samples from hot springs around the Iide Mountains. The estimated seismic velocity and resistivity structures show that a zone with low velocity P- and S-waves, low V_p/V_s ratios and high electrical conductivity are clearly visible at depths of more than 15 km below in the Iide Mountains. The location of the geophysical anomalies correlates with the geographic distribution of hot springs with high $^3\text{He}/^4\text{He}$ ratios similar to MORB-type helium, suggesting that the heat source is due to high-temperature fluid and/or melt derived from mantle materials. Therefore, it is concluded that the geophysical anomaly beneath the Iide Mountains is due to newly ascending magmas in the present-day subduction system. It means that an integrated approach combining geophysical and geochemical methods is useful for detecting crustal magma storage, which has the potential to cause future volcanism in a “non-volcanic” region.

Introduction

Geological hazard assessments are being used to make decisions that may affect society for extended periods of time. For example, the need to make quantitative, long-term estimates of future volcanism, estimates that exceed human timescales are of increasing importance. This is partly as a requirement for constructing nuclear facilities, such as repositories for deep geological disposal of long-lived, high-level radioactive waste in regions with low volcanic risk, tens of kilometers from Quaternary volcanoes. Generally, in order to assess the risk posed by a volcano, it is necessary to determine the age of the last activity by geological and geochronological means and deduce from this whether the volcano poses a credible risk (McBirney and Godoy, 2003). However, it is difficult to carry out volcanic risk assessment in a region consisting of Paleozoic or Mesozoic formations without a record of Pliocene to Quaternary volcanism. In such cases, we would examine the potential for new volcanism using mainly geophysical and geochemical information to elucidate the presence of crustal magma storage in a given region.

Seismic wave velocities can vary mainly depending on fluid contents and temperature. Seismic travel time tomography has been widely applied to investigate the subsurface structure of active volcanoes (e.g. Nakajima and Hasegawa, 2003). Many previous tomographic studies have imaged seismic velocity anomalies that are interpreted as magma chambers, intrusive bodies, gas-filled regions, etc. It is known that low P-wave (V_p), low S-wave velocity (V_s) and low Poisson's ratio (V_p/V_s) observed in the upper crust are caused by inclusions of H_2O with a relatively large aspect ratio, and low V_p , low V_s and high V_p/V_s in the lower crust and the uppermost mantle are caused by melt inclusions (Nakajima *et al.*, 2001). Thus, seismic tomography is considered to be a powerful tool for detecting magma and related fluid in the crust and the upper mantle. Magnetotelluric (MT) methods can provide electrical conductivity images of the crust and upper mantle by measuring natural electromagnetic signals at the Earth's surface in a wide frequency band (e.g. Jones, 1992). A great deal of effort has been made to obtain information about the resistivity structure of active volcanoes and surrounding geothermal fields by MT soundings (e.g. Matsushima *et al.*, 2001). As electrical conductivity is the physical property most sensitive to the configuration of aqueous fluid and/or melt, MT can contribute to the delineation of magma plumbing systems. Accordingly, seismic and electromagnetic studies provide geophysical constraints on crustal magma transfer and storage around volcanic and/or geothermal regions.

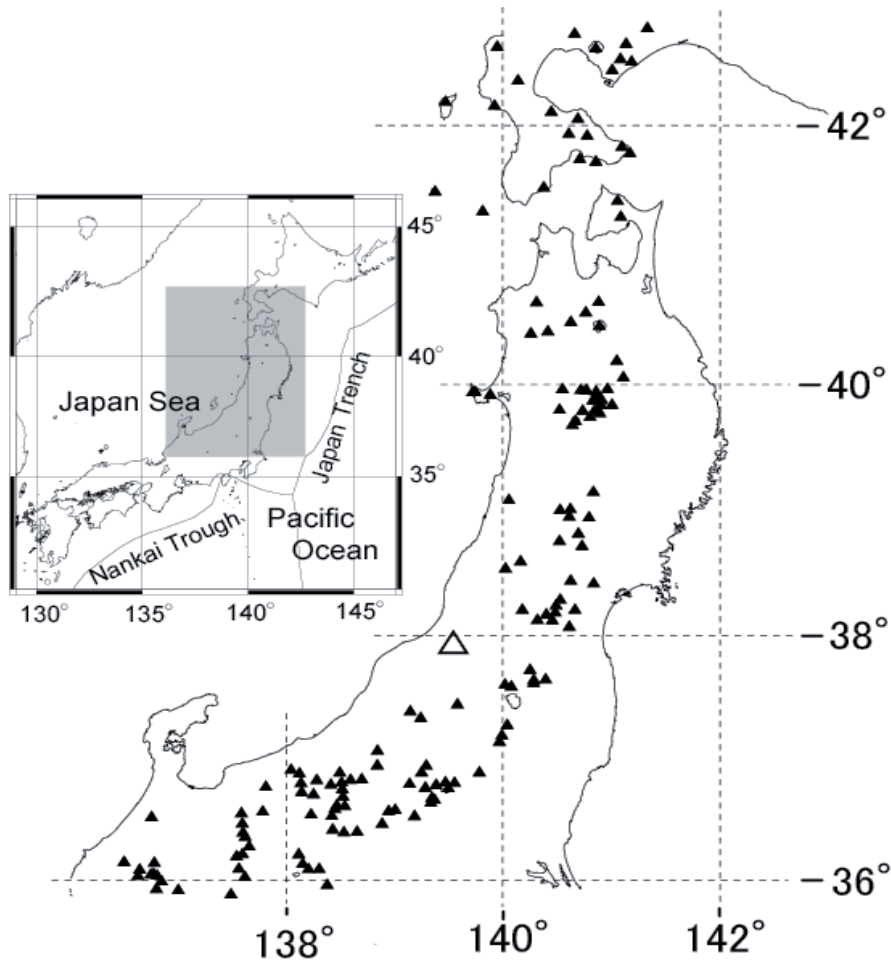
On the other hand, noble gases and their isotopes are excellent natural tracers for mantle-crust interaction in different tectonic provinces. Due to their inert chemical character, they provide durable tracers that are unchanged by the complex chemical processes affecting reactive species. Helium isotopes can be especially, useful geochemical indicators of mantle-derived materials in the crust, owing to the distinct difference in isotopic compositions between the crust ($^3He/^4He$ ratio of $\sim 10^{-8}$) and the upper mantle ($^3He/^4He$ ratio of $\sim 10^{-5}$) (e.g., Ozima and Podosek, 2002). Previous studies have measured helium isotopes in various types of gas samples, and precise $^3He/^4He$ data can provide knowledge on geochemical features of subduction zones (e.g. Sano and Wakita, 1985). The upper limit of $^3He/^4He$ ratios of fumarolic gases and terrestrial waters around volcanoes are commonly similar to those of MORB-type helium, whereas those in the fore-arc regions are significantly lower than the relative to atmospheric value of 1.4×10^{-6} . According to investigations of the $^3He/^4He$ ratio distributions in and around individual volcanoes, there is a general trend for $^3He/^4He$ ratios to decrease with increasing distance from the main cone of each volcano (Sakamoto *et al.*, 1992). This trend is interpreted to be an indication of the presence of magma with a high $^3He/^4He$ ratio, and that the gas supplied from the magma is diluted by atmospheric and/or crustal components with low $^3He/^4He$ ratios with increasing distance from the peak.

As indicated above, seismic tomography, magnetotelluric soundings and determination of helium isotope ratios could provide geophysical and geochemical constraints on the presence of latent magmatic activity beneath crystalline basements in "non-volcanic" regions. This is especially significant if there is no geologic record of Pliocene to Quaternary volcanic events, so that the information obtained would enable us to examine the likelihood of future volcanism. Moreover, integrating evidence from a variety of disciplines could lead to progress in scientific issues regarding magma dynamics and evolution: Are magma reservoirs small or large, shallow or deep, ephemeral or long-lasting? The purpose of this study is to show how these methods were applied to indicate whether or not latent crustal magma storage remains in "non-volcanic" regions.

The Iide Mountains, composed of crystalline basements, are located on the Japan Sea side of Honshu Island along 38.0°N latitude, where the Pacific plate has been subducting beneath the North American plate. The Iide Mountains are located approximately 60 km away from the nearest Quaternary volcano, and there seems to be no evidence of volcanism during either the Pliocene or the Quaternary. However, this area has been recognized to be an unusual "non-volcanic" region as indicated by high heat discharge values observed (Sumi, 1981). In this work, local seismic travel time

tomography and wide-band MT soundings in and around the Iide Mountains were carried out in order to estimate 3-D seismic velocity structure and 2-D resistivity structure, respectively. In addition, we measured helium isotopes in gas samples from hot springs surrounding the Iide Mountains, and examined whether or not the heat source for hot springs originates from recent magmatic activity, based on integrating evidence from a variety of disciplines.

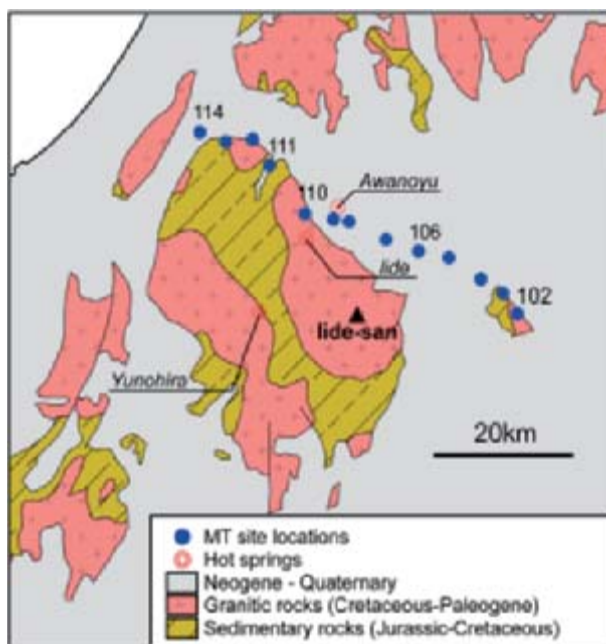
Figure 1. **Location of the Iide Mountains (open triangle). Also shown are Quaternary volcanoes in Northeast Japan (solid triangles)**



Geological background

The Iide Mountains mainly consists of Mesozoic sedimentary rocks and Late Cretaceous to Paleogene granitic rocks (Figure 2). The Mesozoic sedimentary rocks, consisting of massive sandstone, layers of sandstone-shale and bedded chert, are completely metamorphosed by the granitic rocks, and biotite and muscovite are recognized in all the metasediments. The granitic rocks of the Iide Mountains are mostly composed of granite and granodiorite accompanied by garnet-biotite-muscovite granite and granophyre. Notable biotite K-Ar ages of the granodiorite were reported to be 56.3 to 51.3 Ma, and the K-Ar ages of biotite and muscovite from the garnet-biotite-muscovite granite were reported to be 30.3 to 23.9 Ma (Takahashi *et al.*, 1996).

Figure 2. Simplified geological map around the Iide Mountains. Also shown are MT site locations and locations of hot springs



Miocene sediments, unconformably overlying the pre-Neogene basement, are distributed around the Mountains. They are represented by terrestrial and marine sedimentary rocks, with frequent intercalation of volcanoclastic rocks and lava. Intrusive rocks, mainly consisting of biotite rhyolite, orthopyroxene-clinopyroxene andesite and clinopyroxene-olivine basalt intruded into the Late Cretaceous to Paleogene granitic rocks and the Miocene sedimentary rocks (Takahashi *et al.*, 1996). The K-Ar ages of andesitic intrusions were reported to be 12.1 ± 0.3 Ma and 12.6 ± 0.4 Ma (Umeda *et al.*, 2007). It follows that Miocene volcanism continued until around 12 Ma in this region.

In the Iide Mountains, there are several high-temperature hot springs, such as Iide (55°C), Awanoyu (41°C) and Yunohira (56°C). On the basis of their chemical composition, they belong to Na•Ca-Cl•SO₄•HCO₃ type and CO₂-Na-Cl•SO₄ type (Kimbara, 1992), which are similar to those of hot springs in volcanic regions. Although there is no observational data on heat flow in the Iide Mountains, the heat discharge values, estimated using water temperature and volumetric flow rate of the above hot springs, is over 12 mW/m² in the Iide Mountains, whose values are equal to those in volcanic regions in Japan (Sumi, 1980), and cannot be interpreted to be due solely to the radiogenic heat production of the crystalline rocks.

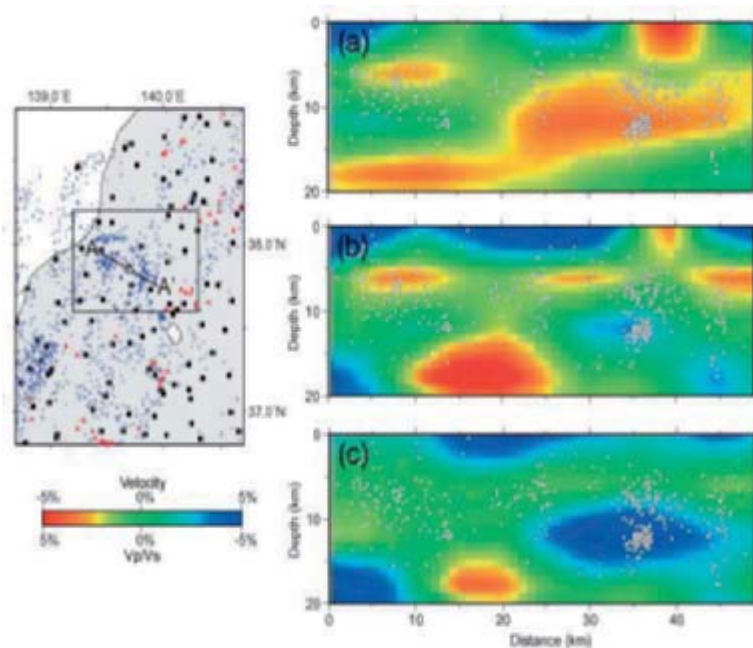
Seismic tomography

Data analysis

We used P and S wave arrival time data from shallow earthquakes in and around the Iide Mountains where over 20 seismic stations are located (Figure 3). These data were collected from a catalog of earthquakes processed with close coordination of the Japan Meteorological Agency (JMA) during the period from January 2002 to February 2006. We used data from 1 688 earthquakes. The accuracy of hypocenter locations is better than 5 km in the inversion. The total numbers of P and S wave arrival times used are 32 790 and 34 557, respectively. The seismic tomography method used was originally developed by Aki and Lee (1976). This work employed the method and computer

programmes developed by Zhao *et al.* (1992a), which are useful for velocity structures with discontinuities in complex geometries. A 3-D grid net was set up in the model space for this area to express the 3-D velocity structure. The P- and S-wave velocities at every grid node were taken as unknown parameters. The velocity at any point in the model space was calculated using a linear interpolation of velocities at the eight grid nodes surrounding that point. For the initial velocity model, we adopted the 1-D velocity structure obtained by Zhao *et al.* (1992b). Grid spacing is 0.10° in the horizontal and 6 km in the vertical directions. We also conducted a checkerboard test (CRT) at different grid spacings to examine the resolution scale of the present data set (Zhao *et al.*, 1992a). To make a checkerboard, we assigned positive and negative velocity perturbations of 3 % to all the 3-D nodes and calculated the travel times for this model to generate synthetic data. The CRT results for the P-waves are also fairly good except for the results at depths from 9 to 15 km. The resolution for the S-wave has very good quality at all depths.

Figure 3. **Vertical cross-sections of (a) P-wave, (b) S-wave and (c) V_p/V_s structure along the line A-A' across the Iide Mountains**

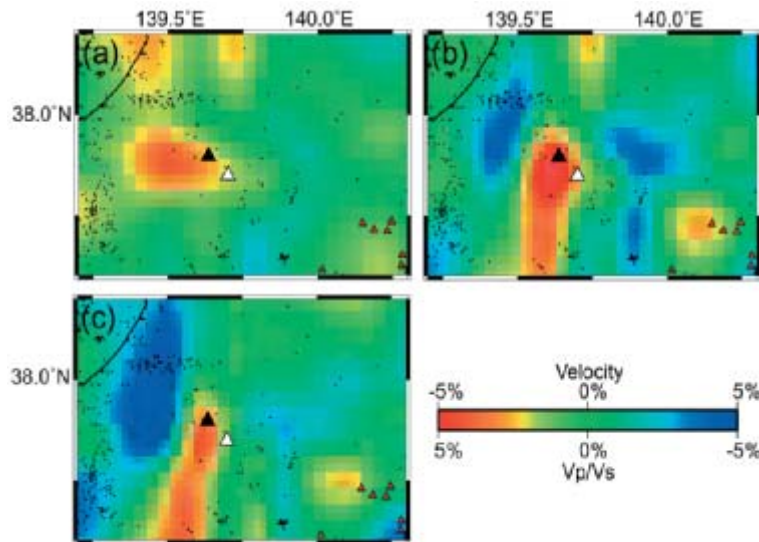


Seismic velocity structure

Figure 3 shows vertical cross-sections of V_p , V_s and V_p/V_s along the line running across the Iide Mountains in an east-west direction (A-A'). The velocity patterns of P- and S-waves are generally similar to each other except for the portion at depths of about 12 km. Low velocity anomalies for the P-wave are distributed in the central to eastern portion of the study area, but cannot be imaged for the S-wave. This is due to the limitation of spatial resolution for the P-wave, because the checkerboard patterns are not well reconstructed in the CRT. It appears that low velocity anomalies are located at depths of more than 15 km beneath the Iide Mountains for both the P- and S-waves. However, the amplitudes of the S-wave anomalies are greater than those of the P-wave anomalies at these depths. High V_p/V_s anomalies are also distributed at depths of more than 15 km, indicating that the seismic velocity anomaly may be related to melt inclusions. Figure 4 shows horizontal cross-sections of V_p , V_s and V_p/V_s at a depth of 18 km in the study area. Low velocity anomalies for the P- and S-waves are visible to the west of the Iide Mountains. The inversion model reveals that there is a seismic velocity anomaly larger than the resolution scale of 10 km in the horizontal direction beneath the Iide Mountains. Seismic wave velocity varies depending on several physical conditions. Variations in fluid

contents and temperature are likely to be the main causes of the velocity anomalies observed in volcanic or geothermal regions (Nakajima and Hasegawa, 2003). On the grounds that hydrothermal activity occurs in the Iide Mountains, the detected seismic velocity anomaly is likely to be the higher temperature and the existence of magma- or a fluid-filled lower crust.

Figure 4. **Horizontal cross-sections of (a) P-wave, (b) S-wave and (c) Vp/Vs structure at a depth of 18 km. The summit location of Iide-san and Kitamata-dake are also shown as white and black triangles, respectively**



Magnetotelluric soundings

Observation

The 50 km long MT profile with 13 recording stations runs across the Iide Mountains (Umeda *et al.*, 2006). The stations were arranged in a N60°W direction, based on the strike of the northeast Japan arc and the distribution of hypocenters of crustal seismicity looking in a NNE-SSW direction (Figure 2). The data were collected using five component (three magnetic and two telluric) wide-band MT instruments (Phoenix MTU-5 system). The data were acquired in the period range from 3×10^{-3} to 2000s. The recording duration for the sites ranged from 3 to 18 days. Because DC electric railways in the area can severely affect the measurements, the time series analysis focused on nocturnal data obtained when there were fewer trains. Two simultaneous remote reference measurements were carried out at the Naruko site (150 km north of the stations) and the Sawauchi site (250 km north of the stations). Using the remote reference technique (Gamble *et al.*, 1979), we were able to reduce unfavorable cultural noise, mainly due to the leakage currents of DC railways around the observation area.

Data analysis

Prior to the 2-D modeling, we checked the dimensionality of the data obtained by Umeda *et al.* (2006), from impedance strike distributions. The strike directions from individual impedance data were estimated by tensor decompositions (Groom and Bailey, 1989), where distortion parameters were set as site-dependent and period-dependent. The result shows that the two-dimensionality is well supported for both N60°W and N30°E directions in the periods from 0.1 to 1 000s. For the modeling, we took the N30°E direction as the regional strike direction, because it follows the strike of the general

northeast Japan arc and the distribution of hypocenters of crustal seismicity looking in a NNE-SSW direction.

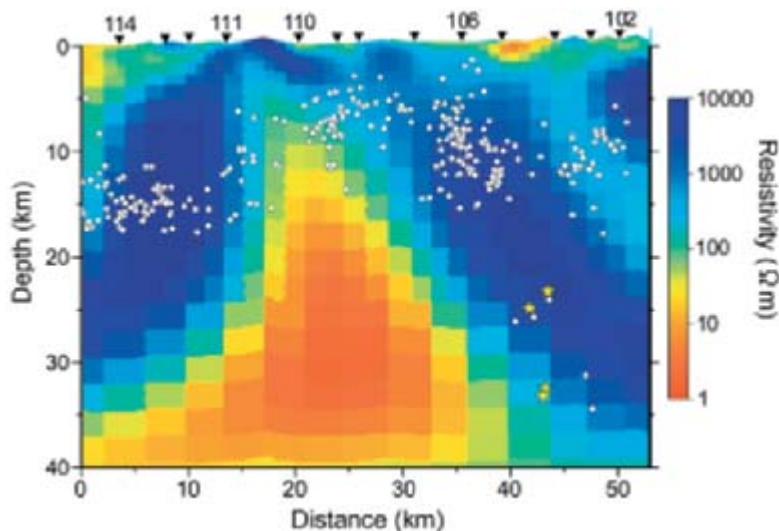
The impedance strikes can be described in terms of distinct modes corresponding to the electric field parallel (TE mode) and perpendicular (TM mode) to the strike direction (N30°E). After fixing the strike direction as N30°E, we decomposed the data from all the sites with period-independent twist and shear. The apparent resistivity and phase data from both the TE and TM modes were inverted simultaneously using the inversion code of Ogawa and Uchida (1996). The model structure and static shifts were used as model parameters. Data misfit, model roughness and static shift norm were simultaneously minimized using Akaike's Bayesian Information Criterion (ABIC). Surface elevation was included in the resistivity model so that a two-dimensional approximation of the effect of topography was reflected in the computations. The first step for the inversion is the design of a suitable finite-difference mesh, which depends largely on the site distribution and the frequency range of the observations. It must have at least one column for each station of the profile but grids preferably consist of a finer mesh where row thickness increases with depth based on the initial resistivity set for the model and the frequencies involved. After trials with different model sizes, we settled upon a mesh of 107 horizontal by 63 vertical cells. All inversions started from 100 Ωm with no static shift. An assumed error floor in the apparent resistivity from 10% to 200% was used together with the equivalent error floor for the phase data. After 25 iterations, the root mean square of data misfit converged to 26%. The calculations were consistent with the observations for the most part.

Resistivity structure

The best fit resistivity model is shown in Figure 5. Also shown are the hypocenters of microearthquakes and deep long period tremors identified by the Japan Meteorological Agency (JMA). The profile shows that there is a resistive part having a resistivity of more than 1 000 Ωm in the upper crust beneath the Iide Mountains, which is concordant with the distribution of the Mesozoic sedimentary rocks and Late Cretaceous to Paleogene granitic rocks. The compact and dry crustal rocks are characterized by elevated electrical resistivity up to 10 000 Ωm (e.g. Schwarz, 1990). Thus, the resistive part may reflect the upper and middle crust probably composed of less permeable meta-sedimentary and granitic rocks. In contrast to the resistive crust, an anomalous conductive body (< 10 Ωm) is clearly visible in the lower crust of the Iide Mountains (below sites 112 to 107). The conductor widens with increasing depth, and extends from the near-surface down to the base of the crust and perhaps into the upper mantle. The resistivity structure is controlled by the presence and connectivity of any fluid and/or melt in the pore spaces and on the conductive minerals, rather than by the resistivity of the host rocks (e.g. Jones, 1992). Although metallic ore bodies can have very high conductivities, they do not generally have spatial dimensions as large as that observed in the Iide Mountains.

The occurrence of crustal seismicity could reflect the thermal structure of the crust. The hypocenters of crustal earthquakes in Northeast Japan are limited to depths of ~ 15 km and the cut-off depth of seismicity probably coincides with the 400 °C isotherm (Ito, 1993). The cut-off depth decreases locally beneath active volcanoes, indicating the presence of magma and related hydrothermal activity. Figure 5 shows that most of the crustal earthquakes occur in the resistive part at depths of less than or equal to ~ 15 km and very few hypocenters are located within the conductor. Note that the cut-off depth decreases toward the Kitamata-dake (below sites 109 to 110), and is in good agreement with the upper boundary of the conductor, implying that the temperature of the conductor is higher than 400°C. The region of thinning of the brittle seismogenic layer is concordant with the distribution of the high-temperature hot springs. Thus, the preferred interpretation for the conductive anomaly beneath the Iide Mountains is the existence of interconnected high-temperature fluid and/or melt.

Figure 5. Two-dimensional resistivity model using both the TM and TE modes. Also shown are hypocenters of microearthquakes (white dots) and deep low-frequency earthquakes (stars)



Helium isotope measurements

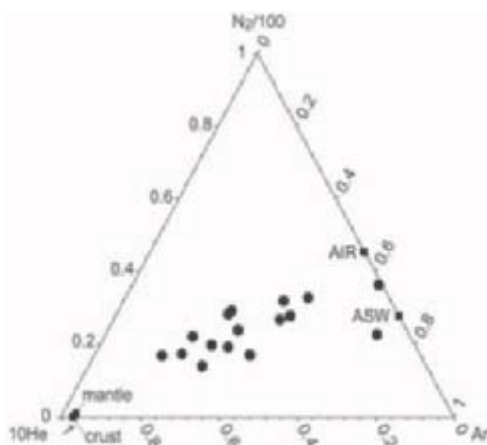
Samples and analytical methods

Samples were collected in glass containers with vacuum cocks at both ends. The gas was introduced into the container by water displacement using an inverted funnel and an injection syringe. Details of sample collection methods can be found in Nagao *et al.* (1981). Major components of the gas samples were determined with gas chromatography. Estimated uncertainty of measurement is $\pm 0.01\%$ for major components, and $\pm 0.001\%$ for He and Ar. The isotope ratios of He and Ne were determined using the MS-III mass spectrometric system (modified VG5400). The ^3He and ^4He ion beams were detected on a double collector system: ^3He by axial counting and ^4He by the high Faraday collector, (feedback resistor = $10\text{ G}\Omega$). A resolving power of 600 allowed the complete separation of the $^3\text{He}^+$ beam from the H_3^+ and HD^+ beams. Neon was released from the cryogenic trap at $45\text{ }^\circ\text{K}$. Measured $^3\text{He}/^4\text{He}$ ratios are normalized to a standard $^3\text{He}/^4\text{He}$ gas ($^3\text{He}/^4\text{He}=1.71\times 10^{-4}$) prepared and stored in a stainless steel container on the inlet line. Blank levels of He and Ne determined were lower than $1\times 10^{-9}\text{ cm}^3\text{ STP}$, respectively. They represent less than 0.1% of the amount of sampled gases, so blank correction was not required. Mass spectrometric details, including purification procedures, have been published elsewhere (e.g. Aka *et al.*, 2001).

Helium isotopes

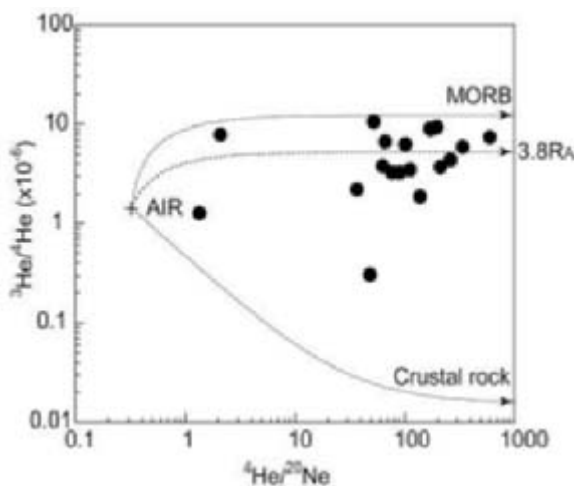
In this section, the characteristics of helium isotopes surrounding the Iide Mountains using both the data obtained in this study and the data reported by Umeda *et al.* (2007) are discussed. Major component analyses of the gas samples show that N_2 is the predominant phase and CO_2 is the next most abundant. They are different from well samples in the Niigata plains, which are dominantly CH_4 rich natural gases. Most of the gas samples show N_2/Ar ratios in the range between 37.7 (air-saturated water) and 83.7 (air). This result indicates that the N_2/Ar ratios are mostly controlled by the atmospheric components. The relative $\text{N}_2\text{-Ar-He}$ compositions of these gases are shown in Figure 6. In this ternary diagram, the hot spring gases fall on a trend between the He and Ar-rich components (Giggenbach, 1996). Therefore, it can be deduced that the source of the gases has a relationship to mantle and/or crust-derived components, in addition to atmospheric components.

Figure 6. Relative N₂-He-Ar composition of gases from hot springs



The $^3\text{He}/^4\text{He}$ ratios of hot spring gases sampled in and around the Iide Mountains ranged from 0.22 to 7.9 RA (RA denotes the atmospheric $^3\text{He}/^4\text{He}$ ratio of 1.4×10^{-6}). Generally, the CO₂ rich samples have higher $^3\text{He}/^4\text{He}$ ratios than the N₂ rich ones. Contribution of atmospheric helium to each sample was estimated using the $^4\text{He}/^{20}\text{Ne}$ ratio, assuming all measured Ne is of atmospheric origin. Figure 7 shows the relationship between the measured $^3\text{He}/^4\text{He}$ and $^4\text{He}/^{20}\text{Ne}$ ratios. Most gas samples have relatively little contamination from air, resulting in small changes to the $^3\text{He}/^4\text{He}$ ratios. Most of the hot spring gases have higher $^3\text{He}/^4\text{He}$ ratios than the atmospheric ratio, indicating remarkable differences in $^3\text{He}/^4\text{He}$ ratio compared with other regions consisting of Mesozoic sediments and Cretaceous granite, away from active volcanoes in Japan. The $^3\text{He}/^4\text{He}$ ratio of arc-related volcanism in Northeast Japan ranged from 1.7 to 8.4 RA and the mean value is 5.1 ± 1.7 RA, consistent with the range of the observed values from hot springs in and around the Iide Mountains (Hilton *et al.*, 2002). Note that the highest $^3\text{He}/^4\text{He}$ ratio of 7.9 RA, which was measured at Iide (No. 7), is close to the value for MORB-type helium with an average value of 8 RA (e.g. Graham, 2002). Although there is no active volcanism around the Iide Mountains, the observed helium ratios of the sampled hot springs are elevated with respect to those expected for a crustal source.

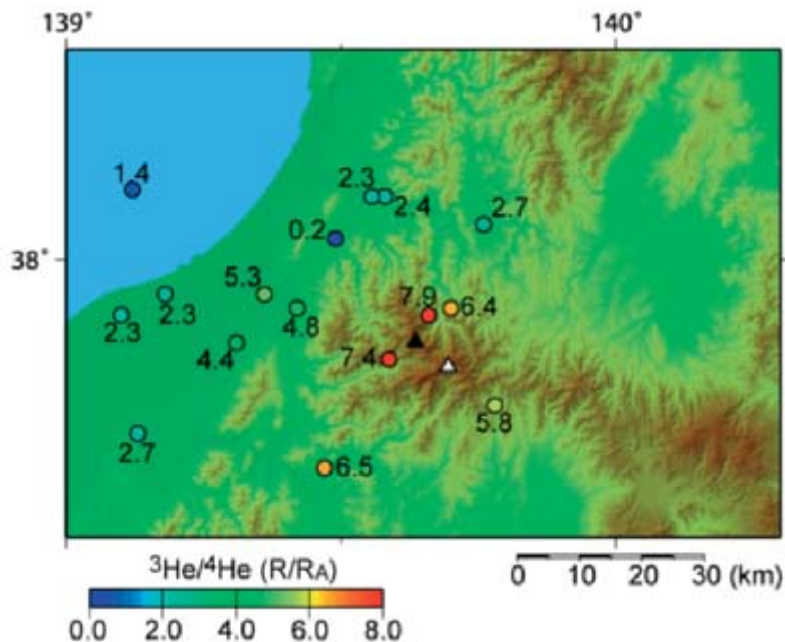
Figure 7. $^3\text{He}/^4\text{He}$ versus $^4\text{He}/^{20}\text{Ne}$ diagram for the hot spring gases



Discussion and Conclusions

As mentioned above, there is a clear correlation with location between the low velocity anomalies and the conductive body, suggesting the existence of high-temperature fluid and/or melt at depths of more than 15 km, toward the Kitamata-dake, one of the peaks in the Iide Mountains. On the other hand, the spatial distribution of the observed $^3\text{He}/^4\text{He}$ ratios for gas samples may reveal the lateral extent of the mantle-derived materials beneath the Iide Mountains. Figure 8 shows the geographic distribution of $^3\text{He}/^4\text{He}$ ratios of gases from hot springs and gas wells. The hot springs having anomalously high $^3\text{He}/^4\text{He}$ ratios are located toward the central part of the Iide Mountains. In contrast, the hot springs and the gas wells having rather low $^3\text{He}/^4\text{He}$ ratios are distributed in the foothills and outside of the Mountains. The trend is similar to the one observed around active volcanoes and their surrounding regions (Sakamoto *et al.*, 1992). The hot spring with the highest $^3\text{He}/^4\text{He}$ ratio at the Iide Hot Spring (7.9 RA) is located in proximity to the Kitamata-dake, suggesting the likelihood that mantle-derived materials are supplying MORB-type helium beneath the Kitamata-dake, and that the mantle helium has been diluted by atmospheric and/or crustal components with lower helium ratios away from the peak. Consequently, the location of the geophysical anomaly correlates with the geographic distribution of hot springs with high $^3\text{He}/^4\text{He}$ ratios similar to MORB-type helium, indicating that the heat source is due to high-temperature fluid and/or melt derived from mantle materials.

Figure 8. Geographic distribution of $^3\text{He}/^4\text{He}$ ratios of gases from hot springs. Numbers indicate $^3\text{He}/^4\text{He}$ ratios as RA unit



The emanation of hot springs with high $^3\text{He}/^4\text{He}$ ratios requires the effective movement of mantle helium to the Earth's surface. Mantle melting is the most likely mechanism responsible for the transfer of mantle helium from the subcrustal lithosphere where the volatiles would be released directly from a magma body to the crustal fluids (e.g. Torgersen, 1993). Considering the apparent lack of volcanism since around 12 Ma, the potential ^3He sources are limited to the following:

- (1) fluid circulation through either the erupted Miocene basalts (~ 12 Ma) or an ancient and non-active magma chamber originally charged with mantle helium; or

- (2) direct addition of mantle helium from newly ascending magma in the present-day subduction system. The initial $^3\text{He}/^4\text{He}$ ratios in the magma emplaced into the crust would be high and similar to those of MORB-type helium. Once the erupted basalt and/or the chamber is isolated and its volatile inventory is no longer being replenished by a mantle source, the helium isotope ratio will decrease with time due to the addition of radiogenic ^4He from U and Th decay, resulting in much lower ratios in the present-day (Craig and Lupton, 1976).

In order to determine whether or not an ancient magma is a possible source of the high $^3\text{He}/^4\text{He}$ ratios in the hot spring gases, we calculated the evolution in $^3\text{He}/^4\text{He}$ ratios of a Miocene basalt with time. The present $^3\text{He}/^4\text{He}$ ratio can be estimated using several assumptions:

- (1) U and Th contents of basalt are 0.5 and 1.0 ppm, respectively (Ebihara *et al.*, 1984);
- (2) the initial ^4He concentration (1×10^{-6} cm³ STP/g) in the basalt was chosen as a reasonable upper limit for non-degassed basalt melt determined from mafic xenoliths (Mamyryn and Tolstikhin, 1984),
- (3) the ^4He production rate P is a function of the U and Th concentrations and can be written in terms of a U concentration parameter and the Th/U ratio as: $P(^4\text{He}) = 0.2355 \times 10^{-12} U^*$ (cm³STP/g/year), $U^* = U \{1 + 0.123 (\text{Th}/U - 4)\}$ (Craig and Lupton, 1976);
- (4) the system is closed. The calculation indicates that the $^3\text{He}/^4\text{He}$ ratio of the aged magma would be 5.3×10^{-6} (3.8 RA) at the present time.

Also shown in Figure 7 is the mixing line between the atmospheric value and the calculated value of 3.8 RA for the ancient magma. Note that most of the gas samples plot above the mixing line. The anomalously high $^3\text{He}/^4\text{He}$ ratios from hot springs cannot be interpreted as a three-component mixture of mantle-derived helium associated with magmatism of Middle Miocene age, radiogenic crustal helium and atmospheric helium. Rather, it is concluded that mantle-derived helium related to newly ascending magma is required to explain the observed $^3\text{He}/^4\text{He}$ ratios, and that recently active crustal magma storage as the heat source for hydrothermal activity has been recognized beneath the Iide Mountains.

In conclusion, local seismic travel tomography and wide-band magnetotelluric soundings are considered as useful geophysical indicators for detecting the presence of high-temperature fluid and/or melt deep underground. Additionally, helium isotope analyses can provide geochemical constraints on the origin of geophysical anomalies, such as active magma storage, a solidified magma plug with high-temperature in deep underground, etc. Therefore, an integrated approach combining evidence obtained from a variety of disciplines, notably by geophysical and geochemical methods, could be available to locate the likelihood of new volcanoes forming at a given site despite an absence in the geologic record of Pliocene to Quaternary volcanic events.

Acknowledgements

We would like to thank Drs. K. Nagao, K. Asamori and T. Negi for helping with the helium isotope measurements, seismic tomography and magnetotelluric soundings, respectively. We are grateful for fruitful discussions with Drs. A. Ninomiya and G. McCrank.

References

Aka, F.T., M. Kusakabe, K. Nagao, and G. Tanyileke, (2001), *Noble gas isotopic compositions and water/gas chemistry of soda springs from the islands of Bioko, São Tomé and Annobon, along with Cameroon Volcanic Line, West Africa, Appl. Geochem.*, 16, 323-338.

- Aki, K., and W.H.K. Lee, (1976), *Determination of the three-dimensional velocity anomalies under a seismic array using first P arrival times from local earthquakes: Part 1. A homogeneous initial model*, *J. Geophys. Res.* **81**, 4381-4399.
- Craig, H., and J.E. Lupton, (1976), *Primordial neon, helium, and hydrogen in oceanic basalts*, *Earth Planet. Sci. Lett.*, **31**, 369-385.
- Ebihara, M., Y. Nakamura, H. Wakita, and T. Konda (1984), *Trace element composition of Tertiary volcanic rocks of northeast Japan*, *Geochem. J.*, **18**, 287-295.
- Gamble, T.D., W.M. Goubou, and J. Clarke, (1979), *Magnetotellurics with a remote reference*, *Geophysics*, **81**, 69-89.
- Groom, R. W., and R. C. Bailey, (1989), *Decomposition of magnetotelluric impedance tensors in the presence of local three-dimensional galvanic distortions*, *J. Geophys. Res.*, **94**, 1913-1925.
- Giggenbach, W.F. (1996), Chemical composition of volcanic gases, in *Monitoring and mitigation of Volcano Hazards*, edited by R. Scarpa, and R.I. Tilling, pp.222-256, Springer Verlag, Berlin.
- Graham, D.W., (2002), Noble gas isotope geochemistry of Mid-Ocean Ridge and Ocean Island Basalts: characterization of mantle source reservoirs, in *Geochemistry and Cosmochemistry, Rev. Mineral. Geochem.*, vol. 47, edited by C.J. Porcelli, D. Ballantine, and R. Wieler, pp. 247-317, Mineral. Soc. Am., Washington DC.
- Hilton, D.R., T.P. Fischer and B. Marty, (2002), Noble gases and volatile recycling at subduction zones, in *Noble Gases in Cosmochemistry and Geochemistry, Reviews in Mineralogy and Geochemistry*, edited by D. Porcelli, C. J. Ballantine, and R. Wieler, **47**, pp. 319-370, Mineralogical Society of America.
- Ito, K., (1993), Cutoff depth of seismicity and large earthquakes near active volcanoes in Japan, *Tectonophys.*, **217**, 11-21.
- Jones, A.G. (1992), Electrical conductivity of the continental lower crust, in *Continental lower crust*, edited by D.M. Fountain et al., pp.81-143, Elsevier, Amsterdam.
- Kimbara, K., 1992, *Distribution map and catalogue of hot and mineral springs in Japan*, 394pp., Geol. surv. Jpn., Tsukuba.
- Mamyrin, B. A., and I. N. Tolstikhin (1984), *Helium isotopes in nature*, 273pp., Elsevier, Amsterdam.
- Matsushima N., H. Oshima, Y. Ogawa, S. Takakura, H. Satoh, M. Utsugi, and Y. Nishida, (2001), Magma prospecting in Usu volcano, Hokkaido, Japan, using magnetotelluric soundings, *J. Volcanol. Geotherm. Res.*, **109**, 263-277.
- McBirney A., and A. Godoy, (2003), Notes on the IAEA Guidelines for Assessing Volcanic Hazards at Nuclear Facilities, *J. Volcanol. Geotherm. Res.*, **126**, 1-9.
- Nagao, K., N. Takaoka, and O. Matsubayashi, (1981), Rare gas isotopic compositions in natural gases of Japan, *Earth Planet. Sci. Lett.*, **53**, 175-188.

- Nakajima, J., and A. Hasegawa, (2003), Tomographic imaging of seismic velocity structure in and around the Onikobe volcanic area, northeastern Japan: implications for fluid distribution, *J. Volcanol. Geotherm. Res.*, *127*, 1-18.
- Nakajima, J., T. Matsuzawa, A. Hasegawa, and D. Zhao, (2001), Three-dimensional structure of V_p , V_s , and V_p/V_s beneath northeastern Japan: implications for arc magmatism and fluids, *J. Geophys. Res.*, *106*, 21843-21857.
- Ogawa, Y., and T. Uchida, (1996), A two-dimensional magnetotelluric inversion assuming Gaussian static shift, *Geophys. J. Int.*, *126*, 69-76.
- Ozima M., and F.A. Podosek, (2002), Noble Gas Geochemistry (Second Edition), 286 pp., Cambridge University Press, Cambridge.
- Sakamoto, M., Y. Sano and H. Wakita, (1992), $^3\text{He}/^4\text{He}$ ratio distribution in and around the Hakone Volcano, *Geochem. J.*, *26*, 189-195.
- Sano, Y., and H. Wakita, (1985), Geographical distribution of $^3\text{He}/^4\text{He}$ ratios in Japan: Implications for arc tectonics and incipient magmatism, *J. Geophys. Res.*, *90*, 8729-8741.
- Schwarz, G., (1990), Electrical conductivity of the earth's crust and upper mantle, *Survey in Geophys.* *11*, 133-161.
- Sumi, K., (1980), Distribution map of heat discharge by hot springs in Japan, Geol. Surv. Jpn., Tsukuba.
- Takahashi, Y., T. Yamamoto, and Y. Yanagisawa, (1996), Geology of the Iidesan district, with geological sheet map at 1:50,000, 52pp., Geol. Surv. Jpn., Tsukuba.
- Torgersen, T., (1993), Defining the role of magmatism in extensional tectonics: Helium 3 fluxes in extensional basins, *J. Geophys. Res.*, *98*, 16257-16269.
- Umeda, K., K. Asamori, T. Negi, and Y. Ogawa, (2006), Magnetotelluric imaging of crustal magma storage beneath the Mesozoic crystalline mountains in a non-volcanic region, Northeast Japan, *Geochem. Geophys. Geosys.*, *7*, doi:10.1042/2006GC001247.
- Umeda, K., K. Asamori, A. Ninomiya, S. Kanazawa, and T. Oikawa, (2007), Multiple lines of evidence for crustal magma storage beneath the Mesozoic crystalline Iide Mountains, northeast Japan, *J. Geophys. Res.*, *112*, B05207, doi:10.1029/2006JB004590.
- Zhao, D., A. Hasegawa, and S. Horiuchi, (1992a), Tomographic imaging of P and S wave velocity structure beneath northeastern Japan, *J. Geophys. Res.*, *97*, 19,909-19,928.
- Zhao, D., S. Horiuchi, and A. Hasegawa, (1992b), Seismic velocity structure of the crust beneath the Japan Islands, *Tectonophys.*, *212*, 289-301.

TABLE OF CONTENTS

Executive Summary	3
Introduction	9
Scope and Objectives of the Workshop	13
Synthesis of the Workshop	15
Poster Session	31
Conclusions	33

Session I

General Framework: Crystalline Rocks as Host Formations

Safety Functions of Crystalline Rock Formations in Deep Geological Disposal and Their Handling in a Safety Case – SKB’s SR-CAN Example	45
Regulatory Expectations Concerning the Confidence in Geosphere Stability and its Handling in an Environmental Safety Case	57

Session II

Examples of Key Processes Affecting the Geosphere for Crystalline Rock

Likelihood of Tectonic Activity Affecting the Geological Stability of a Repository in Japan: Development of NUMO’s ITM Methodology	67
Climate Change and its Potential Impact on Mechanical, Hydraulic and Chemical Conditions	77
Uplift and Erosion: Potential Impact on the Geological Environment	91
Predictability of the Evolution of Hydrogeological and Hydrogeochemical Systems; Geological Disposal of Nuclear Waste in Crystalline Rocks.....	99
Geological and Rock Mechanics Aspects of the Long-term Evolution of a Crystalline Rock Site...	109

Session III

Arguments to Support Confidence in the Stability of Crystalline Rocks as Potential Host Formations

Lithological History and Ductile Deformation: The Lessons for Long-term Stability of Large-scales Structures in the Olkiluoto	123
---	-----

Stability and Predictability in Younger Crystalline Rock System: Japanese Islands Case	133
Developing Confidence in Stability and Predictability of a Repository in Unsaturated Tuffs	147

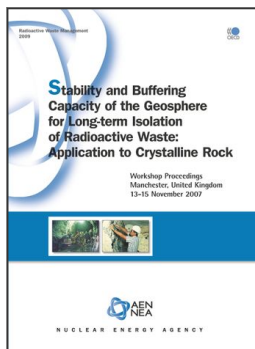
Session IV

Response and Resilience of Crystalline Rock to Natural Perturbations and Geosphere Evolution (buffering)

Fracture Reactivation in Response to Seismic Events	157
Buffering against Intrusion of Groundwater of Undesirable Composition	173
Understanding shield Groundwater Flow Domain Evolution during the Quaternary Period to Build Confidence in Repository Long-term Safety	185
Hydraulic and Hydrochemical Response to Seismic Events	197

Poster Session

Discipline-integrated Modelling Approach for Describing the Olkiluoto Crystalline Site in Finland	207
Study on Characterisation of Quaternary Tectonic Movement by Uplift Estimation using Fluvial Terraces	217
Examination of Earthquake Ground Motion in the Deep Underground Environment of Japan.....	227
Frequency of Fault Occurrence at Shallow Depths during Plio-pleistocene and Estimation of the Incident of New Faults	235
The Role of the Geosphere in Posiva's Safety Case	241
Understanding the Characteristics of Long-term Spatio-temporal Variation in Volcanism and the Continuity of the Related Phenomena for Estimating Regions of New Volcano Development .	247
Numerical Assessment of the Influence of Topographic and Climatic Perturbations on Groundwater Flow Conditions	257
Impacts of Natural Events and Processes on Groundwater Flow Conditions: A Case Study in the Horonobe Area, Hokkaido, Northern Japan	269
Groundwater Flow Prediction Method in Consideration of Long-term Topographic Changes of Uplift and Erosion	277
An Integrated Approach for Detecting Latent Magmatic Activity beneath Non-volcanic Regions: An Example from the Crystalline Iide Mountains, Northeast Japan	289



From:
**Stability and Buffering Capacity of the Geosphere
for Long-term Isolation of Radioactive Waste**
Application to Crystalline Rock

Access the complete publication at:
<https://doi.org/10.1787/9789264060579-en>

Please cite this chapter as:

OECD/Nuclear Energy Agency (2009), "Poster Session", in *Stability and Buffering Capacity of the Geosphere for Long-term Isolation of Radioactive Waste: Application to Crystalline Rock*, OECD Publishing, Paris.

DOI: <https://doi.org/10.1787/9789264060579-11-en>

This document, as well as any data and map included herein, are without prejudice to the status of or sovereignty over any territory, to the delimitation of international frontiers and boundaries and to the name of any territory, city or area. Extracts from publications may be subject to additional disclaimers, which are set out in the complete version of the publication, available at the link provided.

The use of this work, whether digital or print, is governed by the Terms and Conditions to be found at <http://www.oecd.org/termsandconditions>.